EVALUATION OF THE PERFORMANCE OF THE BLASTLOGIC SOFTWARE IN PREDICTING BLASTING FRAGMENTATION DISTRIBUTION IN SURFACE MINES

Milton Munkombwe

A research dissertation submitted to the Faculty of Engineering and the Built Environment, University of the Witwatersrand, in fulfilment of the requirements for the degree of Master of Science in Engineering.

Johannesburg, 2024

DECLARATION

I declare that this report is my own, unaided work. I have read the University Policy on Plagiarism and hereby confirm that no plagiarism exists in this report. I also confirm that there is no copying nor is there any copyright infringement. I willingly submit to any investigation in this regard by the School of Mining Engineering and I undertake to abide by the decision of any such investigation.

Signature of Candidate:

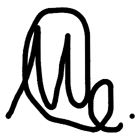

Milton Munkombwe

Date: 26/02/2024

ABSTRACT

Surface mining is a crucial aspect of the mining industry, and one of the most significant factors that affect profitability and efficiency in mining operations is fragmentation. The traditional approach to fragmentation in surface mines involves the use of explosives, which generates a particular fragmentation profile that may not always be targeted size. The objective of this study was to evaluate the performance of the BlastLogic software in predicting fragmentation distribution in surface mines. This was in comparison with Swebrec, Kuz-Ram and Split-Desktop fragmentation results.

Drill pattern designs are created (burden, spacing and hole position) in other design parameter software e.g., Maptek Vulcan, and Micro-station. These patterns are optimised in the BlastLogic software package. It uses advanced algorithms and models to simulate and predict the effects of different blasting parameters on fragmentation.

The study was conducted on 5 surface mines. These were Mogalakwena Platinum Mine, Kolomela Iron Ore Mine, Sishen Iron Ore Mine, Isibonelo Colliery, and Navigation Colliery. The study involved collecting data on the existing fragmentation profile in the mine and the geological characteristics of the ore body. The data was then used to evaluate the performance of the BlastLogic software in predicting fragmentation distribution. The blasting parameters used to achieve this were blast hole diameter, burden and spacing, powder factor and geotechnical factors such as the geology of the rock to be blasted.

By accurately predicting the fragmentation size, engineers and blasting experts can design the blast parameters, such as hole diameter, spacing, and powder factor, more precisely. This allows for better control over the size distribution of the blasted material. Also, knowing the expected fragmentation size allows for the selection of an appropriate amount of

explosive energy. Using too much energy can lead to excessive fracturing and finer fragmentation, while too little energy can result in larger rock fragments. Proper energy management helps achieve the desired size distribution.

The findings of this research demonstrated that the predicted fragmentation distribution created by using BlastLogic software is more effective and profitable than the conventional method. The predicted fragmentation size reduced the amount of oversized material generated during blasting, thereby improving the recovery rate of valuable minerals. The results showed that there were less than 15% of fines produced, with an insignificant amount of oversized material less than 5% for all surface mines under study.

In conclusion, the study evaluated the use of BlastLogic software in predicting fragmentation distribution. The study further highlighted the results of vibration and overpressure results obtained from these improved designs from BlastLogic. It was evident that BlastLogic software is a valuable tool for improving the efficiency and profitability of mining operations. The software offered a more accurate and reliable method of predicting and improving blasting fragmentation distribution for surface mines.

ACKNOWLEDGEMENTS

I want to express my gratitude to God for giving me the knowledge and stamina to finish this research work. I also like to thank the following people and entities:

- The University of Witwatersrand and the support by the Faculty of Engineering during my studies.
- The School of Mining Engineering staff for their positive encouragement and for creating a conducive studying environment.
- Mr. Erhan Uludag, my dissertation supervisor, for his essential advice and direction.
- Co-supervisor, Dr. Nhleko for co-supervision and verifying the final work and inputs.
- Mogalakwena Platinum mine, Navigation Colliery, Isibonelo Colliery, Sishen and Kolomela Iron ore mine for their support during the dissertation.
- My lovely family, wife, and son for the patience throughout my late-night studies.

DEDICATION

Prior to her untimely passing, my late mother, Sr. J. Munkombwe, encouraged me to embark on the master's path. May her spirit rest in peace always.

TABLE OF CONTENTS

CONTENTS **Page**

LIST OF FIGURES

LIST OF TABLES

LIST OF ABBREVIATIONS OR ACRONYMS AND UNITS OF MEASURE

2D	Two-Dimensional
3D	Three-Dimensional
ANN	Artificial Neural Network
BIF	Banded Iron Formation
BL	BlastLogic software
BPM	Bonded Particle Model
BPNN	Back Propagation Neural Network
BRW model	Bergmann, Riggle and Wu model
BWI	Bond Work Index
CDF	Cumulative Distribution Function
CK model	Chung and Katsabanis model
DEM	Discrete Element Method
DWT	Drop Weight Testing
EU	European Union
FEM	Finite Element Method
FIS	Fuzzy Inference System
GDP	Gross Domestic Product
HF	Hardness Factor
JF	Joint Factor
JKMRC	Julius Kruttschnitt Mineral Research Centre

LiDAR	Light Detection And Ranging
MAE	Mean Absolute Error
MVRA	Multivariate Regression Analysis
MWD	Measured While Drilling
MLP	Multi-Layer Perceptron
n	Uniformity index
NBC	Natural Breakage Characteristics
OpenCV	Open-Source Computer Vision
PGEs	Platinum Group Elements
PGM’s	Platinum Group Metals
RRSB	Rosin-Rammler-Sperling-Bennett distribution
RR	Rosin-Rammler
RMD	Rock Mass Description
RDI	Rock Density Influence
RMSE	Root Mean Square
ROM	Run Of Mine
RSA	Republic of South Africa
RBF	Radial Basis Function
S/B ratio	Spacing to Burden ratio
SveDeFO	Swedish Detonation Foundation
SveBeFo	Swedish Rock Research Foundation

SPH	Smoothed Particle Hydrodynamics
t	Metric tonne
UCS	Uniaxial Compressive Strength
USD/$	United States Dollar
USBM	United States Bureau of Mines
UG 2	Upper Group 2
ZAR	South African Rand

1 INTRODUCTION

1.1 Introduction

Chapter 1 provides background information about the importance of using BlastLogic software to predict the fragmentation distribution from blasting activity. This chapter also discusses the importance of different models adopted in the prediction of fragmentation size distribution. The problem statement, research motivation, constraints and scope of the research study are also presented.

1.2 Research Background

Rock fragmentation plays a crucial role in the mining process, as it directly affects downstream activities such as loading and hauling (Bennett, 1936). Incorrect fragmentation can lead to inefficiencies and increased expenses in these operations. Adjusting blast design parameters to achieve the desired fragmentation size is essential for minimising downstream costs (Choudhary, 2019). The controllable and uncontrollable factors influence the blast design parameters that determine the actual fragmentation sizes.

Proper execution of drill and blast activities is crucial to efficient rock excavation (Choudhary, 2013). Brunton *et al*. (2003), investigated the impact of fragmentation size distribution on the efficiency of excavators and loading units in mining operations. They used simulation techniques to model and answer how variations in fragmentation size distribution affected excavation time, loading, and hauling productivity. The authors used the discrete element method (DEM) to simulate the fragmentation size distribution of a rock mass and the subsequent loading of the fragments by an excavator and loading unit. The DEM is a numerical method that simulates the behaviour of individual particles in a granular material (Brunton *et al*., 2003).

Brunton *et al*. (2003) highlighted the relationship between fragmentation profiles and the efficiency of excavation and loading processes. Optimal fragmentation improves loading efficiencies and ensures bucket payload is achieved. The simulation findings showed a 20% increase in loading and hauling productivity due to optimised fragmentation (Brunton *et al*., 2003).

To address the issue of poor fragmentation, various models integrating blast design parameters have been developed. Two common empirical models are the Kuz-Ram model and the Swebrec model (Gheibie *et al*., 2009). The two common models describe particle size distributions in fragmented material. These models consider blast design parameters to analyse and improve the efficiency of blasting and crushing operations (Ouchterlony, 2009).

While both the Kuz-Ram model and the Swebrec function are empirical models used in fragmentation analysis, the Swebrec function offers advantages. These advantages include flexibility in shape representation, accurate data fitting, widespread recognition, and explicit consideration of the characteristic size parameter (Ouchterlony, 2009). The choice between the two methods depends on the specific requirements and characteristics of the fragmentation analysis being conducted (Ouchterlony, 2009).

The five surface mines under study in this thesis are Mogalakwena Platinum Mine, Kolomela Iron Ore Mine, Sishen Iron Ore Mine, Isibonelo Colliery, and Navigation Colliery. These mines are all found in South Africa, and they produce a variety of commodities, including platinum, iron ore, and coal. These mines use a variety of mining methods, including open-pit mining and open-cast.

Mogalakwena Platinum Mine is in Limpopo Province, South Africa (McDonald *et al*., 2005). It is the largest platinum mine in the world, and it produces about 4.5 million ounces of platinum per year. The mine uses of open pit (Gloy, 2005). The targeted fragmentation distribution size for 80% passing is 200-250mm. Some of the problems associated with achieving this fragmentation size include the hardness of the ore, the presence of other minerals, and the depth of the mine (Payne, 2019).

Kolomela Iron Ore Mine is in the Northern Cape Province, South Africa. It is the largest iron ore mine in South Africa, and it produces about 25 million tonnes of iron ore per year (Baxter, 2021). The mine uses the open-pit mining method. The targeted fragmentation distribution size for 80% passing is 250 mm. Some of the problems associated with achieving this fragmentation size include the hardness of the ore, the presence of other minerals, and the depth of the mine.

Sishen Iron Ore Mine is in the Northern Cape Province, South Africa. It is the second-largest iron ore mine in South Africa, and it produces about 20 million tonnes of iron ore per year (Bekker *et al*., 2010). The mine uses the open-pit mining method. The targeted fragmentation distribution size for 80% passing is 250 mm. Some of the problems associated with achieving this fragmentation size include the hardness of the ore, the presence of other minerals, and the depth of the mine.

Isibonelo Colliery is in Mpumalanga Province, South Africa. It is a coal mine, and it produces about 10 million tonnes of coal per year. The mine uses an open-pit mining method. The targeted fragmentation distribution size for 80% passing is 200 mm. Some of the problems associated with achieving this fragmentation size include the hardness of the coal, the presence of other minerals, and the depth of the mine.

Lastly, Navigation Colliery is in Mpumalanga Province, South Africa. It is a coal mine, and it produces about 5 million tonnes of coal per year. The mine uses an open-pit mining method. The targeted fragmentation distribution size for 80% passing is 200 mm. Some of the problems associated with achieving this fragmentation size include the hardness of the coal, the presence of other minerals, and the depth of the mine.

The effect of geological condition on the fragmentation distribution produced by blasting in surface mines is a crucial factor for surface mines (Kinnaird *et al*., 2005). These implications encompass operational efficiency, safety, environmental considerations, processing efficiency, material handling, and effective mining planning distribution. Comprehensively understanding and managing geological conditions is imperative for optimising mining operations (Drebenstedt and Singhal, 2013). It is essential for mitigating risks, minimising environmental impact, boosting equipment efficiency, streamlining material handling, and enabling effective mine planning (Drebenstedt and Singhal, 2013). These combined efforts contribute significantly to achieving operational excellence, ensuring safety, and upholding environmental responsibility in surface mining endeavors (Drebenstedt and Singhal, 2013).

Platinum Ore deposits geology

Platinum ore deposits originate through magmatic, hydrothermal, and placer processes, each with distinct geological characteristics. Magmatic deposits, exemplified by the Bushveld Complex in South Africa, result from the cooling of platinum-rich magma beneath the Earth's surface (Nex *et al*., 2006). Hydrothermal deposits, such as the Merensky Reef, form mineral-rich fluids that circulate through the Earth's crust. Placer deposits, formed through the mechanical concentration of platinum minerals, involve the weathering and erosion of primary sources (Nex *et al*., 2006). Understanding these processes is crucial for efficient extraction, especially in mines like Mogalakwena Platinum, situated within magmatic deposits, where geological knowledge influences blasting strategies (Nex *et al*., 2006).

Iron Ore Deposit Geology

Iron ore deposits encompass massive hematite, magnetite, titanomagnetite, and pisolitic ironstone, each with unique characteristics. Massive hematite deposits, often found in banded iron formations, are easily mined due to their high iron content. Magnetite, known for its magnetic properties, allows for efficient separation and processing. Titanomagnetite, associated with volcanic rocks, offers valuable titanium and vanadium byproducts (Alchin and Botha, 2006). Pisolitic ironstone, with distinctive rounded concretions, is found in tropical environments. The choice of mining type depends on factors like quality, accessibility, and market demand (Alchin and Botha, 2006). As observed in operations like Sishen Iron Ore mine, where efficient blasting is crucial for extracting high iron content hematite (Alchin and Botha, 2006).

Coal Seam Deposit Geology:

Coal formation stages, represented by peat, lignite, bituminous, and anthracite, undergo geological changes with distinct properties at each stage (Kopp, 2019). Peat, originating from partially decayed plant material, is used for domestic heating. Lignite, formed from compressed peat, is brown or black and utilized for electricity generation (Kopp, 2019). Bituminous coal, resulting from further burial, is harder with higher energy content, suitable for electricity generation and industrial processes. Anthracite, the highest coal rank, forms under intense metamorphism, burning cleanly with premium energy content (Kopp, 2019). Understanding these stages is vital for diverse industrial and energy applications, as seen in the continuum of changes at each stage (Kopp, 2019).

Hence the need to incorporate the latest software programs to achieve and manage the desired fragmentation size results and effects from the blasting operations.

Software packages in drill and blast management for surface mines

There are several software programs available for drilling and blasting management in surface mines (Milanović *et al.,* 2019). These programs typically allow users to design blast patterns, calculate explosive requirements, and simulate the effects of the blast. Some of the most popular software programs include:

- BlastLogic
- Deswik
- Micromine
- Vulcan
- 3D Blast
- RockSim

These programs can be used to improve the efficiency and effectiveness of drill and blast operations. They can help to ensure that blast patterns are designed to achieve the desired fragmentation size, and they can help to minimise the environmental impact of blasting.

The software programs mentioned above can also be used to evaluate the fragmentation achieved in a blast. This information can be used to improve the design of future blasts and to ensure that the desired fragmentation size is being achieved.

The evaluation of fragmentation typically involves measuring the size distribution of the blasted rock. This can be done by collecting samples of the blasted rock and then measuring the size of the fragments in the samples. The size distribution of the blasted rock can also be estimated using computer simulations.

BlastLogic software is a popular software program for drill and blast management in surface mines. It is a comprehensive program that offers a wide range of features, including:

- Blast pattern design.
- Explosive calculations.
- Blast simulation.
- Fragmentation evaluation.
- Environmental impact assessment.

BlastLogic software is a user-friendly and easy-to-learn program. This makes it a desirable choice for both experienced and inexperienced users. In addition to its features and ease of use, BlastLogic software is preferred compared to the rest because it is constantly updated with new features and capabilities. This ensures that users have access to the latest technology for drill and blast management (Maptek, 2021).

The BlastLogic software enhances blasting outcomes by utilising the Kuz-Ram and Swebrec models for predicting fragmentation. The Kuz-Ram model delves into particle size distribution based on blast design parameters, while the Swebrec function allows for flexibility in capturing distribution curve shapes (Maptek, 2021).

Compared to other available blasting software, BlastLogic stands out because it uses real-time data from diverse sources, including geological models, drill data, and blasting parameters, to provide precise predictions and simulations of fragmentation results. This information empowers mine engineers to fine-tune blast designs and parameters to attain their desired fragmentation outcomes (Maptek, 2021).

Through the combined use of the Kuz-Ram model and the Swebrec function, BlastLogic enables users to assess and Optimise blast designs by considering their impact on fragmentation results. By simulating and analysing fragmentation data, users can make informed decisions of parameters like hole diameter, spacing, burden, and stemming length, ultimately achieving their desired fragmentation sizes.

One of the important downstream activities affected by inconsistency is the mine-to-mill process. Mine-to-mill optimisation is a total systems approach to the reduction of energy and cost in mining and mineral processing operations. The concept is based on the idea that the efficiency of the entire mining and processing system can be improved by optimising the blast design to produce the desired fragmentation (Chi *et al.*, 1996).

The Mine to Mill concept was first introduced by the Julius Kruttschnitt Mineral Research Centre (JKMRC) in the early 1990s. The JKMRC developed a methodology for determining the impact of blast design on downstream processes, such as crushing and grinding. This methodology was used to develop several optimisation techniques that are effective in reducing energy consumption and costs (Ouchterlony and Sanchidrián, 2019).

The benefits of mine-to-mill optimisation can be significant. For example, one study found that a 10% improvement in fragmentation can lead to a 5% increase in mill throughput. This can translate into significant savings in energy and operating costs (Grundstrom *et al.*, 2011).

The Mine to Mill concept is becoming increasingly important as mining companies look for ways to reduce costs and improve profitability. The methodology is relatively complex, but there are several software tools available that can help mining engineers implement mine-to-mill optimisation (Grundstrom *et al.*, 2011).

The mine-to-mill optimisation process typically involves the following steps:

- Scoping: The first step is to define the goals of the optimisation. This includes identifying the specific areas where improvements are desired, such as energy consumption, costs, or throughput.
- Auditing: The next step is to collect data on the current state of the mining and processing system. This includes information on the rock properties, the blast design, and the performance of the crushing and grinding equipment.
- Modelling and simulation: The data collected in the auditing step is used to develop models of the blasting, crushing, and grinding processes. These models can be used to simulate the impact of different blast designs on the downstream processes.

- Mine-to-mill simulation: The models are then used to conduct mine-to-mill simulations. These simulations allow mining engineers to evaluate the impact of different blast designs on the overall efficiency of the mining and processing system.
- Implementation: The final step is to implement the optimised blast design. This may involve changes to the drilling and blasting practices, the equipment settings, or the design of the crushing and grinding circuits.

Several new technologies are being developed to improve the efficiency of mine-to-mill optimisation (Workman, 2001). These technologies include:

- Real-time monitoring: Real-time monitoring systems can be used to collect data on the performance of the blasting, crushing, and grinding processes. This data can be used to optimise the blast design on an ongoing basis.
- Virtual reality: Virtual reality can be used to simulate the blasting, crushing, and grinding processes. This can help mining engineers to visualize the impact of different blast designs and to identify potential problems.
- Artificial intelligence: Artificial intelligence is being used to develop new optimisation algorithms that can improve the efficiency of Mine to Mill optimisation.

In addition, Workman (2001) goes through the new technologies that are available to control the different stages of the chain from mine to mill. The following technologies of the new mine-to-mill technologies are listed in Table 1.1.

Table 1.1 Modern mine-to-mill enabling technologies. Source: Workman (2001)

Unit operation	Technologies
Drilling	GPS drill position and drill performance monitoring (MWD)
Blasting	Blast design software, targetless laser survey systems, bulk explosive trucks with GPS and on-board computing, fragmentation prediction and measurement
Loading	GPS shovel positioning and shovel performance monitoring
Hauling	Dynamic dispatching and haulage monitoring systems and fragmentation measurements
Crushing and grinding	Continuous fragmentation and energy consumption

Table 1.1 shows the new mine-to-mill technologies and the unit of operations. All units of operation are equally important to the mining cycle.

The Mine-to-Mill concept is a powerful tool that can be used to reduce energy consumption and costs in mining and mineral processing operations. The methodology is complex, but there are several software tools available that can help mining engineers implement mine-to-mill optimisation. The use of new technologies, such as real-time monitoring and virtual reality, is also expected to improve the efficiency of mine-to-mill optimisation in the future.

Overall, blast design parameters are crucial inputs in achieving the desired fragmentation size in the blasting process. The research study aims to evaluate the performance of BlastLogic software in predicting fragmentation distribution.

1.3 Significance and Relevance of the Study

Mining plays a vital role in the socio-economic development of nations, and the Republic of South Africa heavily relies on its mining sector for economic growth and commodity exports. The efficiency and productivity of mining operations have a direct impact on the revenue generated and the overall stability of the country's economy (McMahon and Moreira, 2014).

South Africa possesses vast mineral deposits of platinum, coal, and Iron ore, with an estimated worth of $2.5 trillion, and is a major global supplier of platinum group metals (PGMs) and coal (Nembahe and Ratshomo, 2016). Coal accounts for approximately 72% of South Africa's total primary energy and serves as a primary source for thermal electricity generation (Nembahe and Ratshomo, 2016). Furthermore, South Africa's iron ore industry plays a key role in economic growth, with high-quality iron ore exports contributing significantly to the country's GDP (Kumba Iron Ore, 2011).

The mining sector's contribution to the economy heavily relies on the productivity and efficiency of mining operations (Orica, 2021). Optimising mining processes using modern technologies, such as Blastmap software, BlastIQ software, Blast timing software, Laser Profiling, 3D Laser Scanning and Seismic Monitoring can lead to increased profitability and revenue generation (Ediriweera and Wiewiora, 2021). BlastLogic software, being a drilling and blasting management software, has the potential to optimise the blasting process, which directly impacts downstream activities like loading, hauling, and crushing (Bowa, 2015).

Fragmentation plays a vital role in mining operations as it affects the efficiency of loading, hauling, and milling processes (Bhandari, 1997).

Optimised blasting design parameters are crucial in achieving the desired fragmentation size, leading to improved effectiveness and cost reduction in subsequent mining unit operations (Thornton *et al*., 2001 and Bowa, 2015). By effectively utilising BlastLogic software to optimise blasting, mining operations can enhance their productivity, reduce operational costs, and minimise adverse environmental impacts caused by blasting (Ndibalema, 2008).

The significance of this research study extends beyond the specific case of BlastLogic software used in the evaluation of performance and predicting fragmentation distribution. Successful fragmentation optimisation through improved blast design parameters can benefit other surface mines in South Africa that employ similar software and technologies. By reducing costs and improving operational efficiency, mining operations can increase their profitability while ensuring environmental sustainability (Gomes-Sebastiao and de Graaf, 2017).

Moreover, the research study aligns with the global trend in the mining industry towards technology-driven optimisation processes and environmentally acceptable practices. It expands the knowledge in the field of blast design parameters and their influence on fragmentation muckpile through the adoption of BlastLogic software technology in surface mines. By conducting this evaluation, the research study contributes to the advancement of mining practices, cost reduction efforts, and operational efficiency in the mining sector, not only in South Africa but also globally.

In summary, the research study on the evaluation of the performance of BlastLogic software in predicting fragmentation distribution holds significant significance and relevance for the South African mining sector. It addresses the need for optimisation in mining operations, the importance of blast design parameters in achieving optimal fragmentation, and the potential benefits of BlastLogic software in enhancing productivity and reducing operational costs. The study's findings and insights contribute to the broader understanding of blast design parameters and their impact on fragmentation muckpile, ultimately advancing mining practices and operational efficiency in the industry.

1.4 Problem Statement

While there have been establishments and attempts of continuous improvements to blast fragmentation prediction analysis and optimisation, surface mines continue to face challenges with inconsistent fragmentation results (Kemeny *et al*., 2002). The inconsistencies of fragmentation sizes at the surface mines under study (Mogalakwena Platinum Mine, Isibonelo Colliery, Navigation Colliery, Kolomela Iron Ore Mine, and Sishen Iron Ore Mine) highlight the challenges of inadequate rock fragmentation evaluation and predicting. The following paragraphs in the problem statement discuss the issues at each mine under study, their target size and what they are achieving.

The problem under investigation revolves around the accurate prediction of fragmentation distribution in surface mines. Also, the environmental aspect of the fragmentation results obtained in terms of vibration, and overpressure in surface mines.

In examining the surface mining sites studied, it becomes evident that fragmentation challenges experienced are consistent. These challenges include excessive boulders, difficulties in excavation, and fragmentation distribution inconsistencies. These issues have direct repercussions on efficiency, productivity, safety, and operational costs. For example, Mogalakwena Platinum Mine faced the challenge of fragmentation exceeding the target size of 250mm, impacting efficiency and safety. Kolomela Iron Ore Mine struggled with inconsistent fragmentation, leading to excavator difficulties and prolonged loading times. Isibonelo Colliery and Navigation Colliery confront issues of coal pulverization resulting in smaller-than-desired fragment sizes, affecting coal quality and operational costs. Sishen Iron Ore Mine struggled to achieve the target fragment size of 200mm. This negatively impacts the efficiency and loading times.

Optimising fragmentation size is crucial for cost reduction in subsequent mining activities. The traditional methods of gathering and analysing data for blast design have been cumbersome, thus making informed decisions challenging (Roy *et al*., 2016). Given these challenges, utilizing tools like BlastLogic software becomes essential to efficiently predict fragmentation sizes, overpressure, and vibration levels.

The research aims to address the critical need for accurate fragmentation predictions in surface mining operations and assess the capabilities of BlastLogic software in meeting these requirements. By doing so, the study aims to contribute valuable insights to the mining industry, improving efficiency, productivity, and safety while minimizing environmental impact.

Traditional static drilling and blasting methods imposed a significant burden on engineers in terms of gathering, analysing, and manipulating the data necessary for efficient blast design (Maptek, 2021). This made it difficult for engineers to make instant and informed decisions before blasting and predicting the fragmentation size. Because of this, it is crucial to make sure that the drilling and blasting operations are optimised using the information and data that is accessible. The surface mines under study struggled with fragmentation sizes. BlastLogic software was suggested as a tool to efficiently predict the fragmentation size from the selected blast designs.

1.5 Research Question

"Can BlastLogic Software be efficiently used to predict the fragmentation size, overpressure and vibration levels?"

1.6 Research Objectives

This study was aimed at evaluating BlastLogic software’s accuracy in predicting, fragmentation distribution size, ground vibration, and overpressure in surface mines. The objectives of the research were to:

- Evaluate the performance of BlastLogic software in predicting fragmentation distribution for surface mines.
- Predict vibration and overpressure levels using BlastLogic software.

1.7 Dissertation Overview

Chapter 1 introduced the background and further described the problem of the study. The significance and the objectives of the study were also discussed in Chapter 1. Chapter 2 discusses the literature study and provides an overview of the various fragmentation models, analysis, and their most popular models. Geology and geotechnical parameters were included for different surface mines. Chapter 3 discusses the methodology followed to evaluate the performance of the BlastLogic software in predicting fragmentation distribution. This covers the discussion of the methodology used for data gathering, costing analysis, and the research study's underlying assumptions. The input of the chosen design criteria for the chosen pattern across the studied commodities is highlighted in Chapter 4's data for the study. Chapter 5 discusses and analyses the results. The conclusion and recommendations drawn from the research study's data are presented in Chapter 6.

2 FRAGMENTATION MODEL DISCUSSIONS

2.1 Overview of Chapter 2

This chapter comprises ten sections that provide an overview of blast fragmentation. The mechanisms and factors that affect rock fragmentation were discussed before an in-depth look at the fragmentation prediction models. The fragmentation models were compared before concluding by looking at how the fragmentation can be measured and analysed in the field.

2.2 Mechanism of Rock Fragmentation

Rock fragmentation refers to the process of breaking rock into smaller fragments. In mining operations, this is typically achieved through controlled blasting. The mechanism of rock fragmentation involves the generation and propagation of shockwaves and the application of high-pressure forces on the rock (Ouchterlony and Sanchidrian, 2019).

During the blasting process, explosives are used to create a controlled release of energy (BME, 2021). When the explosive charge is detonated, a shockwave is generated and rapidly propagates through the rock mass. This shockwave is a high-pressure wave that travels faster than the speed of sound in the rock (Baumgardt *et al*., 1975).

The shockwave interacts with the rock, inducing stress waves and generating high-pressure zones. These high-pressure zones create tensile and shear stresses within the rock, causing it to fracture and fragment. The rock fractures along pre-existing planes of weakness, such as joints, faults, and bedding planes. The shockwave also causes the generation of microcracks within the rock (Ouchterlony and Sanchidrian, 2019).

The shockwave is followed by the expansion of high-pressure gases, which further contribute to rock fragmentation. The sudden release of these gases applies additional pressure on the rock, causing it to break into smaller pieces (Cundall and Strack, 1979). The crushed zone concept is illustrated in Figure 2.1.

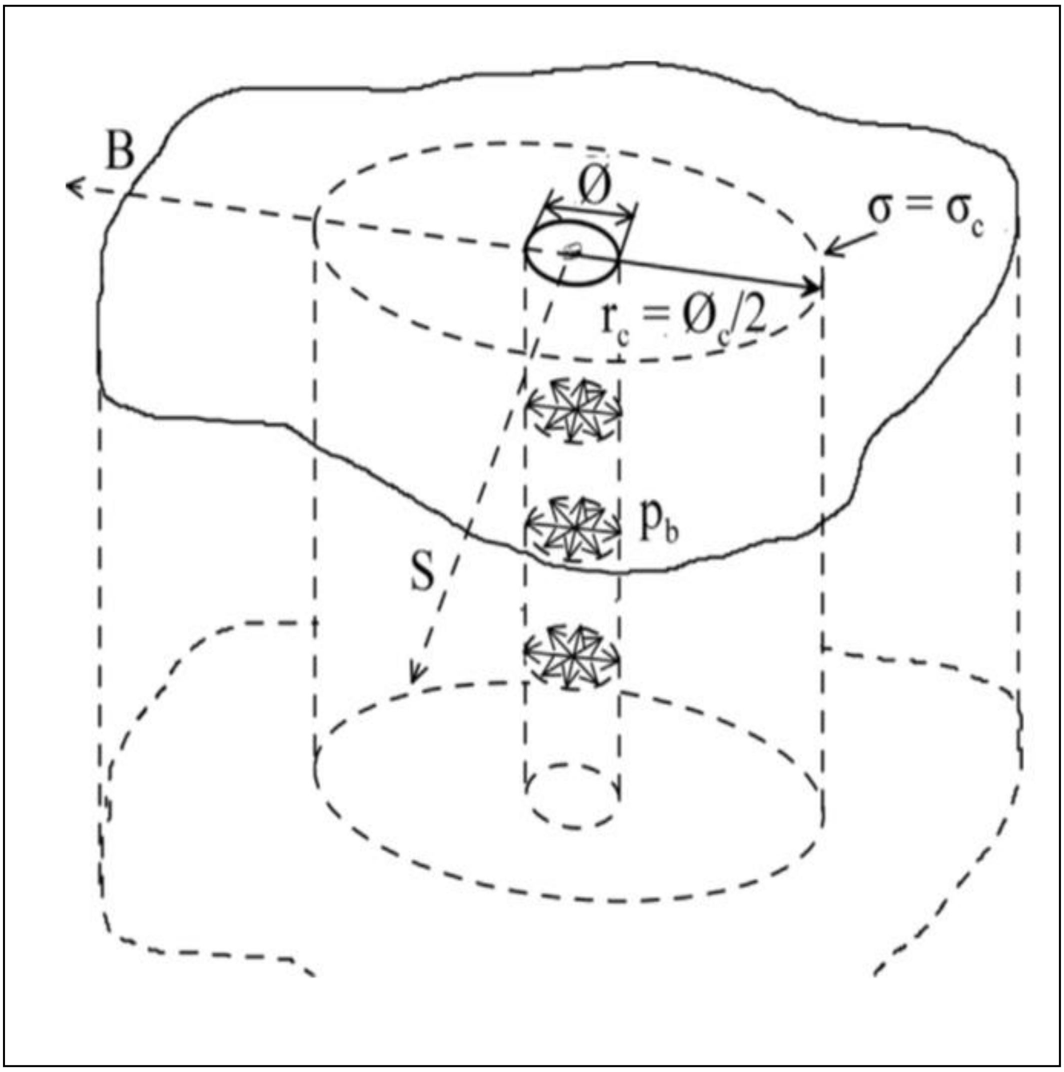

Figure 2.1 CZM crushed zone concept. Source: Ouchterlony and Sanchidrian (2019)

Figure 2.1 shows the crushed zone concept and the radius of stressed zones. The model predicts the fraction of fines F_c having a size of more than 1mm. Equations 2.1 and 2.2 introduced the crushed zone concept and the stressed zone concept.

$F_c = V_c /(BS)$ 2.1

Where:

V_c is $\pi(\emptyset_c{}^2 - \emptyset_h{}^2)/4$ 2.2

Where:

$\emptyset_c$ is unconfined compressive strength.

The joining point for rocks having σ_C more than 50MPa is x_{50} while for σ_C less than 50MPa is x_{90}. The graph of mass percentage passing against mesh size splicing point x_{50} is illustrated in Figure 2.2.

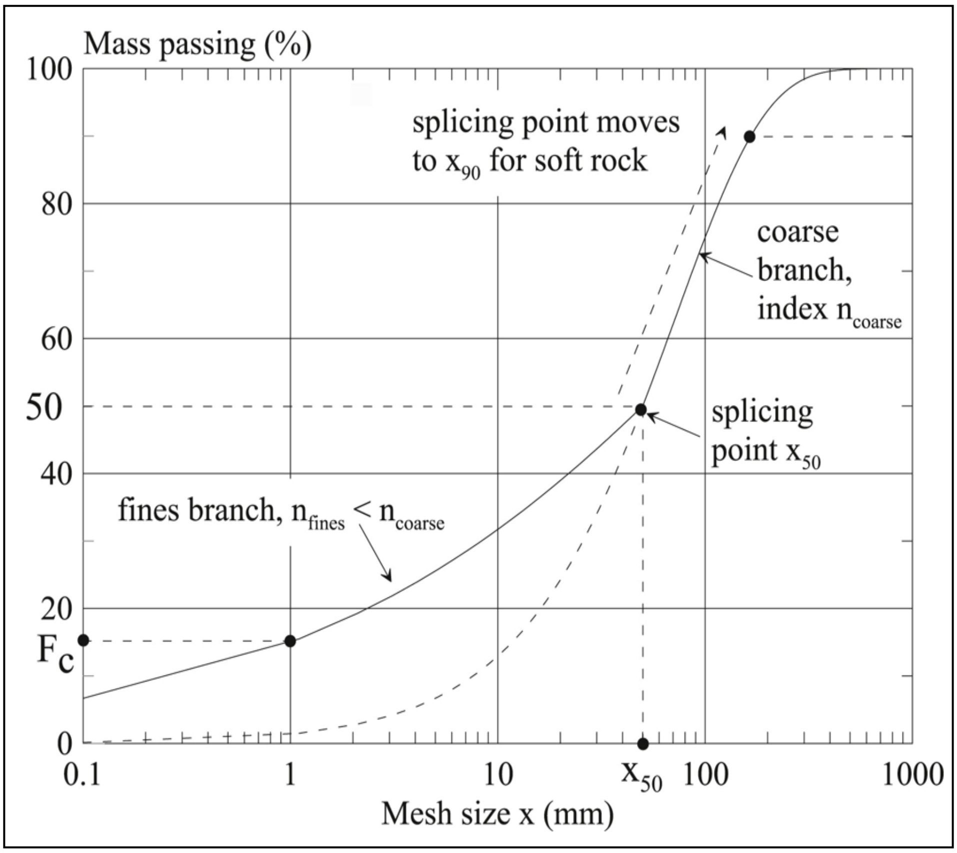

Figure 2.2 CZM coarse and fine branches splicing point at mean fragmentation size. Source: Ouchterlony (2003)

Figure 2.2 shows the Crush Zone Model for coarse and fine particles. The model predicts that fines with sizes less than 1mm are generated in the crushed zone only (Ouchterlony, 2003). The fines sizes of more than 1mm are generated beyond the crushed zone.

The performance of rock blasting is influenced by various factors, including the properties of the rock and the explosive used. Rock properties such as strength, toughness, and jointing affect how the rock responds to the shockwave and pressure. Weaker and more brittle rocks are generally easier to fragment compared to stronger and tougher rocks. The presence of pre-existing fractures and planes of weakness also play a role in determining the pattern and extent of fragmentation (Ouchterlony, 2003).

The explosive properties, including detonation velocity, brisance, and fragmentation index, also influence rock fragmentation. Detonation velocity refers to the speed at which the explosive wave travels through the rock (Gaudin, and Meloy, 1962). Brisance measures the ability of the explosive to shatter the rock, while fragmentation index is an indicator of the explosive's ability to produce a uniform size distribution of rock fragments (Ouchterlony, 2003).

In summary, rock fragmentation occurs through the generation and propagation of shockwaves, coupled with the application of high-pressure forces. The shockwave induces stresses within the rock, leading to fractures along existing planes of weakness. The expansion of high-pressure gases further contributes to the fragmentation process (Ouchterlony, 2003).

2.3 Factors Affecting Fragmentation Distribution Size

Understanding the factors that influence fragmentation size distribution is essential for optimising blasting practices and achieving desired outcomes. Several key factors contribute to the variation in fragmentation sizes, such as rock properties, blast design parameters, drilling accuracy, blast energy distribution, blast-hole configurations explosive type and quantity, and weather conditions (Abdallah *et al*., 2019).

In addition to these factors, there are other factors that can affect fragmentation size distribution, such as the use of stemming, the type of blasting cap used, and the depth of the holes (Dumakor-Dupey *et al*., 2021). It is important to consider these factors when designing a blast to achieve the desired fragmentation size distribution (Chen *et al*., 2018). A well-designed blast will produce a more uniform fragmentation size distribution, which will make it easier to load, transport, and crush the blasted rock (Barakat, 1976).

2.3.1 Rock properties

The strength of the rock is one of the most important factors affecting fragmentation size distribution. Stronger rocks will tend to fragment into larger pieces, while weaker rocks will fragment into smaller pieces. This is because stronger rocks require more energy to break, so they will not fragment as easily as weaker rocks (Ozturk *et al*., 2014).

The rock strength must be high to withstand breaking pressures. This is dependent on both the characteristics of the discontinuities and the characteristics of the intact rock mass. Rock strength has significant effects on the design of both underground and open mines as well as drilling efficiency (Ozturk *et al*., 2014).

Resistance to breaking forces is referred to as rock power. This is dependent on the characteristics of both the discontinuities and the intact rock mass. According to Ozturk *et al*., (2014) and Heinz (2009), rock strength has significant effects on the architecture of both underground and surface mines.

Sometimes the terms "rock strength" and "rock hardness" are used interchangeably. Rock hardness and the power of the rock material, as determined by the uniaxial compressive strength (UCS), are correlated. (Heinz, 2009). Heinz (2009) suggested that sticking with the word "strength" to describe the complete rock mass is more appropriate. While "hardness" can be used to refer to a rock's strength and resilience to permanent deformation (Heinz, 2009). For mining, rock hardness is typically of utmost importance. Simple mechanical tests are more consistently and easily used to characterize hardness (Heinz, 2009).

Compressive strength refers to a material's ability to resist applied forces. These data can be used to forecast the strength of the rocks in a mining block and to create a hardness index. The difficulty of crushing the rock is highly correlated with its UCS value. (Adeyemo and Olaleye, 2012). While there is only a weak link between UCS and Bond Work Index BWI, there has been some correlation and relationship between the strength (UCS) and hardness (DWT) (Bye, 2005). To characterise breakage characterisation for comminution processes, both tests are used.

‘Strike’ and ‘dip’ expressions are used to describe the rock orientation. The strike is the horizontal direction of the structure on the rock surface. The dip is the angle of the structure relative to the horizontal rock surface. This is shown in Figure 2.3.

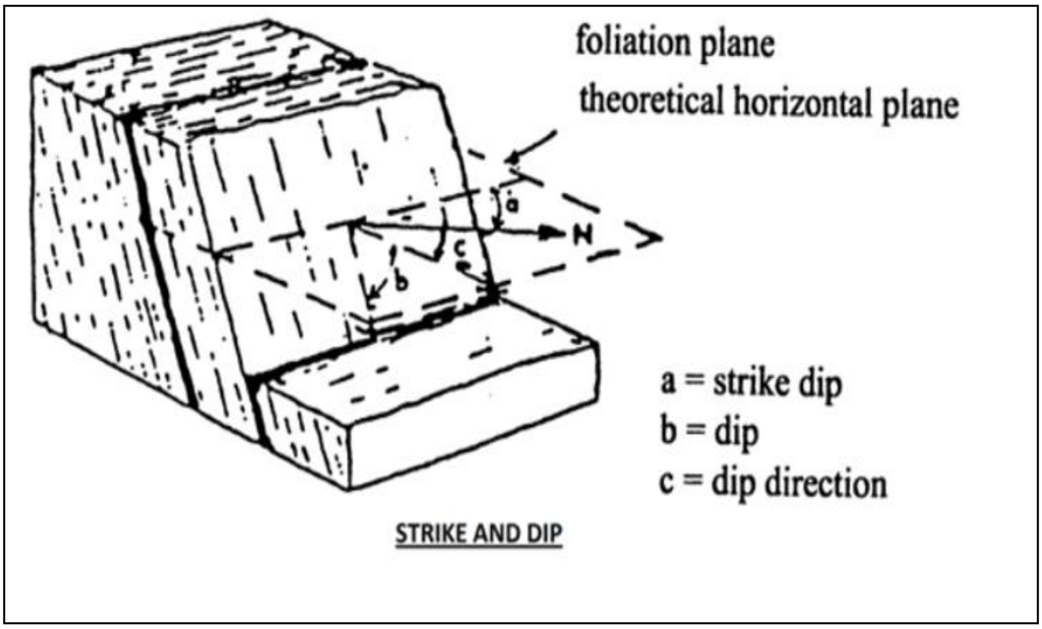

Figure 2.3 Strike and dip. Source: Sharma (2011)

Figure 2.3 shows the foliation plane and theoretical horizontal plane on a rock surface. The strike dip, dip and dip direction are all shown to explain how they influence the movement of rock when breaking.

2.3.2 Tensile strength of the rock

The tensile strength of a rock is defined as the pulling force, required to rapture a rock divided by the cross-sectional area (Zhang, 2016). It gauges the failure of rock mass issues, making it a crucial mechanical parameter in mining. The Brazilian test, which yields a more accurate result than the more widely used compression strength, is typically used to ascertain this. Cunningham (2005) asserts that rocks with tensile strengths of more than 15 MPa tend to fragment coarsely, while those with tensile strengths of less than 6 MPa fracture finely.

Zhang (2019) investigated how granite tensile strength affected loading rates. As a result, especially in dynamic loading, the loading rates varied according to the tensile strength of the rocks being loaded. Always larger than static tensile strength is the dynamic tensile strength of rock (Zhang, 2016).

Tensile failure in rock will occur when the effective stress becomes tensile and equals or exceeds rock strength. Equation 2.3 shows the relationship between the failure mode and stress applied to the rocks.

$$\sigma'_3 = -T_0 \qquad 2.3$$

Where:

σ'_3 are the minimum effective principal tensile stresses.

T_0 is the uniaxial tensile strength.

Most rock types have a compression strength which is 8 to 10 times greater than the tensile strength. These properties are crucial factors in rock blasting and are shown in Table 2.1.

Table 2.1 Tensile and compressive strength. Source: Sharma (2011)

Type of rock	Compressive strength (kg/cm^2)	Tensile strength (kg/cm^2)
Granites	2000-3600	100-300
Diabase	2900-4000	190-300
Marble	1500-1900	150-250
Limestone	1300-2000	170-300
Shale	1300-2000	300-1300
Sandstone, hard	3000	300

Table 2.1 shows the different rock compressive strengths and tensile strengths. Shale has the highest tensile strength of up to 1 300 kg/cm^2. Granites have tensile strength in the range of 100-300 kg/cm^2. Rocks with higher compressive strength are more resistant to breaking under compression forces. In blasting, understanding the compressive strength helps determine the amount of explosive energy needed to break the rock effectively. For example, rocks with high compressive strength may require more explosive energy to achieve satisfactory fragmentation.

Young’s modulus of the rock

The uniaxial compressive test was the foundation for Young's Modulus idea. It gauges a solid material's tensile or compressive stiffness when a force is applied longitudinally. However, tangent, secant, and average modulus can all be used to calculate it (Makowski *et al*., 2018). A coarser fragmentation is expected for rocks with the same tensile strength at a lower Young’s modulus of less than 50GPa.

Material with a high modulus, under extreme strain the material resists the first force and recovers well. For a lower modulus material, strain stresses and can break. The stress and strain figure are illustrated in Figure 2.4.

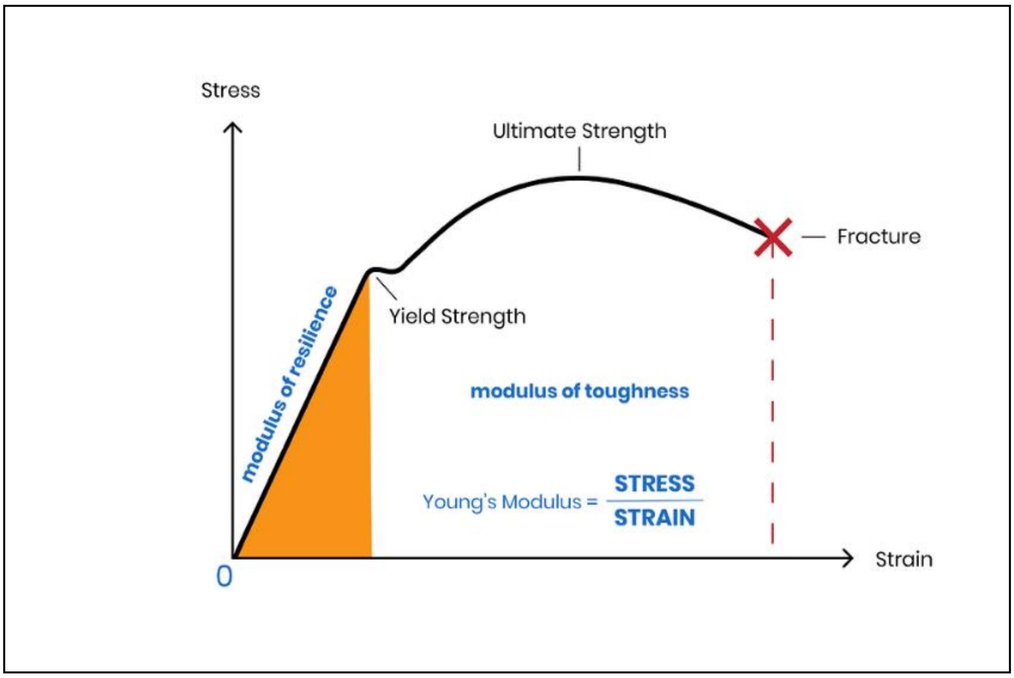

Figure 2.4 Stress and strain curve. Source: Thread (2019)

Figure 2.4 shows the stress and strain concept graph for different materials under load. The first part of the curve describes the ability of a wire, cable, yarn, or thread to resist elastic deformation under load. It describes the material's ability to withstand or retain shape after being stretched, pulled, twisted, or compressed (Thread, 2019).

2.3.3 The density and P-wave velocity of the rock

The impedance of the boulder is defined as the rock's P-wave velocity multiplied by its density. According to the statistical analysis, saturated samples yield greater P-wave velocity values while dry samples yield lower values (Kassab and Andreas, 2015).

Research on P-wave velocity and uniaxial tensile strength was conducted by Singh and Sarkar (2005). They concluded that the uniaxial strength and P-wave velocity both decreased with increasing quartz concentration and increased moisture content, respectively. According to the research, P-wave velocity decreased as silica content rose.

The regression model is analysed with the relationship between P-wave velocity and physical-mechanical properties. The relationship between wave velocity and Unified Compressive strength is illustrated in Figure 2.5.

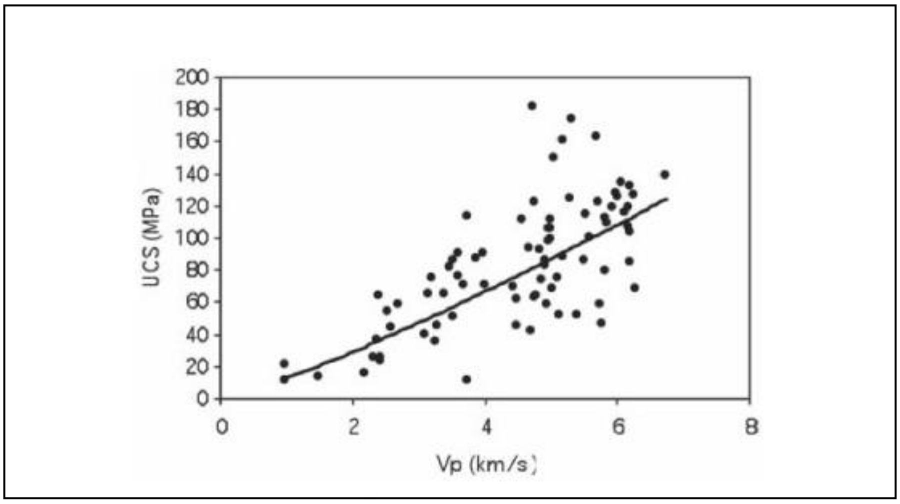

Figure 2.5 The relationship between the P-wave velocity and UCS of rocks. Source: Altindag (2012)

Figure 2.5 shows the linear relationship between Uniaxial compressive strength UCS (MPa) and P-wave velocity (Vp), km/s. P-wave velocity is higher for rocks with a higher UCS. The velocity is higher because the UCS is higher.

2.3.4 Blast design parameters

The burden, spacing, hole diameter, stemming length, and initiation timing are all important blast design parameters that affect fragmentation size distribution. The burden is the distance between the centre of one blast hole and the centre of the next blast hole. The spacing is the distance between the centres of adjacent blast holes in the same row. The hole diameter is the diameter of the blast hole. The stemming length is the length of the stemming material that is placed in the blast hole. The initiation timing is the sequence in which the blast holes are detonated.

Burden

The burden is the shortest distance between the hole and the exposed bench face. The burden is one of the most important blast design parameters affecting fragmentation size distribution. It directly affects the confinement of the explosive energy within the rock mass during blasting. The large burden requires increased energy. Increased energy will result in fine fragments (Petropoulos, 2015).

Explosive type and quantity

An explosive is a chemical compound or mixture of chemicals ignited by impact, shock or heat or a combination of the presence of these ignition initiators. When an explosive ignites, it decomposes rapidly in detonation and releases heat and large quantities of high-pressure gases that expand. The effects of the energy released by detonation produce rock fragmentation; rock displacement; ground vibration; and air blast (Service, 1999).

The type and quantity of explosive used in the blast also affect fragmentation size distribution. In general, more powerful explosives will produce smaller fragments, while less powerful explosives will produce larger fragments. This is because more powerful explosives release more energy, which results in more fragmentation. In addition, some explosives like water gel explosives work well in water conditions (Service, 1999).

An accepted theory of explosives is that the detonation of the explosives charge causes a high-velocity shock wave and a huge release of gas pressure. The shock wave cracks and crushes the rock near the explosives and creates visible cracks around the rock. The gases expand and fill the cracks until the gas pressure is worn to expand the cracks further or are vented from the rock (Service, 1999).

Explosives are to be selected based on the adaptation of the actual rock conditions before the blast. Explosive choice influences fragmentation due to the explosive properties. These properties are as follows:

- Energy content.
- Gas volume.
- Detonation velocity.
- Density.

To have useful energy released by the explosive is dependent on factors such as:

- Properties of the explosive.
- Confinement of the explosive.
- Hole diameter.
- Degree of coupling.

The reasons for choosing an explosive and range from specifications of the product are dependent on price, availability, and reliability. The following are the properties of explosives.

- Velocity is for good fragmentation; the actual results are when the detonation velocity is at or near the sonic velocity of the rock. If mass movement is a priority or large size rock sizes, then detonation velocity should be notably below the rock's sonic velocity.
- Sensitivity is for when using charges in small diameter boreholes, sensitivity products such as cap-sensitive emulsions or water gels are needed. The smaller the holes, the more sensitive the hole.
- Gas or Pressure Release is the amount of gas pressure released when the blasting agent or explosive detonates. The more the gas released, the more heave or displacement that is possible.

Drilling accuracy

The accuracy of the drilling also affects fragmentation size distribution. Drill accuracy is the degree to which the blast holes are drilled in the correct location, direction, and depth. Drill accuracy is important for fragmentation size distribution because it affects how the blast wave propagates through the rock. If the holes are not drilled accurately, the blast wave will not be able to propagate as effectively through the rock, resulting in a more heterogeneous fragmentation size distribution (Sharma *et al*., 2019).

Several factors can affect drill accuracy, including the type of drill rig used, the skill of the driller, and the rock conditions. In general, more accurate drilling results in a more uniform fragmentation size distribution. Some of the benefits of drilling blast holes accurately :

- Improved and consistent fragmentation size distribution size, and better drill accuracy result in a more uniform fragmentation size distribution.
- Reduced secondary blasting and better drill accuracy can reduce the need for secondary blasting, which can save time and money.
- Improved safety and better drill accuracy can reduce the risk of accidents, such as fly-rock and misfires.

Achieving drill accuracy involves several factors, including the selection of appropriate drilling equipment, proper training of drill operators, and effective drilling practices. Modern drilling technologies, such as GPS-guided systems and automated drilling rigs, can enhance drill accuracy by ensuring precise hole placement and alignment. Regular monitoring and quality control measures should be implemented to verify drill accuracy and address any deviations promptly (Sharma *et al*., 2019).

Stemming length

The stemming length is the length of the stemming material that is placed in the blast hole such as sand, gravel, or other inert material. Stemming retains the explosive gases within the blast hole for as long as possible to ensure the energy is not lost through the collar of the blast hole (Sharma *et al*., 2019). The length of stemming is dependent on the application. The shorter stemming length may result in venting (loss of energy) resulting in coarse fragments while a long stemming length may contain the gases but may result in capping. The stemming length affects fragmentation size distribution by preventing the blast wave from propagating too far into the rock. A shorter stemming length will result in smaller fragments, while a longer stemming length will result in larger fragments. This is because a shorter stemming length will prevent the blast wave from spreading out as much, resulting in more fragmentation (Sharma *et al*., 2019).

Delay timing

The delay timing is the sequence in which the blast holes are detonated. The delay timing affects fragmentation size distribution by influencing how the blast wave propagates through the rock. A well-designed delay timing will result in a more uniform fragmentation size distribution, while a poorly designed delay timing will result in a more heterogeneous fragmentation size distribution (Sharma *et al*., 2019).

Understanding and optimising these factors in blast design and execution can help control and tailor fragmentation size distribution to meet specific requirements. By adjusting rock properties, explosive properties, blast design parameters, considering geological characteristics, and managing energy distribution, mining operations can achieve the desired fragmentation outcomes. This, in turn, improves the efficiency of downstream processes, reduces costs associated with handling and processing of fragmented material, and enhances safety by controlling fly rock and ground vibration (Sharma *et al*., 2019).

The significance and interplay of these factors may vary depending on the specific mining operation, rock types, and site conditions. Conducting comprehensive site-specific studies and consulting with blasting experts is crucial for understanding the specific impact of these factors on fragmentation size distribution in each context.

2.4 Prediction of Fragmentation Models

The prediction of fragmentation from blasting operations plays a crucial role in various industries, including mining, construction, and quarrying (Singh, 2013). Accurate fragmentation prediction models are essential for optimising blasting parameters, improving operational efficiency, and minimizing downstream processing costs. Over the years, researchers and practitioners have developed several models and formulas to estimate fragmentation size distribution based on various blasting parameters (Dindarloo and Ataei, 2020).

One widely used model for fragmentation prediction is the Kuz-Ram model, proposed by Kuznetsov and Ramazanov in the 1960s (Kuznetsov and Ramazanov, 1965). The Kuz-Ram model utilizes blast design parameters such as blast hole diameter, burden (distance between blast holes), spacing (distance between rows), rock properties, and explosive properties to estimate the median fragment size. This model assumes a power-law relationship between the median fragment size and the blast design parameters (Jimeno *et al*., 2020).

Another commonly used fragmentation prediction model is the Modified Kuz-Ram model, which was introduced by Cunningham in 1983. The Modified Kuz-Ram model extends the original model by incorporating additional variables such as explosive energy, rock density, and rock strength. This model provides a more comprehensive prediction of fragmentation size distribution compared to the original Kuz-Ram model.

In recent years, there has been a growing interest in using advanced computational techniques, such as Artificial Neural Networks (ANNs) and machine learning algorithms, for fragmentation prediction. These models leverage large datasets containing blasting and fragmentation data to develop more accurate prediction models (Dindarloo and Ataei, 2020). ANNs can capture complex nonlinear relationships between blasting parameters and fragmentation outcomes, leading to improved prediction accuracy.

Formulae used in fragmentation prediction models typically involve mathematical expressions that relate blasting parameters to fragmentation size distribution. These formulae may include empirical constants and coefficients that are derived from experimental data and calibration procedures. The accuracy of these formulae depends on the quality and representativeness of the underlying dataset used for model development (Dindarloo and Ataei, 2020).

For this research study, the researcher reviewed and compared various fragmentation prediction models used in blasting operations. The underlying principles, assumptions, and mathematical formulae used in these models were examined. Additionally, we discuss the advantages and limitations of different modelling approaches, including empirical models like the Kuz-Ram and Modified Kuz-Ram models, as well as data-driven techniques such as ANNs. By understanding the strengths and weaknesses of different models, practitioners can make informed decisions regarding the selection and application of fragmentation prediction models in their specific blasting operations (Dindarloo and Ataei, 2020).

2.4.1 Artificial neural-based

Artificial Neural Network(ANN) based models are a class of computational models inspired by the structure and functioning of biological neural networks. These models consist of interconnected nodes, called neurons, which are organized into layers. ANN models have gained significant popularity in the field of fragmentation prediction due to their ability to capture complex relationships between blasting parameters and fragmentation outcomes (Dindarloo and Ataei, 2020).

The basic architecture of an ANN consists of an input layer, one or more hidden layers, and an output layer. Each neuron in a layer is connected to neurons in the adjacent layers through weighted connections. The values of these weights are adjusted during a training process, where the model learns from the input-output patterns in the training dataset. The training process involves the forward propagation of inputs through the network, computing the outputs, and comparing them to the desired outputs. The error between the predicted and desired outputs is used to update the weights, iteratively improving the model's performance (Dindarloo and Ataei, 2020).

Examples of ANN-based fragmentation prediction models include feedforward neural networks, radial basis function networks, and recurrent neural networks. These models have been applied to various blasting scenarios to predict fragmentation size distribution. For instance, feedforward neural networks have been used to predict fragmentation in surface mining operations based on parameters such as blast hole diameter, spacing, burden, and rock properties (Dindarloo and Ataei, 2020).

Monjezi *et al*. (2010) used fuzzy logic to study and forecast rock fragmentation caused by blasting at the Gol-E-Gohar Iron Ore Mine. The model makes use of a fuzzy inference method and regression analysis

(FIS). The fuzzy estimator was found to perform noticeably better than the statistical approach. The flaw in the fuzzy logic approach is that it causes numerous, time-consuming experiments to apply fuzzy logic on standard hardware. Fuzzy logic is less effective at recognizing patterns than neural networks in machine learning, which receives less attention in data science. (Entemann, 2000).

Oraee and Asi (2006) created an ANN model to forecast various particle diameters at the Gol-e-Gohar Iron Ore Mine in Iran. Input variables for the ANN included the type of boulder, specific gravity, spacing, stemming, explosive length, weight, and type, detonation, water depth in blast holes, and prescribed factors. A single input layer, two hidden layers, and an output layer were used to create the ANN in MATLAB. The network used 15 records for assessment and 60 records for training. According to the sensitivity analysis, the spacing and specific charge are the most crucial factors. Using gold-size software, the results of the Kuz-Ram model picture analysis were compared to the output of the ANN. When the forecasts of ANN and the Kuz-Ram model were evaluated, it was evident that ANN gave superior results with higher precision. The Kuz-Ram model is alleged to be unreliable because it does not adequately assess the impact of rock mass requirements (Oraee and Asi 2006).

Moghadam et *al*. (2006) developed an ANN model to predict the spread of muck-pile fragmentation based on blast patterns produced using radial basis function neural networks. The results were shown as equivalent screen sizes that pass 80% of the blasted materials, equivalent screen sizes that pass 63.2% of the blasted materials, and an index of uniformity. As input parameters, they employed the diameter of the blast hole, the number of holes, the burden, the spacing, the depth of the hole stemming, the number of rows, the detonation velocity, the charge per delay, the powder factor, and the blastability index.

Monjezi *et al*. (2010) developed an Artificial Neural Network to predict fragmentation in the Iranian Sarcheshmeh Copper Ore mine. The burden-to-spacing ratio, hole diameter, stemming, total charge per delay, powder factor, number of rows, maximum holes per delay, point load index, and the delay between the rows were some of the input variables used to determine the aim variable, which was fragmentation size. 132 datasets were used to train the model using the back-propagation method. It was found that a four-layer ANN works best with architecture 9-8-5-1. To validate the predictions of the ANN, a model for multivariate regression analysis was also developed. Root Mean Square (RMSE), Mean Absolute Error (MAE), and Mean Relative Error were used to evaluate the models (Er). The models' comparison revealed that the ANN model performed better than the regression model (Monjezi *et al*., 2010). According to the study, the elements with the highest impacts on fragmentation were the burden-to-spacing ratio, powder factor, total charge-per-delay, and delay between the rows. Factors like stemming, number of holes per delay, number of rows, hole width, and point load index have less of an impact on the output.

Kulatilake *et al*. (2012) used neural networks and multivariate regression to calculate the mean particle size prediction in rock blast fragmentation. They found that the trained neural network models and multivariate regression models' forecasting capabilities were superior to those of the most popular fragmentation prediction model currently in use. The use of several groupings of blast data was one of the created model's major elements. It was shown that the improvements to the multivariate regression analysis and neural network models are suitable for usage in mines (Kulatilake *et al*., 2012).

An Artificial Neural Network was also created by Bahrami *et al*. (2010) to forecast fragmentation in the Sangan Iron Ore mine. The goal variable was the percentage of fragmentation, and the input variables were the hole diameter, average hole depth, burden, spacing, powder factor, blast stability index, particular drilling, stemming length, and charge per delay. The back-propagation method was used to train the model using two hundred and twenty datasets. They concluded that an effective method to forecast rock fragmentation appears to be an Artificial Neural Network with high correlation capability. The results of the model were compared with the results of the regression model. For the regression method, *R*2 and RMSE were calculated, and the following values were obtained 0.701 and 1.958, respectively.

The primary reason why the statistical method is less effective could be due to the linearity hypothesis that was used. To identify the elements that influence rock fragmentation that are most sensitive, they used the cosine amplitude method (CAM). According to the study's findings, the factors that affected rock fragmentation the most effectively were the blast stability index, charge per delay, burden, and powder factor. The least efficient fragmentation parameters were average hole depth, specific drilling, spacing, stemming length, and hole diameter (Bahrami *et al*., 2010).

Kulatilake *et al*. (2012) looked at the blast database that was produced in one of their tests. In situ, block size, elastic modulus, explosive characteristics, and explosion design parameters are all included in the database. Based on the stiffness of the intact rock, a rigorous study split the blast data into two comparable groups. The group structures were supported by the discriminant analysis. The solitary hidden layer of the back propagation neural network model was trained using a subset of this blast data. The objective was to predict the mean particle size of the explosive fragmentation for each of the determined similarity groupings. They found that seven main factors affect the average particle size. For each of the layers, the right number of units for the concealed layer should be. To determine the ideal number of units for the concealed layer for each of the identified similarity groups, a thorough analysis was conducted. The learned neural network models were validated using the blast data that was not used for training (Kulatilake *et al*., 2012).

Multivariate regression models were created to forecast mean particle size for the same two identity groups. Comparing forecasts with measured mean particle size values and predictions based on one of the most widely used fragmentation prediction models allowed researchers to assess the performance of the developed neural network models and multivariate regression models (Silva *et al*., 2017). The trained neural network models and multivariate regression models' predictive power was found to be robust and superior to that of the currently most widely used fragmentation prediction model. One of the most crucial features of the developed models is the use of various groups of blast data (Kulatilake *et al*., 2012).

Shi *et al*. (2013) used the input variables rock joints protodyakonov's coefficient, burden, the time interval of a millisecond, detonation velocity, explosive specific charge, stemming length, and hole-space to develop a back-propagation neural network (BPNN). This was improved by a genetic algorithm (GA-BP) to predict mean particle size (X_{50}). Shi *et al*. (2013) concluded that it is possible to forecast the distribution of particle size in bench blasting using an Artificial Neural Network (ANN). After using the real data for training and testing, the Multivariate Regression Analysis (MVRA) were expected to have mean relative errors (RE) of 11.15% and 7.38%, respectively, while GA-BP had a RE of 3.09%.

ANN-based models assume that there exist complex, nonlinear relationships between blasting parameters and fragmentation outcomes. These relationships may not be explicitly captured by traditional empirical models. By utilising a large dataset containing historical blasting and fragmentation data, ANNs can learn and generalise these relationships, enabling accurate prediction of fragmentation size distribution (Shi *et al*., 2013).

Equations used in ANN-based models are derived from the mathematical operations performed by neurons within the network. These equations involve the computation of weighted sums of inputs, activation functions to introduce nonlinearity and adjustment of weights through backpropagation algorithms. The specific equations vary depending on the architecture and type of neural network used (Shi *et al*., 2013).

It is important to note that ANN-based models require a representative and diverse training dataset to ensure accurate predictions. The quality and quantity of the dataset influence the model's ability to capture the underlying relationships effectively. Additionally, ANN models may suffer from overfitting, where the model becomes too specific to the training data and underperforms on new, unseen data. Regularisation techniques and validation procedures are commonly employed to address overfitting and ensure model generalisation (Shi *et al*., 2013).

In summary, ANN-based models for fragmentation prediction are based on the principles of artificial neural networks, which emulate the structure and functioning of biological neural networks. These models capture complex, nonlinear relationships between blasting parameters and fragmentation outcomes and have demonstrated success in accurately predicting fragmentation size distribution in various blasting operations (Shi *et al*., 2013).

2.4.2 Mechanistic

A mechanistic model for fragmentation prediction is a model that is based on the physical and mechanical properties of the rock material undergoing blasting (Chung and Katsabanis, 2000). These models aim to simulate the fragmentation process by considering the behaviour of individual rock particles during the blasting operation (Ouchterlony *et al*., 2018). They are often derived from fundamental principles of mechanics, such as energy transfer and rock breakage mechanisms.

One example of a mechanistic fragmentation model is the Discrete Element Method (DEM) (Schunnesson *et al*., 2020). DEM simulates the behaviour of a collection of discrete particles, representing the rock material, subjected to external forces such as blasting (Chen and Zhang, 2021). It accounts for particle-particle interactions, as well as the response of particles to applied loads, leading to the prediction of the resulting fragment size distribution.

Another commonly used mechanistic model is the Bonded Particle Model (BPM) (Potyondy and Cundall, 2004). BPM considers the rock material as an assembly of bonded particles and simulates the breakage process by considering the fracture mechanics and strength properties of individual bonds. This model provides insights into the mechanisms of crack propagation and fragmentation based on rock material properties.

Mechanistic models assume that the behaviour of rock particles can be described using physical principles and mechanical properties of the rock material. These models consider parameters such as rock strength, elasticity, fracture toughness, and energy transfer during blasting (Singh, 2007).

Equations used in mechanistic models are derived from fundamental physical principles and rock mechanics theories. These equations describe the behaviour of individual particles or bonds, considering forces, stresses, and deformations. The specific equations depend on the underlying model and its assumptions.

Mechanistic models have been used in various applications, including mining, quarrying, and construction. They are employed to optimise blasting parameters, assess the impact of different explosive properties, evaluate the effects of rock properties on fragmentation, and design blasting operations to achieve desired fragmentation outcomes.

2.4.3 Numerical models

A numerical model for fragmentation prediction is a computational model that utilizes numerical methods to simulate the fragmentation process in blasting operations (Shi *et al*., 2017). These models employ mathematical equations and algorithms to simulate the behaviour of rock material and predict the resulting fragment size distribution.

One example of a numerical fragmentation model is the Finite Element Method (FEM) (Lu and Wang, 2020). FEM divides the rock material into small elements and approximates their behaviour based on numerical discretization techniques. It considers factors such as stress distribution, strain energy, and fracture mechanics to simulate the rock breakage process during blasting.

Another commonly used numerical model is the Smoothed Particle Hydrodynamics (SPH) method (Randles and Libersky, 1996). SPH treats the rock material as a continuous medium and represents it using particles. It uses fluid dynamics principles to simulate the deformation and fragmentation of the rock material under the influence of blast-induced forces.

Numerical models are based on fundamental principles of physics and mechanics, such as the conservation of mass, momentum, and energy. They consider the properties of the rock material, including elasticity, strength, and fracture toughness, as well as the characteristics of the explosive and the blasting process.

Equations used in numerical models are derived from the governing equations of physics, such as the equations of motion, stress-strain relationships, and fracture mechanics theories (Munjiza, 2004). These equations are solved using numerical methods, such as finite element analysis or particle-based methods like SPH, to approximate the behaviour of the rock material during the fragmentation process.

Assumptions in numerical models may include the homogeneity and isotropy of the rock material, the neglect of thermal effects, and simplifications in the modeling of particle interactions or fracture propagation. These assumptions are made to simplify the computational complexity and allow for feasible simulations.

Numerical models are used to optimise blasting designs, evaluate the effects of different parameters on fragmentation, and assess the structural response to blasting-induced vibrations (Latham and Ouchterlony, 2019). They provide insights into the detailed behaviour of the rock material during blasting and aid in the design of more efficient and safer blasting operations.

2.4.4 Empirical models

An empirical model for fragmentation prediction is a model that is derived from observed data and statistical analysis (Kou and Rustan 1993). These models establish relationships between blasting parameters and fragmentation outcomes based on empirical observations. Empirical models are widely used due to their simplicity and practicality in estimating fragmentation size distribution (Adebola *et al*., 2016).

Empirical models assume that there exist empirical relationships between blasting parameters and fragmentation outcomes. These relationships are established through statistical analysis of field data, experimental data, or a combination of both. Empirical models do not consider the underlying physical mechanisms governing fragmentation but rely on observed patterns and correlations (Adebola *et al*., 2016).

Equations used in empirical models are derived from regression analysis or curve-fitting techniques applied to the available data. These equations express the relationship between the blasting parameters and the predicted fragmentation size distribution. The specific form of the equation depends on the assumptions and functional form chosen for the model (Adebola *et al*., 2016).

Assumptions in empirical models may include the representativeness and validity of the dataset used for model development, as well as assumptions about the functional form of the relationship between the blasting parameters and fragmentation outcomes. These assumptions can influence the accuracy and applicability of the model in different blasting scenarios (Adebola *et al*., 2016).

The modified Kuz-Ram model, which was introduced in 2005 (Ouchterlony and Sanchidrián, 2019), resembles the preceding Kuz-Ram model. However, the difference is the modification of the Kuznetsov equation by applying a 0.073 multiplier to help the model perform better in predicting the mean fragmentation size (Gheibie *et al.,* 2009). The Kuz-Ram uniformity index is also substituted by an upgraded uniformity index.

Kuznetsov-Rumyantsev-Ouchterlony

The Kuznetsov-Rumyantsev-Ouchterlony (KCO) model is an empirical fragmentation model used for predicting fragmentation size distribution in blasting operations. This model aims to estimate the median fragment size based on various blast design parameters and rock properties (Ouchterlony, 1989).

The KCO model is based on the empirical observation of relationships between blasting parameters and fragmentation outcomes. It assumes a power-law relationship between the median fragment size (D_{50}) and the blast design parameters, such as blast hole diameter (D_n), spacing (S_n), burden-to-charge ratio (BWi), and rock properties. The equation of the KCO model can be represented as:

$$D_{50} = K(D_n)^a \times (S_n)^b \times (BWi)^c \quad 2.6$$

where K, a, b, and c are empirical constants derived from statistical analysis of field data.

Assumptions in the KCO model include the power-law relationship between the blasting parameters and fragmentation size distribution, as well as the representativeness and validity of the dataset used for model calibration. The model assumes that the fragmentation outcomes can be approximated using these empirical relationships without explicitly considering the underlying physical mechanisms governing fragmentation.

The KCO model is commonly used in blasting operations to estimate fragmentation size distribution and guide blast design. It provides a practical and straightforward approach to predict fragmentation outcomes based on easily measurable blasting parameters and rock properties (Ouchterlony, 1989)

Swebrec

The Swebrec fragmentation model is widely utilised in the mining industry to estimate fragmentation size distribution. It is based on the concept of energy distribution and the breakage behaviour of the rock material during blasting (Borisson, 2003). The model considers the blast design parameters, such as burden, spacing, and explosive energy, as well as the rock properties.

The Swebrec model assumes that the energy distribution in the blasting process is logarithmically normal. It uses the concept of the energy-size distribution to estimate the fragmentation characteristics. The model utilises an equation to calculate the median fragment size. This is shown in Equation 2.7.

$$P_{Swe}\ (x) = 1/\ \{1 + [\frac{ln(x_{max}\ /x)}{ln(x_{max}/x_{50}}].^{b}\ \} \qquad 2.7$$

$$P_{Swe}\ (x)\ is\ valid\ when \quad x < 0 < x_{max}$$

Where:

$P(x)$ is the cumulative small size.

x_{max} is the maximum size of ore particles, (mm).

x is the normal size (mm).

x_{50} is a sieve size that retains 50% of the material, (mm).

This is a three-parameter size distribution model, which is different from the most popular models in ore processing. The variables are b, x_{max}, and x_{50}. The inflection point moves towards x = $x_{max}$when b is equal to 1, and towards x = x_{50} when b is equal to 2. It has the shape parameter b, sometimes known as the undulation exponent or occasionally the Natural Breakage Characters, along with the two size parameters x_{50} and x_{max}. (NBC) exponent (Ouchterlony, 2009). In this sense , $P_{Swe}(x)$ is comparable with rescaled or transformed RR functions.

In addition to understanding more about the Swebrec models, Moser (2005) investigated fine fragmentation studies. Moser (2005) provided information on the European Union (EU) initiative "Less Fines," which involved blasting and sieving numerous rock and mortar cylinders. Similar research was conducted by Less Fines' collaborator Swedish Rock

Research (SveBeFo) and the Montanuniversitaet Leoben. The Swebrec function was found in the fragmentation studies (Ouchterlony, 2003) and (Ouchterlony and Sanchidrian, 2009). The sieving curves deviated from the Rossin Rammler RR are defined in two significant ways: (i) there is naturally the largest boulder size x_{max} and (ii) the fines tail is not linear in a $log_{10}P(x)$ vs. $log_{10}x$ diagram. Hardly any wide-range sieving data for blasted and crushed rock looks like RR, not even Kuz-Rams data (Kuznetsov, 1973).

SweDeFo

The SweDeFo (Swedish Defense Research Agency) SweDeFo empirical models are widely used for fragmentation prediction in blasting operations. These models were developed based on extensive field testing and data collection, specifically for Swedish rock types (Persson, 2002). SweDeFo models provide practical tools to estimate the fragmentation size distribution and optimise blasting operations.

The SweDeFo models are based on the statistical analysis of large datasets, encompassing various blast design parameters, rock properties, and explosive properties. These models aim to capture the empirical relationships between these parameters and the resulting fragmentation size distribution.

SveDeFo's fragmentation equations were shown in Equations 2.8 and 2.9 (Hjelmberg, 1983).

$$x_{50} = 0.143 \times f\left(L_{\frac{t_0 t}{H}}\right) \times \left\{B^2 \sqrt{\frac{1.25}{{}^{S}/_{B}}}\right\}^{0.29} \left(\frac{C_{rock}}{SD_r q}\right)^{1.35}$$

2.8

$$P_x = 1 - 2^{-\left({}^{x}/_{x_{50}}\right)^{1.35}}$$

2.9

Where:

L is the total charge length, (m).

f is1+4.67 (1- L_{tot}/H).

S is spacing, (m).

SDr is the weight strength of the explosive.

H is hole depth, (m).

B is burden, (m).

C_{rock} is rock constant.

Q is the specific charge, (kg/m^3).

The SweDeFo models are employed to estimate fragmentation size distribution, optimise blasting parameters, and assess the impact of different factors on fragmentation outcomes. These models provide practical and reliable tools for the Swedish mining and construction industry.

2.4.5 Empirical computer based models

Empirical computer-based models are software programs and commercial tools that have been developed to predict fragmentation distribution size based on empirical models such as the Kuz-Ram model , SveDeFo, Swebrec to assist in fragmentation prediction and blast design optimisation. They provide a practical and efficient approach to predict fragmentation outcomes without the need for complex physical or numerical simulations. JKSimblast, fragmentation analyst, BlastLogic software, o-pit blast software and Blasting software.

Below are some of the software packages used in the industry to predict fragmentation.

The JKSimBlast is a software package developed by JKTech. It incorporates the Kuz-Ram model as one of the fragmentation prediction models (Thornton *et al.*, 2001).

- Fragmentation Analyst: A software tool developed by Split Engineering, which utilizes the Kuz-Ram model to estimate fragmentation size distribution and provides visualization and analysis of fragmentation data (Higgins *et al*., 1999).
- BlastLogic software: A software tool developed by Maptek company, which utilizes the Kuz-Ram model and Swebrec to estimate fragmentation size distribution and provides visualization and analysis of fragmentation data (Maptek, 2021). It further provides vibration and overpressure analysis. Figure 2.6 shows the BlastLogic software workflow.

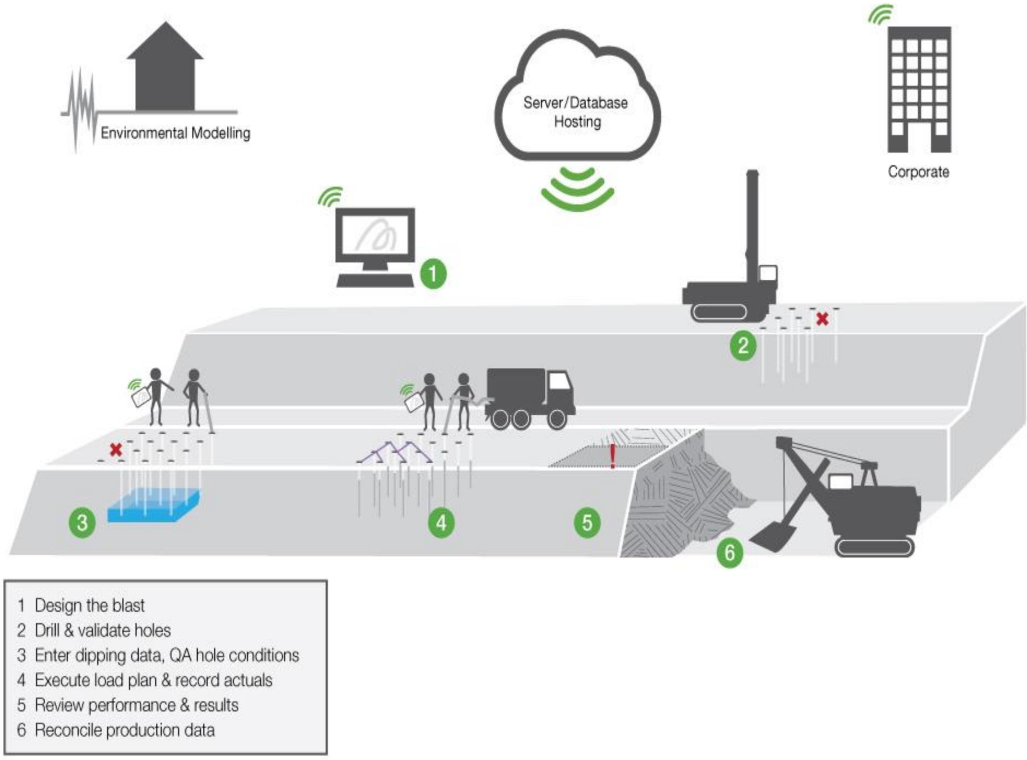

Figure 2.6 BlastLogic software workflow. Source: (Maptek, 2021)

All the stages in the workflow are shown a centralised record of all operational blast data. The server or database hosting is very important as it allows live data to be available all the time dependent on the network connectivity. Additionally, the BL interfaces with the drill navigation system. The blast performance is achieved by fusing distinct data sets associated with mine planning, drill guidance, field survey, load design parameters and post-blast evaluation to create a blast design (Maptek, 2021).

2.5 Comparison of Fragmentation Models

The knowledge attained from fragmentation models, including empirical, mechanistic, Artificial Neural Network (ANN), and numerical models, provides valuable insights and guidance in the field of blasting engineering. These models offer different perspectives and approaches to predict fragmentation outcomes based on various factors and parameters.

A discussion on what can be deduced from these models and how they can be improved:

Empirical models provide a practical and simple approach to estimating fragmentation size distribution based on observed relationships between blasting parameters and fragmentation outcomes. They are often preferred in situations where limited data or resources are available. From empirical models, one can deduce the empirical relationships between blasting parameters and fragmentation outcomes specific to the dataset or context. These models offer quick estimations but may have limitations in generalizability due to the specific dataset used for model development. To improve empirical models, one can expand the dataset by incorporating more diverse and representative data from different blasting scenarios or consider incorporating additional variables to enhance prediction accuracy.

Mechanistic models are based on the physical and mechanical properties of rock materials and aim to simulate the fragmentation process. They provide insights into the underlying mechanisms of rock breakage during blasting. From mechanistic models, one can deduce the behaviour of individual rock particles, crack propagation, and energy transfer during blasting. These models can offer a more detailed understanding of the fragmentation process but may require more computational resources and specific input parameters. Improving mechanistic models involves refining the representation of rock material properties, considering more complex fracture mechanics, and validating the models against experimental data.

ANN models leverage advanced computational techniques to capture complex relationships between blasting parameters and fragmentation outcomes. They can handle nonlinearities and interactions that may be challenging for other models (Wang *et al*., 2021). From ANN models, one can deduce the nonlinear patterns and correlations between the input parameters and fragmentation size distribution. ANN models can be improved by incorporating more comprehensive and diverse datasets, optimising the network architecture and parameters, and ensuring robust validation and testing procedures (Dimitraki *et al.,* 2018).

Numerical models, such as finite element analysis and smoothed particle hydrodynamics, simulate the behaviour of rock material during blasting using numerical methods (Zhou *et al*., 2023). They can provide detailed predictions of stress distribution, deformation, and fragmentation. From numerical models, one can deduce the complex interactions between particles, stress distribution, and energy transfer. Improving numerical models involves refining the material models, accounting for more realistic boundary conditions, and increasing the computational efficiency for larger-scale simulations.

Each model has its strengths and limitations, and the choice of model depends on the specific needs and available resources in the blasting operation. A comprehensive approach can involve integrating different models or combining the strengths of different approaches to improve accuracy and applicability.

2.6 Rock Fragmentation Measurement

Rock fragmentation measurement is the process of quantifying and assessing the size distribution and characteristics of rock fragments resulting from blasting or other mechanical fragmentation methods. It provides crucial information for optimising blasting operations, evaluating the efficiency of rock breakage, and determining downstream processing requirements in various industries such as mining, construction, and quarrying.

The concept of rock fragmentation measurement involves capturing data on the size distribution, shape, and other relevant properties of the fragmented rock material. This information helps in understanding the efficiency and effectiveness of blasting operations and allows for adjustments and improvements in blast design parameters. Field observations, sieving and digital image processing are methods commonly used for rock fragmentation measurement.

One of the most common rock fragmentation measurements is Split Desktop. Split-Desktop program is a resource used in image processing to calculate the size distribution of rock fragments through digital image analysis in grayscale. Digital images can be acquired using digital camera or cell phone (Souza *et al*., 2018). After image acquisition, analysis of fragmentation from the blasting is conducted in five stages: opening of the images by the program; delineation of images; manual delineation edition to minimise errors; determination of images scale; analysis of the particle size of each image and blasting (Souza *et al*., 2018). The acquisition and scheduling of the images were obtained with the aid of two spherical objects that were positioned apart in the lower and upper parts of the image. So that their diameters were perpendicular to the optical axis of the image for it did not differ from the real size (Souza *et al*., 2018).

Significant Role in Fragmentation Measurement:

- Accurate Size Distribution Analysis: Split Desktop plays a significant role in accurately determining the size distribution of rock fragments. By delineating individual fragments and providing statistical data, it allows for a precise assessment of the range of fragment sizes present in the muckpile.

Souza *et al*. (2018) demonstrated the accuracy of Split Desktop in size distribution analysis, highlighting its capability to capture variations in fragment sizes with high precision.

- Efficient Shape Analysis: The software's tools enable efficient shape analysis of rock fragments, including metrics such as aspect ratio, roundness, and angularity. This information is crucial for understanding the geometric characteristics of the fragments.

The study by Souza *et al*. (2018) showed the effectiveness of Split Desktop in providing detailed insights into the shape attributes of rock fragments, aiding in the optimization of blasting practices.

- Quick and Repeatable Results: Split Desktop offers a user-friendly interface and efficient workflow, allowing for quick and repeatable fragmentation analysis. This aspect is crucial for timely decision-making in mining operations.

Research by Souza *et al*. (2018) emphasised the speed and reliability of Split Desktop, highlighting its role in delivering consistent results for real-time decision support in the mining industry.

- Integration with Blasting Optimisation: The software's capabilities go beyond mere analysis, contributing to the integration of fragmentation data with blasting optimisation strategies. This integration facilitates a continuous improvement loop in blasting practices.

Souza *et al.* (2018) demonstrated how the integration of Split Desktop results with blasting optimization models led to improved fragmentation outcomes and overall operational efficiency.

Split Desktop emerges as a powerful and versatile tool for rock fragmentation measurement in mining operations compared to other fragmentation software. Its ability to provide accurate size distribution and shape analysis, coupled with its efficiency and integration capabilities, positions it as a significant asset in optimizing blasting practices and enhancing overall operational efficiency. This allows field observations to visually assess the fragmentation distribution.

2.7 Field Observations

Field observations in the context of rock fragmentation refer to the process of visually assessing and recording the fragmentation outcomes resulting from blasting or other mechanical fragmentation methods. These observations provide valuable insights into the actual fragmentation characteristics, patterns, and distribution in the field.

During field observations, various aspects of rock fragmentation can be assessed, including fragment size distribution, shape, fines content, oversized material, and the presence of undesirable rock conditions such as overbreak or underbreak. Visual inspections can be supplemented with measurements using simple tools such as tape measures, rulers, or reference objects to estimate fragment sizes or provide scale.

To improve field observations in rock fragmentation, the following aspects can be considered:

- Systematic Data Collection: Implementing a systematic approach to data collection during field observations is essential. This can involve defining specific observation points, ensuring consistent lighting conditions, and establishing standard protocols for recording observations.

- Use of Technology: Utilizing technology can enhance field observations. For instance, digital cameras or mobile devices can be used to capture photographs or videos of the fragmented rock material, providing a visual record for further analysis. This enables detailed documentation and the ability to review and share observations.
- Reference Standards: Having reference standards or objects of known size can assist in estimating fragment sizes during field observations. These standards can be placed next to or within the fragmented material to provide a scale reference for accurate size estimation.
- Field Testing: Conducting field tests using specialized equipment, such as sieves or image analysis tools, can complement visual observations and provide more precise data on fragment size distribution, fines content, and other fragmentation parameters.
- Documentation and Reporting: Thoroughly documenting field observations, including photographs, sketches, and written descriptions, is important for reference and future analysis. Clear and comprehensive reporting of the observations, including any notable findings or issues, facilitates effective communication and subsequent decision-making (Harris, 1968).

Regular training and experience in field observations can also improve the accuracy and reliability of assessments. Collaboration with experts or consulting specialists in rock fragmentation analysis can provide valuable insights and guidance in conducting field observations.

2.8 Digital Image Processing

Digital image processing is a field that focuses on the manipulation, analysis, and interpretation of images using computational algorithms and techniques. It involves transforming digital images acquired from various sources into more useful and meaningful forms. Digital image processing finds applications in diverse fields such as medicine, surveillance, remote sensing, and computer vision (Broadbent and Callcott, 1956).

The concept of digital image processing revolves around the acquisition, enhancement, analysis, and interpretation of digital images. It involves a series of steps, including:

- Image acquisition: Digital images are obtained from various sources such as digital cameras, scanners, or satellite sensors. The images are typically represented as a grid of pixels, where each pixel corresponds to a specific colour or intensity value.
- Image enhancement: Enhancement techniques are applied to improve the quality, clarity, and visibility of the acquired images. These techniques can involve adjusting brightness, contrast, sharpness, noise reduction, or colour correction to enhance specific image characteristics.
- Image analysis: Analysis techniques are employed to extract useful information or features from the images. This can include image segmentation, which divides the image into meaningful regions or objects, or feature extraction, which identifies and quantifies specific patterns, edges, textures, or shapes present in the image.
- Image interpretation: Interpretation techniques are used to analyse and make sense of the extracted information. This can involve object recognition, classification, or decision-making based on the interpreted image features.

Onederra *et al*. 2014 explored the use of image analysis to quantify the fragmentation of muck piles. The majority of the run-of-mine (ROM) fragmentation studies have used two-dimensional (2D) imaging systems based on photography to quantify particle size.

High data density describes the ability to detect small, overlapped particles, the smallest particle size that can be reliably detected, and the resolution of size classes detectable, making it one of the key criteria for particle size measurement (Dehran, 2018). Understanding the expected spatial distance between measured 3D points is crucial, as illustrated by the analysis region in Figure 2.7.

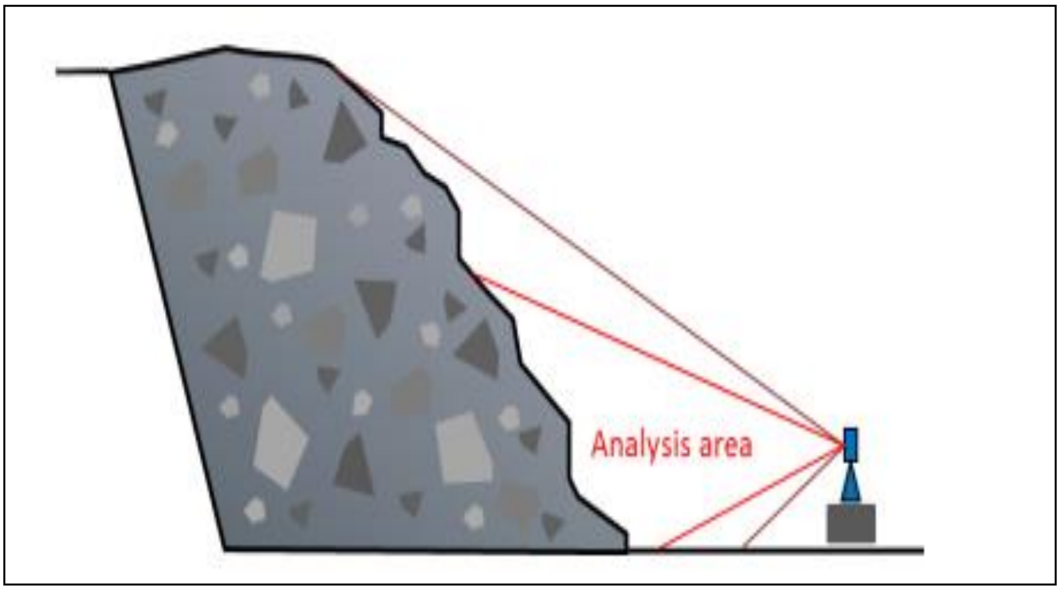

Figure 2.7 Measurement geometry and analysis area. Source: Onederra *et al*., (2014)

The measurement geometry is illustrated in Figure 2.7 as a case study. In this approach, the measured data is further cropped to ±12° in the horizontal plane and -5° to +12° in the vertical plane. There is no special reason for choosing precisely 12° but it was chosen as a balance between a high spatial resolution of 3D points and a sufficiently large field of view of the rock pile (Onederra *et al*., 2014).

Potts and Ouchterlony (2006) voiced strong reservations about 2D imaging when measuring the fragment size distribution in a muckpile or from a belt in an accurate manner. They did this in their evaluation of another commercial photographic-based 2D system. If the lighting circumstances are not too variable and the cover glasses for the camera lenses are kept clean, it could probably identify rough behaviours in fragmentation variations. They also stated that the system was applied incorrectly because of "caused the truncated, bimodal distributions to, misleadingly, show up as unimodal curves." This revealed a significant restriction on the system's capacity to identify variations in the fragment size distribution. In the surface environment used, the variation in lighting conditions can be extreme and their research ensures that 2D photographic imaging can only be highly erroneous without substantial manual particle delineation, which introduces inconsistencies due to human operator error.

Additionally, if a bimodal distribution is present, using a fragmentation assessment method that is unable to identify it will probably prevent its detection. Because of the model's dependability and robustness, disintegration models were chosen. Instead of attempting to depict the real fragmentation in the captured images, this is a type of distribution. There is a chance to create methods that could get around the constraints of current 2D image-based systems thanks to the 3D imaging technology's quick development and increased accessibility. This includes the capability of obtaining data free from the effects of lighting, shadowing, or texture differences, as well as the capacity to autonomously delineate particles without the need for human editing (Potts and Ouchterlony, 2006).

3D data offers a clear indication of size, as shown by Thurley and Kim (2005). Thurley (2014) offers the capability to size these various classes of material in various ways, produce size distributions based on volume information, and categorise delineated regions as overlapped particles, non-overlapped particles, or areas of fines. Few papers have dealt with particle size measurement in a surface environment using 3D imaging (Thurley, 2014).

Noy (2013) discussed the challenges of getting a system to function well in such a setting while demonstrating work on a stereo camera setup attached to a shovel. There was no comparison of the readings to sieving data, and no illustrations of particle delineation were given. They presented research that, without statistical remapping to an anticipated size distribution, determines the size of the non-overlapped particles and the areas of fines. This research is based on Thurley (2014). Additionally, examples of the findings of the particle delineation are provided, and the particle delineation is divided into areas with fines, overlapped rocks, and non-overlapped rocks. The only published algorithms that eliminated the bias were those supplied by Thurley (2014). This resulted from different sizing overlapped particles as if they were smaller non-overlapped particles and detected areas of fines.

Any measurement device that takes a sample or image from the visible surface is subject to additional sources of error. Segregation and grouping error, also referred to as the Brazil-nut effect, is the most important of these (Rosato *et. al*.,1987). When vibrated, a collection of rocks tends to separate into materials of various sizes. Although this is a poor way to describe blasting, it is also illogical to presume that the blast will homogenize the rock pile. Therefore, it is not anticipated that the pile surface at any time will represent the entire pile. Therefore, to collect a representative and statistically significant sample, measurements during different stages of the material extraction have been performed for each blast.

2D image analysis had its disadvantages like the lack of ability to differentiate particles that are beneath the muck pile. The disadvantages of 2D photographic systems are significant and have been noted variously by Thurley and Kim (2005), Thurley (2014) and Noy (2013) include:

- Severe particle delineation errors due to uneven lighting conditions which can be extreme outdoors, excessive shadowing; and/or colour and texture variation in the material.
- No direct measure of scale and perspective distortion.

- Lack of the capability to distinguish between overlapped and non-overlapped particles.
- An inability to automatically detect visible fines realistically.

Improvements in digital image processing can be achieved through various means:

- Algorithmic Advancements: Developing and refining image processing algorithms can enhance the accuracy, speed, and efficiency of image analysis tasks. This includes advancements in noise reduction, edge detection, image registration, segmentation, and pattern recognition algorithms.
- Machine Learning and Deep Learning: Utilizing machine learning and deep learning approaches can improve the performance of image processing tasks. These techniques can automatically learn from large datasets, extract complex patterns, and make predictions or classifications based on learned features.
- Hardware Acceleration: Utilizing specialized hardware, such as graphics processing units (GPUs), can significantly accelerate image processing tasks, allowing for real-time or near real-time analysis of images.
- Integration with Other Technologies: Integrating digital image processing with other technologies, such as artificial intelligence, augmented reality, or virtual reality, can enhance the capabilities and applications of image processing systems.

There are several software programs available for digital image processing, offering a range of functionalities and features. Some popular examples include:

- MATLAB: MATLAB provides a comprehensive set of image-processing functions and tools for various image analysis tasks. It offers a user-friendly environment and allows for the prototyping and development of custom image-processing algorithms.

- Wipfrag image analysis Software allows instant particle size distribution analysis of digital images collected at the muckpile after a blast. It is compatible with drones to generate comprehensive data quickly and safely with precise geographic information.
- Split desktop method of determining fragmentation particle size by Split-Desktop system involves five stages: image scaling, rock fragments segmentation dedicating, issuing permission to edit the rock fragments, analysing the marked pieces, and the final phase is displaying the diagram of size distribution results. It allows the resulting size distributions to be plotted in various forms (linear-linear, log-linear, log-log, and Rosin-Rammler).
- Gold Size is a Windows™ based computer program to estimate the sizes of objects in photographs. Principally its use to date has been in the estimation of blast fragmentation size distributions. Some features, such as fines correction to estimate the amount of material too small to be seen, are specifically tailored to fragmentation analysis. Also, the sizes, by default, are empirically adjusted to match the results obtained when rock fragments are sieved.
- OpenCV: OpenCV (Open-Source Computer Vision Library) is an open-source software library that provides a collection of algorithms and tools for computer vision and image processing tasks. It supports multiple programming languages and platforms.
- ImageJ: ImageJ is a free, open-source image processing software that offers a wide range of features and plugins for image analysis, visualization, and measurement. It has a user-friendly interface and supports various file formats.

Advantages of digital image processing software include:

- Automation: Software enables automated image analysis, reducing manual effort and increasing efficiency.

- Flexibility: Software allows for the development and customization of algorithms to suit specific image processing tasks.
- Speed and Accuracy: Software can process images quickly and provide accurate results, even for large datasets.
- Visualization: Software provides visual representations of images and analysis results, aiding in interpretation and decision-making.

Disadvantages of digital image processing software include:

- Learning Curve: Some software programs may have a steep learning curve, requiring time and effort to master.
- Cost: Certain software programs may come with a cost, especially for commercial or advanced versions.
- Hardware Requirements: Complex image processing tasks may require powerful hardware resources, which can add to the overall cost.

To improve rock fragmentation measurement, the following aspects can be considered:

• Sampling Techniques: Ensuring representative and unbiased sampling is critical to obtaining accurate fragmentation data. Developing standardized protocols for sample collection and randomization techniques can improve the reliability of the measurements.

• Automation and Advanced Technologies: Incorporating automation and advanced technologies, such as machine learning algorithms and computer vision, can enhance the efficiency and accuracy of the measurement process. These technologies can automate data collection, image analysis, and size distribution calculations.

• Integration of Multiple Measurement Methods: Combining different measurement methods, such as sieving, image analysis, and laser scanning, can provide a more comprehensive assessment of rock fragmentation. Integration of multiple methods can help capture a broader range of fragment sizes and improve the accuracy of the measurement.

- Calibration and Validation: Regular calibration and validation of the measurement techniques against known standards or reference samples can help ensure accuracy and reliability. Developing calibration procedures and validation protocols can enhance the quality of fragmentation data.

Rock fragmentation measurement is an ongoing field of research and development, aiming to improve the accuracy, efficiency, and reliability of assessing rock fragment sizes and characteristics. These advancements contribute to optimising blasting operations, downstream processing, and overall operational efficiency.

To improve rock fragmentation measurement, the following aspects can be considered:

- Sampling Techniques: Ensuring representative and unbiased sampling is critical to obtaining accurate fragmentation data. Developing standardized protocols for sample collection and randomization techniques can improve the reliability of the measurements.
- Automation and Advanced Technologies: Incorporating automation and advanced technologies, such as machine learning algorithms and computer vision, can enhance the efficiency and accuracy of the measurement process. These technologies can automate data collection, image analysis, and size distribution calculations.
- Integration of Multiple Measurement Methods: Combining different measurement methods, such as sieving, image analysis, and laser scanning, can provide a more comprehensive assessment of rock

fragmentation. Integration of multiple methods can help capture a broader range of fragment sizes and improve the accuracy of the measurement.

- Calibration and Validation: Regular calibration and validation of the measurement techniques against known standards or reference samples can help ensure accuracy and reliability. Developing calibration procedures and validation protocols can enhance the quality of fragmentation data.

Rock fragmentation measurement is an ongoing field of research and development, aiming to improve the accuracy, efficiency, and reliability of assessing rock fragment sizes and characteristics. These advancements contribute to optimising blasting operations, downstream processing, and overall operational efficiency.

It is important to select the appropriate software based on specific requirements, considering factors such as functionality, ease of use, compatibility, and support (Liu *et al*., 2023).

2.9 Chapter Summary

The chapter discussed the process of rock fragmentation by blasting, which is the first step of ore extraction in mining operations. The chapter further explains the mechanisms of rock fragmentation, such as stress wave propagation, gas pressure expansion, and crack initiation and propagation. The chapter reviews the factors affecting rock fragmentation, such as rock mass properties, blast design parameters, explosive characteristics, and environmental conditions. Different fragmentation models, empirical models, mechanistic models, empirical computer-based models, numerical models, and artificial neural-based models were discussed. Furthermore, the chapter evaluated the advantages and disadvantages of each model. It then described the model into which

BlastLogic software falls. The chapter concluded by reviewing the methods of rock fragmentation measurement and analysis, such as manual sieving, image analysis, laser scanning, and 3D reconstruction. The next chapter discusses the research methodology.

3 RESEARCH METHODOLOGY

3.1 Introduction

Chapter 3 provides a comprehensive description of the research process in investigating fragmentation distribution in surface mines. It emphasizes the use of quantitative research techniques to analyse historical data, focusing on correlations between variables. It also discusses the use of BlastLogic software for blast prediction and concludes with a focus on the validity and reliability of the findings. This chapter lays the groundwork for further analyses and discussions on surface mines' dynamics and efficiency.

3.2 Research Design

The research methodology used is quantitative.

Experimental Studies: Conduct controlled experiments where BlastLogic predictions are compared against actual fragmentation outcomes. Collect quantitative data on fragmentation sizes, distribution, and other relevant parameters.

Statistical Analysis: Use statistical methods such as regression analysis to assess the correlation between BlastLogic predictions and observed fragmentation. This can involve measures like correlation coefficients, absolute error and root mean square error.

3.3 Data Collection

This research study focused on BlastLogic software-licensed surface mines, specifically platinum group metals (PGMs), collieries, and iron ore mining companies in South Africa. The BlastLogic software was utilised as the primary data source due to its widespread availability. The data retrieved from the BlastLogic software encompasses information on drilling, and blasting cycles, ensuring the provision of reliable data for the companies under investigation. The dataset used for this study was obtained from the BlastLogic server database, with explicit permission granted for research purposes. The data included the geometric blast design, explosive data, and rock parameters data in the pit.

Collecting geometric data is integral to the evaluation process as it allows for a comprehensive assessment of how well BlastLogic aligns with the actual physical characteristics of the mining site. This evaluation is crucial for determining the software's reliability, effectiveness, and practical utility in predicting blasting fragmentation distribution in surface mines.

Forty blasts from each of the five surface mines were considered due to the blasting schedules and the blast data available.

The surface mines with data analysed for this study are:

- Mogalakwena Platinum mines (Anglo American Platinum Mine).
- Navigation Colliery and Isibonelo Colliery (Thungela resources).
- Kolomela mine and Sishen mine (Kumba Iron ore).

3.4 Data Analysis

The collection of blast design parameters is initiated to facilitate the prediction of fragmentation through the utilisation of the BlastLogic software. This process serves as a guide in manipulating various blast parameters to achieve the targeted fragmentation size. Once the prediction of a specific distribution is attained, the subsequent step involves the practical implementation of the blast. Post-blast detonation, the researcher proceeds to capture images or photographs of the resultant muckpile as part of the data collection process. Subsequently, relevant software is employed to analyse the resulting fragmentation.

The ensuing phase of the study involves a comparative analysis between the predicted fragmentation, obtained through BlastLogic, and the actual fragmentation distribution derived from the post-blast muckpile images. This comparative assessment serves as a crucial step in determining the accuracy and reliability of BlastLogic's predictions in replicating the actual outcomes of the blasting operation.

3.4.1 Fragmentation prediction

The expected fragmentation distributions from the input blast parameters were obtained from the S-Curve graph on the BlastLogic dashboard. A rock factor is given by the technical person from the mines or can be calculated based on the rock factor parameters (Otterness *et al*., 1991). Users are also able to explicitly specify a value for a rock factor.

The shape of the S-curve graph can be modified by altering correction factors. Timing factors also affect the timing data of curves. Figure 3.1 shows the fragmentation profile modelling done in BlastLogic software.

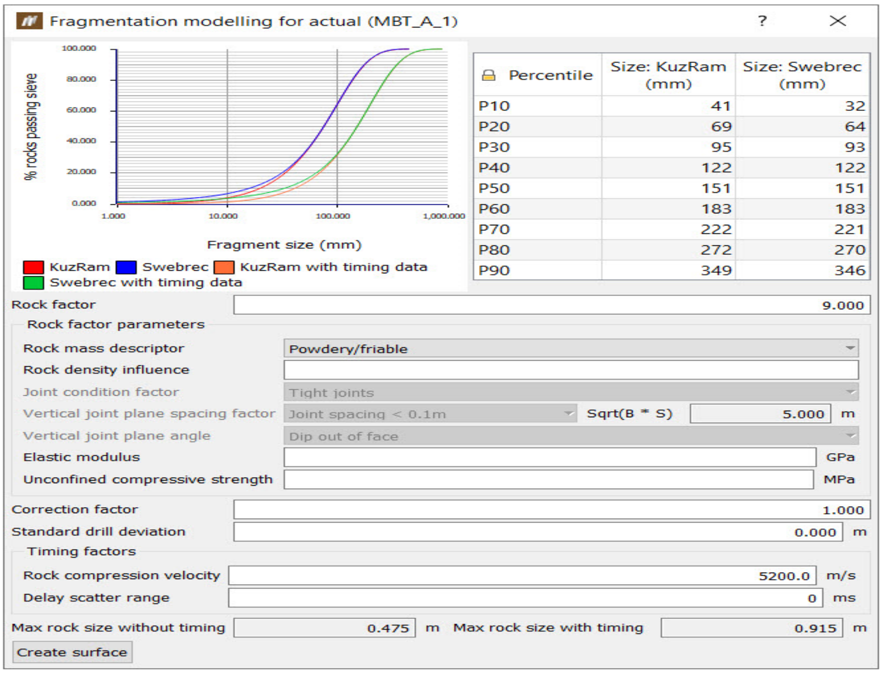

Figure 3.1 Fragmentation modelling in BlastLogic software. Source: Maptek (2021)

Figure 3.1 shows the estimated fragmentation sizes as calculated by the Kuz-ram and Swebrec models. These estimations provide a visual representation of the average fragmentation size distribution and are depicted through fragmentation curves. The utility of this data becomes even more evident when you utilise the "create surface" function, which generates a surface representing these fragmentation characteristics (Maptek, 2021).

3.4.2 Fragmentation analysis after blast

Split-Desktop® fragmentation analysis software was used to analyse the images to quantitatively assess the fragmentation of the blasts at the mine. Ten images were analysed for each blast and the individual image results were combined by the software to represent the fragmentation of the blast. The images were delineated automatically after the scales were set but the results of the auto delineation were not representative of the image such that bigger fragments were split into several small, delineated fragments while the smaller fragments were merged and delineated as one object in the image (Choudhary and Gupta, 2012). To ensure that the fragments were delineated properly, the images were edited manually by drawing borders around each rock fragment to completely delineate it and help the software to effectively estimate and measure the size of rock particles present in the images.

A fine factor of 50% was used for the images because the software cannot delineate finer particles (less than 10mm) hence using a fines factor the finer particle sizes present can be estimated. Voids between fragments were masked while areas of fine fragments whose edges were not clear enough to be delineated were masked as fines. The rest of the Split-Desktop data is presented in the Appendix 8.2.

The scaling objects were selectively excluded so that they are not considered as rock fragments. Figure 3.2 shows a well delineated image in Split-Desktop® from Mogalakwena Platinum mine.

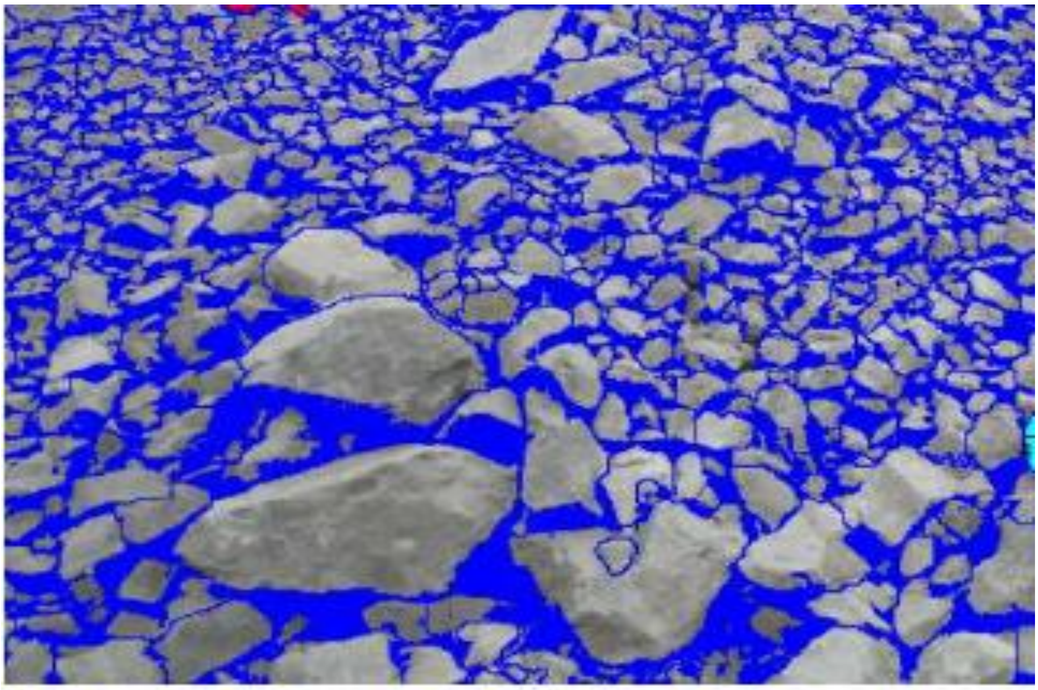

Figure 3.2 Delineated muck pile image for Mogalakwena Platinum mine

Figure 3.2 shows the delineated muck pile image sample for Mogalakwena Platinum mine. After the delineations were compiled and processed, the results were displayed in a table form in Appendices Table 8.3.

3.4.3 Fragmentation estimation

After data collection, the geometric, explosive, and rock parameters were used for the prediction of the fragmentation output for each of the blasts under study. The prediction was done using the Kuz-Ram and Swebrec models incorporated in BL, chosen due to the following reasons:

- They are the most used models in mining applications.
- They are incorporated into the BlastLogic software.

- The Swebrec model was introduced to remove some of the weaknesses of the Kuz-Ram model.
- The data required as input for these models adopted in BlastLogic software were obtained from the site.

3.4.4 Costing

Fragmentation costing analysis is a process of estimating the costs associated with various levels of fragmentation in a mining operation. The goal of fragmentation costing analysis is to identify the optimal level of fragmentation that minimises costs while still meeting the desired production goals.

The costs associated with fragmentation can be divided into two main categories:

Direct costs: These are the costs that are related to the size of the fragments, such as the cost of loading and hauling the blasted rock, the cost of crushing and screening the rock, and the cost of waste disposal.

Indirect costs: These are the costs that are not related to the size of the fragments, but that are still affected by fragmentation, such as the cost of downtime, the cost of rework, and the cost of lost production.

Here's an overview of the key steps involved in fragmentation costing analysis:

- Data collection: Gather data on the fragmentation sizes resulting from various blasting activities in the mining operation. This data can be obtained through post-blast fragmentation analysis using optical imaging systems, laser scanners, or sieving equipment to measure the size distribution, shape, and strength of the fragmented material.
- Cost estimation: Identify the relevant cost components associated with the mining operation. These costs may include drilling and

blasting costs, material handling costs, crushing, and grinding costs, and transportation costs.

- Fragmentation size classification: Categorize the fragmented material into different size ranges based on the collected data. Typically, fragmentation sizes are classified into specific size intervals.
- Volume and weight estimation: Calculate the volume and weight of material within each size range. This step is essential as different size distributions may result in varying amounts of material to handle, transport, and process.
- Cost allocation: Allocate the relevant operational costs to each size range. This involves determining the proportion of each cost component attributed to the specific fragmentation size.
- Cost analysis: Analyse the total costs associated with each fragmentation size range. This analysis will reveal the cost implications of different fragmentation sizes on the mining operation.
- Productivity evaluation: Evaluate the impact of fragmentation sizes on overall productivity. For instance, smaller fragmentation sizes may lead to increased energy consumption during crushing and grinding, while larger sizes may require additional material handling efforts.
- Economic optimisation: Identify the fragmentation size range that minimizes operational costs while maximising productivity. The goal is to find an economically optimal fragmentation size that balances costs and productivity.
- Sensitivity Analysis: Conduct sensitivity analysis to assess the effect of changes in key factors, such as blasting parameters or cost components, on the overall cost and productivity outcomes.
- Decision-Making: Based on the results of the fragmentation costing analysis, make informed decisions on optimising blasting

parameters, fragmentation sizes, and operational practices to achieve cost-efficient mining operations.

Fragmentation costing analysis is crucial for mining companies to optimise their blasting and fragmentation practices, reduce operational costs, and enhance overall productivity. By understanding the economic implications of different fragmentation sizes, mining operations can make data-driven decisions to improve their efficiency and profitability.

The methodology and steps followed for the study are as follows:

- Step 1: Selection of Blasting Sites and Data Collection.

Identify a set of blasting sites in surface mines with diverse rock properties, geological conditions, and explosive characteristics.

Obtain historical data from these blasting sites, including detailed information on rock properties, explosive properties, drilling and initiation patterns, and in-situ geology.

- Step 2: BlastLogic Software Implementation

Install and configure the BlastLogic software on a suitable computer system.

Input the collected data from the selected blasting sites into the software, including rock properties, explosive properties, drilling and initiation patterns, and in-situ geology.

- Step 3: Fragmentation Prediction with BlastLogic Software

Utilize the BlastLogic software's mechanistic model to predict the fragmentation distribution for each blasting site based on the input data.

Record the predicted fragmentation distributions for further analysis.

- Step 4: Actual Fragmentation Measurement

Conduct post-blast fragmentation analysis at each blasting site to determine the actual fragmentation distribution.

Utilize optical imaging systems, laser scanners, or sieving equipment to measure fragment size distribution, shape, and strength.

Record the actual fragmentation distribution data for each blasting site.

- Step 5: Statistical Analysis

Use MS Excel software packages to analyse the predicted and actual fragmentation distribution data. Calculate statistical metrics such as mean, median, standard deviation, and correlation coefficients to compare the predicted and actual fragmentation distributions.

- Step 6: Performance Evaluation

Compare the predicted fragmentation distributions with the actual fragmentation distributions using the statistical metrics.

Assess the accuracy, precision, and robustness of the BlastLogic software in predicting fragmentation distribution.

- Step 7: Sensitivity Analysis

Perform sensitivity analysis by varying input parameters within a reasonable range to observe how changes in rock properties, explosive properties, drilling patterns, and in-situ geology affect the accuracy of the predictions.

Instruments Used

Computer System: To install and run the BlastLogic software for fragmentation prediction.

Optical Imaging Systems: To capture images of fragmented material and measure fragment size and shape distribution.

Laser Scanners: To obtain 3D data of fragmented material for precise size and shape analysis.

Sieving Equipment: To separate and measure fragmented material based on size distribution.

Statistical Software Packages: To perform data analysis, calculate statistical metrics, and visualize the results. Microsoft Excel was used.

Through this methodology, the performance of the BlastLogic software in predicting fragmentation distribution can be assessed, providing valuable insights into its reliability and applicability in mining and blasting operations. Figure 3.3 summarises the method followed by this research study.

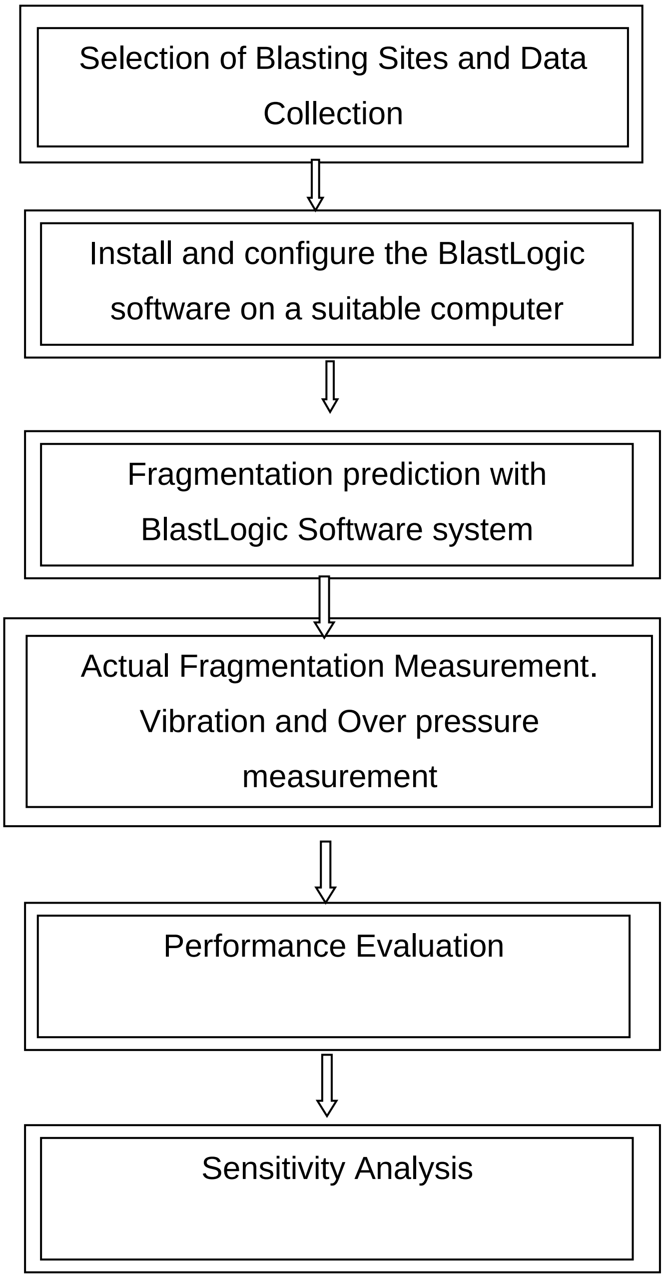

Figure 3.3 Research process flow. Source: Maptek (2021)

This methodology flow description summary outlines the key steps and procedures used in evaluating the BlastLogic software's performance in predicting fragmentation distribution sizes.

3.5 Chapter Summary

The approach of this research project as discussed in Chapter 3 is summarised in Figure 3.3. The chapter outlined the sources of data that were considered for the determination of the optimised fragmentation muck pile profile using the different blast design parameters. The data was confirmed to address inconsistencies that could affect the analysis of the optimised fragmentation muck pile profile. BlastLogic software and the adoption of Kuz-Ram and Swebrec models were a key component applied to fragmentation size distribution and the data for study is presented in Chapter 4.

4 DATA FOR THE STUDY

4.1 Introduction

This chapter presents the geometric blast design data input used for the study. Data used was obtained from the BlastLogic database. The data generated from the images taken from the much pile is also presented.

4.2 Geometric Blast Design Data Input and Explosive Parameters Used

The geometric blast design parameters are crucial for ensuring the success of any blasting operation. These parameters include the burden, spacing, hole depth, and diameter (Eloranta, 1995). Table 4.1 shows the design blast parameters for different surface mines used in BlastLogic software.

Table 4.1 Geometric blast design parameters for design surfaces for mines understudy

Description	Units	Mogalakwena Platinum Mine	Isibonelo Colliery	Navigation Colliery Mine	Kolomela Iron Ore Mine	Sishen Iron Ore Mine
Hole Diameter	(mm)	245	160	160	250	250
Average hole length	(m)	16.8	12.9	14	15	15
Spacing	(m)	6.2	5	6	5.5	5.5
Burden	(m)	5.4	5	6	5.0	5.0
Cup Density	(g/cc)	1.11-1.22	0.99- 1.08	0.99-1.08	1.12-1.23	1.12-1.23
Final Stemming Length	(m)	4	3	3	4.5	4.5
Powder Factor	kg/m^3	0.70	0.56	0.56	0.88	0.88
Drill pattern		staggered	square	square	staggered	staggered

The blast design parameters outlined in Table 4.1 proved to be pivotal factors influencing the ultimate outcomes of fragmentation. Specifically, the selection of hole spacing, burden, and stemming length emerged as critical determinants in achieving the desired fragmentation pattern. This deliberate choice effectively facilitated the even distribution of blast energy, thereby contributing to the desired results. Moreover, the careful consideration of the powder factor, tailored to the specific rock density, played a pivotal role in ensuring efficient rock breakage (Bergmann *et al*., 1973). This approach prevented the release of excessive energy, promoting a controlled and effective fragmentation process. Considering these findings, it becomes evident that blast design parameters wield a direct and significant impact on the rock fragmentation process. Consequently, their optimisation is of paramount importance to enhance the overall efficiency of surface mining operations (Leng *et al*., 2020). Table 4.2 to Table 4.6 show the explosive parameters for the surface mines under study. The rest of the parameters are in the Appendix 8.3

Table 4.2 Explosive parameters at Mogalakwena Platinum mine

Blast Number	Total Charge(kg)	Tons blasted (tons)	Powder Factor	Density (kg/m^3)
1	69 300	76 157	1.46	2 200
2	71 764	89 456	1.47	2 200
3	56 980	76 465	1.46	2 200
4	33 572	67 348	1.47	2 200
5	44 660	78 946	1.47	2 200
6	70 840	896 768	1.47	2 200
7	95 788	110 229	1.46	2 200
8	61 600	126 738	1.47	2 200
9	77 904	124 233	1.47	2 200
10	63 120	121 002	1.47	2 200
11	69 345	97 565	1.38	2 200
12	120 849	162 278	1.46	2 200
13	82 020	90 282	1.47	2 200
14	83 739	90 998	1.47	2 200
15	94 493	109 364	1.47	2 200
16	77 349	89 443	1.38	2 200
17	23 484	62 384	1.46	2 200
18	90 201	166 675	1.47	2 200
19	118 282	189 978	1.47	2 200
20	61 600	99 565	1.47	2 200
21	57 904	87 562	1.38	2 200
22	43 156	78 620	1.46	2 200
23	69 345	97 659	1.47	2 200
24	110 841	219 675	1.47	2 200
25	82 920	104 435	1.47	2 200
26	61 633	92 565	1.38	2 200
27	57 954	81 562	1.46	2 200
28	43 129	72 720	1.47	2 200
29	77 039	101 234	1.47	2 200
30	57 994	88 562	1.38	2 200

Table 4.3 Explosive parameters of blasts at Isibonelo Colliery

Blast Number	Total Charge(kg)	Tons blasted (tons)	Powder Factor	Density (kg/m^3)
1	17 640	25 200	0.70	1 200
2	13 770	24 097	0.68	1 200
3	12 960	22 680	0.65	1 200
4	16 200	28 350	0.60	1 200
5	17 460	30 555	0.70	1 200
6	18 360	32 130	0.68	1 200
7	10 260	17 955	0.65	1 200
8	9 360	16 380	0.60	1 200
9	18 000	31 500	0.70	1 200
10	16 290	28 507	0.68	1 200
11	16 940	25 998	0.65	1 200
12	14 773	25 097	0.60	1 200
13	12 560	22 380	0.70	1 200
14	16 500	28 150	0.68	1 200
15	17 469	30 555	0.65	1 200
16	18 360	32 130	0.65	1 200
17	10 460	17 955	0.65	1 200
18	9 369	16 383	0.65	1 200
19	18 500	31 550	0.65	1 200
20	16 290	28 950	0.65	1 200
21	16 290	30 055	0.65	1 200
22	16 940	32 930	0.65	1 200
23	14 773	17 455	0.68	1 200
24	12 560	16 382	0,65	1 200
25	16 500	28 150	0.68	1 200
26	17 469	30 055	0.65	1 200
27	18 360	32 930	0.68	1 200
28	10 460	17 455	0.65	1 200
29	9 369	30 055	0.68	1 200
30	14 773	25 197	0.60	1 200

Table 4.4 Explosive parameters of blasts at Navigation Colliery

Blast Number	Total Charge(kg)	Tons blasted (tons)	Powder Factor	Density (kg/m^3)
1	18 424	22 540	0.61	1 200
2	18 620	25 074	0.61	1 200
3	24 010	35 237	0.61	1 200
4	18 424	22 071	0.61	1 200
5	18 620	25 047	0.62	1 200
6	19 502	25 237	0.62	1 200
7	22 540	22 574	0.62	1 200
8	19 797	22 914	0.62	1 200
9	19 992	25 074	0.62	1 200
10	10 192	21 111	0.62	1 200
11	19 424	25 074	0.69	1 200
12	18 720	22 927	0.69	1 200
13	24 010	35 114	0.69	1 200
14	18 425	21 074	0.69	1 200
15	18 120	25 102	0.69	1 200
16	18 424	25 174	0.69	1 200
17	18 820	25 074	0.69	1 200
18	24 910	22 074	0.69	1 200
19	18 424	25 074	0.69	1 200
20	18 820	25 174	0.69	1 200
21	24 910	31 500	0.69	1 200
22	18 524	28 507	0.69	1 200
23	18 720	25 998	0.69	1 200
24	24 910	31 500	0.69	1 200
25	18 624	28 120	0.69	1 200
26	18 820	28 424	0.69	1 200
27	24 915	28 820	0.69	1 200
28	18 464	28 120	0.69	1 200
29	18 821	24 910	0.69	1 200
30	19 425	20 074	0.69	1 200

Table 4.5 Explosive parameters of blasts at Kolomela Iron Ore mine

Blast Number	Total Charge(kg)	Tons blasted (tons)	Powder Factor	Density (kg/m^3)
1	139 725	201 291	1.44	3 200
2	120 690	198 238	1.44	3 200
3	104 490	188 273	1.44	3 200
4	134 055	204 292	1.44	3 200
5	94 365	175 901	1.44	3 200
6	85 860	156 282	1.44	3 200
7	80 190	168 281	1.44	3 200
8	99 225	178 091	1.44	3 200
9	100 845	182 451	1.44	3 200
10	39 690	88 472	1.44	3 200
11	113 837	178 859	1.44	3 200
12	98 271	188 574	1.44	3 200
13	129 291	178 289	1.44	3 200
14	99 719	154 747	1.44	3 200
15	103 372	299 273	1.44	3 200
16	91 387	992 829	1.44	3 200
17	171 282	320 192	1.44	3 200
18	182 282	281 893	1.44	3 200
19	182 928	291 095	1.44	3 200
20	92 914	179 459	1.44	3 200
21	79 928	154 282	1.44	3 200
22	100 290	128 383	1.44	3 200
23	90 382	168 943	1.44	3 200
24	112 031	172 483	1.44	3 200
25	98 318	124 483	1.44	3 200
26	108 239	285 953	1.44	3 200
27	112 390	298 389	1.44	3 200
28	98 498	128 489	1.44	3 200
29	139 081	298 182	1.44	3 200
30	90 414	177 459	1.44	3 200

Table 4.6 Explosive parameters of blasts at Sishen Iron Ore mine

Blast Number	Total Charge(kg)	Tons blasted (tons)	Powder Factor	Density (kg/m^3)
1	139 725	171 282	1.45	3 200
2	171 282	282 182	1.50	3 200
3	182 582	282 928	1.50	3 200
4	172 928	292 914	1.50	3 200
5	62 915	179 928	1.50	3 200
6	89 978	140 290	1.50	3 200
7	110 290	190 372	1.50	3 200
8	95 382	200 031	1.50	3 200
9	112 231	98 318	1.50	3 200
10	95 318	133 382	1.50	3 200
11	93 839	168 943	1.50	3 200
12	82 023	172 483	1.50	3 200
13	83 139	124 481	1.50	3 200
14	93 491	285 950	1.50	3 200
15	74 344	168 949	1.50	3 200
16	78 484	172 483	1.50	3 200
17	91 201	181 283	1.50	3 200
18	102 292	122 292	1.50	3 200
19	192 945	289 292	1.50	3 200
20	128 481	181 381	1.50	3 200
21	112 231	98 318	1.50	3 200
22	95 318	133 382	1.50	3 200
23	93 839	168 943	1.50	3 200
24	112 231	172 483	1.50	3 200
25	95 318	98 318	1.50	3 200
26	73 094	148 493	1.50	3 200
27	85 860	112 182	1.50	3 200
28	99 225	100 845	1.50	3 200
29	100 845	239 690	1.50	3 200
30	104 389	189 479	1.50	3 200

The interplay between these explosive parameters and the resultant fragmentation size holds paramount importance when it comes to optimising blasting outcomes within the mining industry (Spathis *et al*., 2017). A comprehensive understanding of how to manipulate the total mass of explosives and the powder factor emerges as a critical factor in attaining the intended fragmentation size (Spathis, 2006). This, in turn, has far-reaching implications for downstream processes such as crushing and grinding, as well as for addressing safety and environmental concerns (Garg *et al.*, 2021). Indeed, the ability to exercise control over fragmentation is pivotal. Not only does it impact cost reduction, but it also enhances overall productivity. Additionally, by ensuring consistent and controlled fragmentation, mining operations can operate safely and efficiently during subsequent activities, underscoring the holistic importance of achieving the targeted fragmentation distribution in the mining sector (Malkowski *et al*., 2018).

4.3 Rock Parameters Input

Data obtained included the following:

- Uniaxial Compressive strength.
- rock density, joint spacing and Young’s modulus.
- Rock mass description (RMD).

The assumption of the rock parameters at these surface mines is that there is no significant change in the rock parameters during the duration of the study. Table 4.7 summarises the rock parameters at the surface mines under study.

Table 4.7 Rock characteristics for surface mines

Parameters	Mines and Collieries				
	Mogalakwena	Isibonelo	Navigation	Kolomela	Sishen
Uniaxial Compressive Strength (MPa)	210	21.9	21.9	147	147
Joint Spacing (m)	1.5	0.8	0.8	1.3	1.3
Rock Density (kg/m^3)	3 000	1 350	1 350	7 200	7 200
Young's Modulus (GPa)	97	6	6	198	198
Rock Type	Pyroxenite	Bituminous	Bituminous	Manganore Iron	Manganore Iron
Rock Description	Strong	Soft	Soft	Strong and hard	Strong and hard

The data essential for understanding the rock's key characteristics was extracted from the geological database of the mines under investigation, as presented in Table 4.7. This dataset encompassed critical parameters such as the Uniaxial Compressive Strength, Rock Density, and the specific rock type. It's important to note that these fundamental data points were already available before the initiation of blast pattern design.

The collected data was incorporated and used within the BlastLogic software for vibration and fly-rock analysis. The collected blast design parameters were documented and reported. This documentation ensures that the data is readily available for future reference, research, or decision-making processes related to fragmentation analysis, mine planning, or optimisation of blasting operations.

4.4 Fragmentation Distribution Image Sampling

For each blast, a minimum of forty pictures of the blasted muck piles were captured using a digital camera. Some of the pictures are found in (Appendices 8.1). In each of these images, scaling objects such as a safety helmet and a soccer ball were included. These objects were placed at separate locations within the images and served as reference-sized objects. Split-Desktop® software utilised these scaling objects to estimate the size of the fragments. The specific sizes of the safety helmet and soccer ball were not mentioned in the given paragraph (Babaeian *et al*., 2019).

4.5 Chapter Summary

This chapter presented the geometric design input parameters used. It explains the use of the geometric design input parameters and how they were used in BL. The chapter went on to incorporate the rock parameters and how they play a key role in the fragmentation, vibration and overpressure models. Lastly, the fragmentation distribution image sampling in Split Desktop was investigated. The next chapter discusses the results and analysis.

5 DISCUSSION AND ANALYSIS OF RESULTS

5.1 Introduction

Chapter 5 presents the costing analysis associated with the fragmentation size distribution. The fragmentation analysis and the evaluation of the BL performance are explained in detail. In addition, vibration and over-pressure analysis is included in Chapter 5. The cost analysis showed exactly when the BL software was implemented to show the improvements.

Costing analysis

Fragmentation costing analysis is crucial for mining companies to optimise their blasting and fragmentation practices, reduce operational costs, and enhance overall productivity. By understanding the economic implications of different fragmentation sizes, mining operations can make data-driven decisions to improve their efficiency and profitability (Gates, 1915). Table 5.1 compares average target and actual fragmentation sizes and their associated costs.

Table 5.1 Average cost reduction and efficiency gains through BlastLogic software implementation in a fragmentation analysis

	Mogalakwena mine		Isibonelo Colliery.		Navigation Colliery		Kolomela mine		Sishen mine	
	Target	Actual	Target	Actual	Target	Actual	Target	Actual	Target	Actual
Fragmentation size P50 (mm)	255	250	200	200	200	200	220	220	220	220
Vibration (m/s)	12.6	10	12.6	12	12.6	12	12.6	12	12.6	10
Over-pressure (dB)	120	120	120	120	120	120	120	120	120	120
Muckpile shape	Heave	Heave	Heave	Scattered	Scattered	Heave	Heave	Heave	Heave	Heave
Cost (R)	R190 Million	R101 Million	R90 Million	R69 Million	R101 Million	R61 Million	R231 Million	R122 Million	R211 Million	R145 Million

Table 5.1 shows the impact of the BlastLogic software implementation on cost reduction, as shown by the table showing a decrease in costs. The data reflects the cost efficiencies achieved by accurately predicting fragmentation sizes using the BlastLogic software, leading to improved decision-making and cost reduction in the mining operations.

5.2 Fragmentation Results and Cost Analysis

The results and discussions for the fragmentation, vibration, and overpressure prediction in BlastLogic software were analysed before conducting the blast. After the blast, the image analysis was done in Split-Desktop® software is presented in this section. Appendix 8.3 shows figures with vibration and over-pressure measuring stations. The fragmentation size distribution curves and results for each of the blasts considered at the 5 different mines under study are presented.

5.2.1 Mogalakwena Platinum Mine results

The target fragmentation P50 size was 250mm. The pattern design chosen was 5.7m burden and 6.6m spacing or 5.4m burden and 6.2m. The diameters used for the patterns were 270mm and 250mm, respectively. The environmental impact of vibration and overpressure was evaluated for the chosen blast design parameters. Table 5.2 and Table 5.3 show the fragmentation results for the Mogalakwena Platinum mine.

Table 5.2 Mogalakwena Platinum mine results 1

Blast No:	Fragmentation				Vibration (mm/s)	Over-pressure (dB)	Comment
	P50 target (mm)	P50 prediction BlastLogic Kuz-Ram (mm)	P50 prediction BlastLogic Swebrec (mm)	P50 Split desktop (mm)			
1	255	250	253	252	11	133	No boulders
2	255	254	255	254	10	144	No boulders
3	255	253	254	254	11	124	No boulders
4	255	254	255	255	12	145	No boulders
5	255	253	255	199	12	131	No boulders
6	255	254	254	254	11	119	Slight boulders
7	255	250	251	252	10	90	No boulders
8	255	249	253	254	10	89	Slight boulders
9	255	253	255	255	12	117	No boulders
10	255	250	255	256	12	110	No boulders
11	255	253	255	255	11	119	Slight boulders
12	255	254	254	254	10	90	No boulders
13	255	253	254	255	10	89	Slight boulders
14	255	254	254	254	12	117	No boulders
15	255	253	255	255	12	110	No boulders
16	255	247	250	254	11	119	Slight boulders
17	255	253	255	255	10	90	No boulders
18	255	261	258	257	10	89	Slight boulders
19	255	253	255	255	12	117	No boulders
20	255	254	254	254	12	110	No boulders

Table 5.3 Mogalakwena Platinum Mine Results 2

Blast No:	Fragmentation				Vibration (mm/s)	Over-pressure (dB)	Comment
	P50 target (mm)	P50 prediction BlastLogic Kuz-Ram (mm)	P50 prediction BlastLogic Swebrec (mm)	P50 Split desktop (mm)			
21	255	253	254	255	11	133	No boulders
22	255	254	255	253	10	144	No boulders
23	255	250	253	254	11	124	No boulders
24	255	251	255	255	12	145	No boulders
25	255	254	255	252	12	131	No boulders
26	255	253	255	255	11	119	Slight boulders
27	255	253	254	254	10	90	No boulders
28	255	254	255	255	10	89	Slight boulders
29	255	253	254	254	12	117	No boulders
30	255	253	255	255	12	110	No boulders
31	255	254	254	254	11	119	No boulders
32	255	253	255	255	10	90	No boulders
33	255	253	255	254	10	89	Slight boulders
34	255	254	255	255	12	117	No boulders
35	255	253	254	256	12	110	No boulders
36	255	253	255	255	11	119	No boulders
37	255	254	254	257	10	90	No boulders
38	255	253	255	257	10	89	No boulders
39	255	253	254	255	12	117	No boulders
40	255	254	254	254	12	110	No boulders

Table 5.2 and 5.3 presents a visual representation of the target fragmentation distribution and then proceed to compare it against the predictions generated by the BlastLogic software. Among the two models, the Swebrec model exhibited the closest alignment with the intended target fragmentation size. However, it's important to note that there were instances of small boulders observed within the mining pit. These

deviations from the target fragmentation size can be attributed to a constellation of contributing factors, including the explosive performance and the precision of the drilling process.

Cost Analysis for Mogalakwena Mine

Cost-benefit analysis for fragmentation size distribution was critical in showing whether the BlastLogic software implementation helped the mines. This was from a period when BlastLogic software was implemented and used on site for drilling and blasting management processes. Figure 5.1 shows the costs before and after BlastLogic software was implemented.

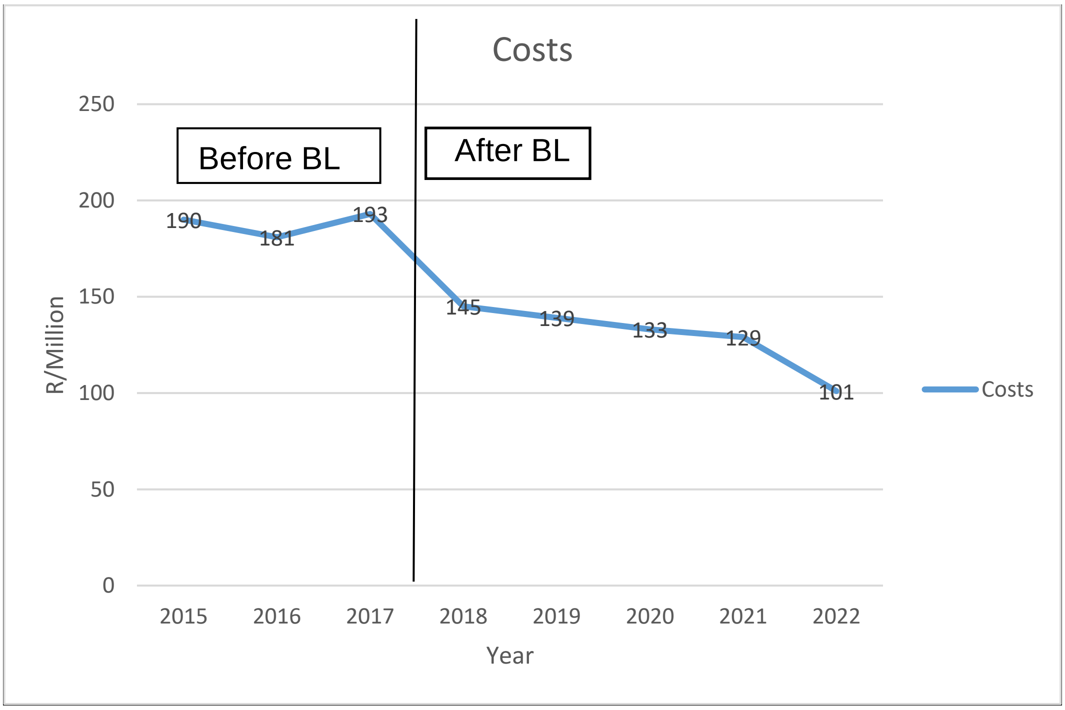

Figure 5.1 Cost analysis for Mogalakwena Platinum mine

Figure 5.1 shows a comprehensive analysis of fragmentation costs over a five-year period during which the BlastLogic software was implemented on-site. The graph reveals a notable and consistent downward trend in costs associated directly with the size of fragmentation resulting from blasting activities. This decline in costs can be directly attributed to the successful integration and utilisation of the BlastLogic software within the mining operation. However, it's worth noting that in 2017, there was a temporary increase in costs hence This spike can be attributed to a rise in the price of explosives, which, although causing a temporary setback, does not negate the overall positive impact of the BlastLogic software on cost reduction over the broader period.

5.2.2 Isibonelo Colliery results

The expected fragmentation P50 size was 200mm. From the processing plant, they would now crush and sort according to the market requirement. The pattern design chosen was 4.5 m burden and 5.0 m. The diameter used for the pattern was 161mm diameter. The environmental impact of vibration and overpressure were evaluated for the chosen blast design parameters. Table 5.4 and Table 5.5 show the fragmentation results at Isibonelo Colliery.

Table 5.4 Isibonelo Colliery results 1

Blast No:	Fragmentation				Vibration (mm/s)	Over-pressure (dB)	Comment
	P50 target (mm)	P50 prediction BlastLogic Kuz-Ram (mm)	P50 prediction BlastLogic Swebrec (mm)	P50 Split desktop (mm)			
1	200	206	197	199	11	133	No boulders
2	200	198	199	200	10	144	No boulders
3	200	195	200	199	11	124	No boulders
4	200	199	199	199	12	145	No boulders
5	200	198	199	200	12	131	No boulders
6	200	198	201	199	11	119	No boulders
7	200	198	199	199	10	90	No boulders
8	200	197	197	199	10	89	No boulders
9	200	198	199	199	12	117	No boulders
10	200	198	196	199	12	110	No boulders
11	200	198	199	200	11	119	No boulders
12	200	198	200	199	10	90	No boulders
13	200	197	197	199	10	89	No boulders
14	200	198	200	199	12	117	No boulders
15	200	198	199	196	12	110	No boulders
16	200	205	201	199	11	119	No boulders
17	200	198	199	201	10	90	No boulders
18	200	197	200	199	10	89	No boulders
19	200	198	199	199	12	117	No boulders
20	200	198	199	199	12	110	No boulders

Table 5.5 Isibonelo Colliery results 2

Blast No:	Fragmentation				Vibration (mm/s)	Over-pressure (dB)	Comment
	P50 target (mm)	P50 prediction BlastLogic Kuz-Ram (mm)	P50 prediction BlastLogic Swebrec (mm)	P50 Split desktop (mm)			
21	200	203	199	199	11	133	No boulders
22	200	198	198	199	10	144	No boulders
23	200	198	199	199	11	124	No boulders
24	200	202	200	199	12	145	No boulders
25	200	198	199	200	12	131	No boulders
26	200	197	199	199	11	119	No boulders
27	200	200	199	200	10	90	No boulders
28	200	197	199	199	10	89	No boulders
29	200	195	202	199	12	117	No boulders
30	200	198	199	199	12	110	No boulders
31	200	198	199	200	11	119	No boulders
32	200	198	200	199	10	90	No boulders
33	200	197	199	199	10	89	No boulders
34	200	198	200	199	12	117	No boulders
35	200	198	199	199	12	110	No boulders
36	200	198	199	200	11	119	No boulders
37	200	198	200	199	10	90	No boulders
38	200	197	199	200	10	89	No boulders
39	200	198	199	199	12	117	No boulders
40	200	193	198	201	12	110	No boulders

Table 5.2 and 5.3 represents the target fragmentation distribution results and then proceed to compare it against the predictions generated by the BlastLogic software. Among the two models, the Swebrec model exhibited the closest predictions of the fragmentation size.

Cost Analysis for Isibonelo Colliery

Cost analysis was critical in showing how the project added value to the surface mine. This was from a period when BlastLogic software was implemented and used on site for drilling and blasting management processes. Figure 5.2 shows the cost analysis associated with the fragmentation distribution.

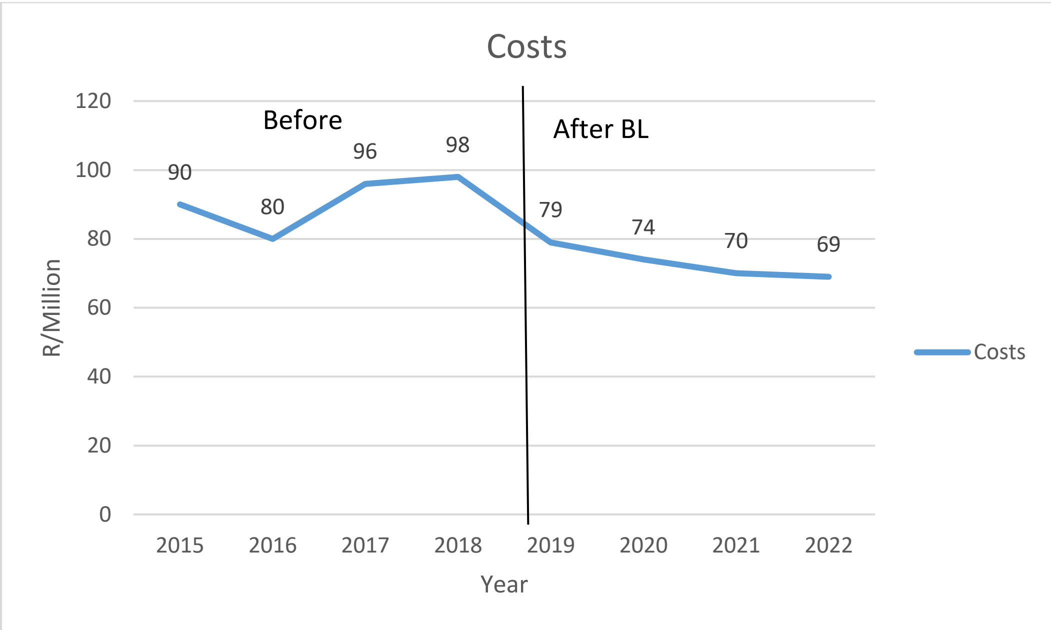

Figure 5.2 Cost analysis for Isibonelo Colliery

Figure 5.2 shows a comprehensive analysis of fragmentation costs over an eight-year period during which the BlastLogic software was implemented on-site. The graph reveals a notable and consistent downward trend in costs associated directly with the size of fragmentation resulting from blasting activities. This decline in costs can be directly attributed to the successful integration and utilisation of the BlastLogic software within the mining operation. However, between 2018 and 2019, there was a temporary decrease in costs. This can be attributed to a decrease in the price of explosives. The combination of both low explosive price and the adoption of BL software contributed to the

5.2.3 Navigation Colliery results

The expected fragmentation P50 size was 200mm. From the processing plant, they would now crush and sort according to the market requirement. The pattern design chosen was 4.5 m burden and 5.0 m. The diameter used for the pattern was 161mm diameter. The environmental impact of vibration and over pressure were evaluated for the chosen blast design parameters. Table 5.6 and 5.7 showed the fragmentation results.

Table 5.6 Navigation Colliery results 1

Blast No:	Fragmentation				Vibration (mm/s)	Over-pressure (dB)	Comment
	P50 target (mm)	P50 prediction BlastLogic Kuz-Ram (mm)	P50 prediction BlastLogic Swebrec (mm)	P50 Split desktop (mm)			
1	200	198	202	200	11	133	No boulders
2	200	198	199	199	10	144	No boulders
3	200	198	199	199	11	124	No boulders
4	200	211	204	199	12	145	No boulders
5	200	198	199	200	12	131	No boulders
6	200	208	199	206	11	119	Slight boulders
7	200	195	199	196	10	90	No boulders
8	200	197	199	199	10	89	Slight boulders
9	200	198	199	199	12	117	No boulders
10	200	198	199	199	12	110	No boulders
11	200	198	201	202	11	119	Slight boulders
12	200	206	200	199	10	90	No boulders
13	200	209	199	196	10	89	Slight boulders
14	200	190	196	199	12	117	No boulders
15	200	198	206	207	12	110	No boulders
16	200	198	204	202	11	119	Slight boulders
17	200	191	197	199	10	90	No boulders
18	200	197	200	199	10	89	Slight boulders
19	200	209	195	199	12	117	No boulders
20	200	198	199	199	12	110	No boulders

Table 5.7 Navigation Colliery result 2

Blast No:	Fragmentation				Vibration (mm/s)	Over-pressure (dB)	Comment
	P50 target (mm)	P50 prediction BlastLogic Kuz-Ram (mm)	P50 prediction BlastLogic Swebrec (mm)	P50 Split desktop (mm)			
21	200	203	203	199	11	133	No boulders
22	200	198	198	199	10	144	No boulders
23	200	198	198	199	11	124	No boulders
24	200	202	202	199	12	145	No boulders
25	200	198	198	200	12	131	No boulders
26	200	197	197	199	11	119	Slight boulders
27	200	200	200	200	10	90	No boulders
28	200	197	197	199	10	89	Slight boulders
29	200	195	195	199	12	117	No boulders
30	200	198	198	199	12	110	No boulders
31	200	198	198	200	11	119	Slight boulders
32	200	198	198	199	10	90	No boulders
33	200	197	197	199	10	89	Slight boulders
34	200	198	198	199	12	117	No boulders
35	200	198	198	199	12	110	No boulders
36	200	198	198	200	11	119	Slight boulders
37	200	198	198	199	10	90	No boulders
38	200	197	197	200	10	89	Slight boulders
39	200	198	198	199	12	117	No boulders
40	200	193	193	201	12	110	No boulders

Table 5.6 and 5.7 shows the target fragmentation distribution and compares it to what is predicted from BlastLogic software. The Swebrec model was the closest to the target fragmentation size. However, there are some small boulders observed in the pit, which can be attributed to various contributing factors such as the explosive performance used and drilling accuracy.

Cost Analysis for Navigation Colliery

Cost-benefit analysis was critical in showing how the project added value to the surface mine. This was from a period when BlastLogic software was implemented and used on site for drilling and blasting management processes. Figure 5.3 shows the cost analysis associated with the fragmentation size distribution.

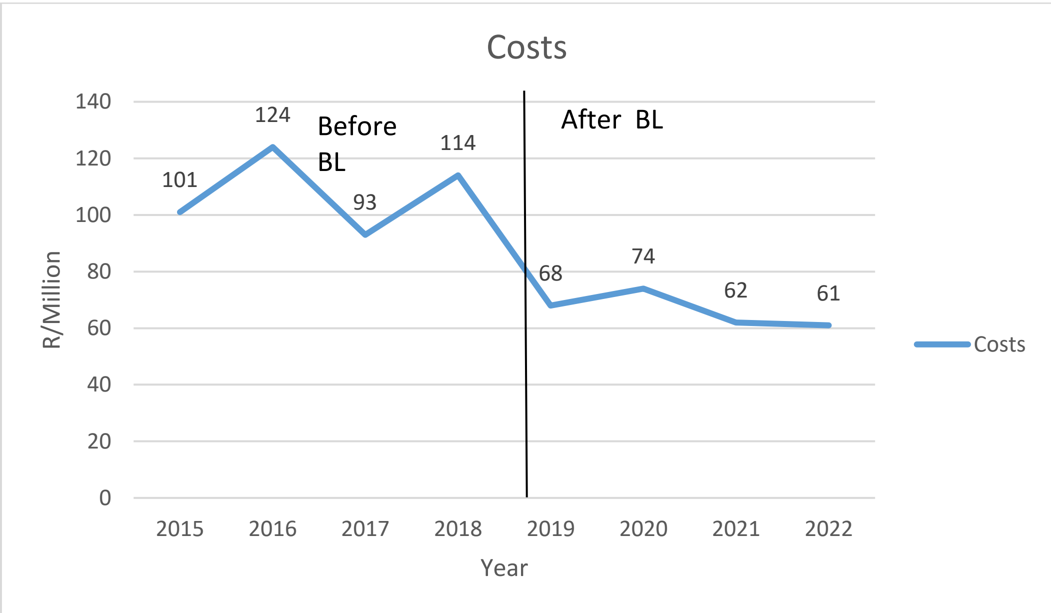

Figure 5.3 Cost analysis for Navigation Colliery

Figure 5.3 provides an analysis of the fragmentation costs spanning four years during which BlastLogic software was actively implemented on-site. The graph within this figure notably illustrates a consistent downward trend in costs, directly attributed to the optimisation of blasting fragmentation sizes over time. One intriguing observation within the graph is the noticeable peak in 2016. This spike can be attributed to a deliberate acceleration in production during that year. However, it's essential to note that this surge was soon followed by a return to a more stable cost trajectory in 2016 as production targets were exceeded. Furthermore, the year 2017 stands out as another notable peak in fragmentation costs. This upswing was primarily driven by a significant increase in explosive costs from the supplier. The rise in expenses associated with explosive materials during this period had a discernible impact on the overall fragmentation cost analysis.

5.2.4 Kolomela Iron Ore Mine results

The expected fragmentation P50 size was 200mm. The pattern design chosen was 4.8m burden and 5.5m spacing. The diameter used for the patterns was 160 mm diameter. The environmental impact of vibration and overpressure were evaluated for the chosen blast design parameters. Table 5. 8 and 5.9 showed the results for Kolomela Iron Ore Mine.

Table 5.8 Kolomela Iron Ore mine results 1

Blast No:	Fragmentation				Vibration (mm/s)	Over-pressure (dB)	Comment
	P50 target (mm)	P50 prediction BlastLogic Kuz-Ram (mm)	P50 prediction BlastLogic Swebrec (mm)	P50 Split desktop (mm)			
1	200	204	200	199	11	133	No boulders
2	200	208	211	210	10	144	No boulders
3	200	200	200	200	11	124	No boulders
4	200	200	199	199	12	145	No boulders
5	200	198	200	199	12	131	No boulders
6	200	200	200	201	211	119	No boulders
7	200	211	202	203	10	90	No boulders
8	200	211	203	199	10	89	No boulders
9	200	198	195	199	12	117	No boulders
10	200	198	200	200	12	110	No boulders
11	200	211	199	199	11	119	No boulders
12	200	207	201	199	10	90	No boulders
13	200	200	201	200	10	89	No boulders
14	200	198	198	199	12	117	No boulders
15	200	198	203	200	12	110	No boulders
16	200	198	197	199	11	119	No boulders
17	200	198	199	199	10	90	No boulders
18	200	205	201	200	10	89	No boulders
19	200	209	199	198	12	117	No boulders
20	200	200	197	199	12	110	No boulders

Table 5.9 Kolomela Iron Ore mine results 2

Blast No:	Fragmentation				Vibration (mm/s)	Over-pressure (dB)	Comment
	P50 target (mm)	P50 prediction BlastLogic Kuz-Ram (mm)	P50 prediction BlastLogic Swebrec (mm)	P50 Split desktop (mm)			
21	200	200	198	200	11	133	No boulders
22	200	200	200	200	10	144	No boulders
23	200	200	211	202	11	124	No boulders
24	200	200	211	203	12	145	No boulders
25	200	200	198	195	12	131	No boulders
26	200	200	198	200	11	119	Slight boulders
27	200	200	200	200	10	90	No boulders
28	200	200	211	202	10	89	Slight boulders
29	200	200	211	203	12	117	No boulders
30	200	200	198	195	12	110	No boulders
31	200	200	198	200	11	119	Slight boulders
32	200	200	200	200	10	90	No boulders
33	200	200	211	202	10	89	Slight boulders
34	200	200	211	203	12	117	No boulders
35	200	200	198	195	12	110	No boulders
36	200	200	198	200	11	119	Slight boulders
37	200	200	200	200	10	90	No boulders
38	200	200	211	202	10	89	Slight boulders
39	200	200	211	203	12	117	No boulders
40	200	200	198	195	12	110	No boulders

Tables 5.8 and 5.9 shows the target fragmentation distribution and compare it to what is predicted from BlastLogic software and the actual sizes from split desktop results. The Swebrec model was the closest to the target fragmentation size. However, there are some small boulders observed in the pit, which can be attributed to various contributing factors such as explosive performance and drilling accuracy.

Cost Analysis for Kolomela Mine

The cost-benefit analysis was critical in showing how the project added value to the surface mine. This was from a period when BlastLogic software was implemented and used on-site for drilling and blasting management processes. Figure 5.4 shows the cost analysis associated with the fragmentation size distribution.

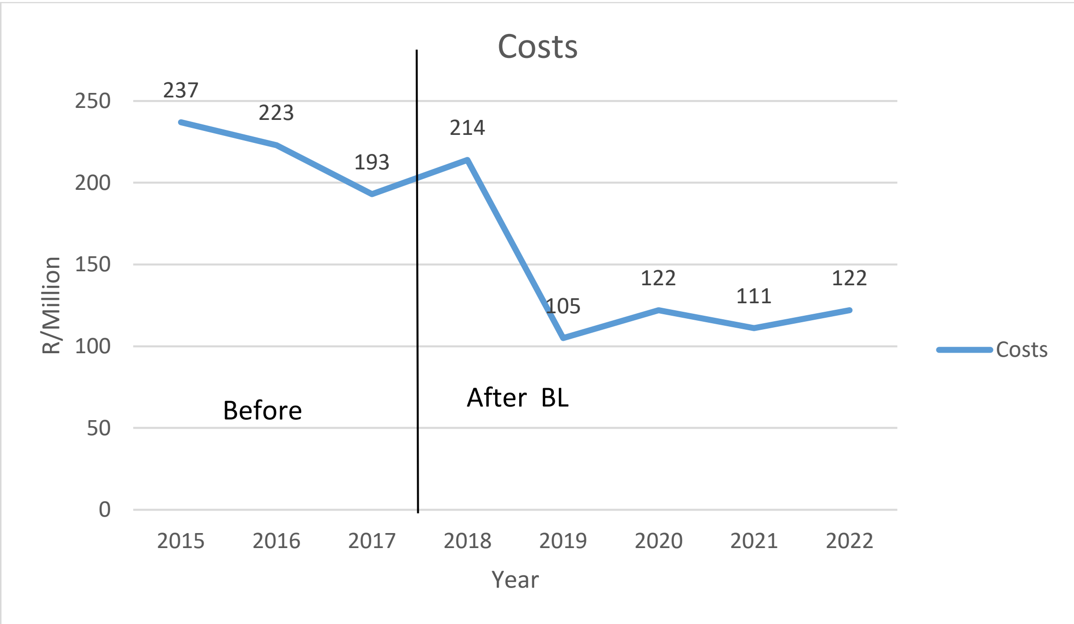

Figure 5.4 Cost analysis for Kolomela Iron Ore mine

Figure 5.4 presents a comprehensive analysis of the fragmentation benefits observed over four years during the deployment of BlastLogic software on our site. This graph effectively shows a consistent downward trend in costs directly associated with blasting size fragmentation. The data within this figure highlights the progressive reduction in fragmentation-related expenses, highlighting the positive impact of BlastLogic software on our operations over the eight years. In the year 2017 showed a spike after BL software was implemented due to the poor adoption of the system on the system on site.

5.2.5 Sishen Iron Ore Mine results

The expected fragmentation P50 size was 200 mm. The pattern design chosen was 5m burden and 5.5m spacing. The diameter used for the patterns was 161mm. The environmental impact of vibration and overpressure was evaluated for the chosen blast design parameters. Tables 5.10 and 5.11 show the fragmentation results 1 and result 2.

Table 5.10 Sishen Iron Ore mine results 1

Blast No:	Fragmentation				Vibration (mm/s)	Over-pressure (dB)	Comment
	P50 target (mm)	P50 prediction BlastLogic Kuz-Ram (mm)	P50 prediction BlastLogic Swebrec (mm)	P50 Split desktop (mm)			
1	200	198	199	199	11	133	No boulders
2	200	198	199	199	10	144	No boulders
3	200	198	199	199	11	124	No boulders
4	200	200	199	199	12	145	No boulders
5	200	198	199	199	12	131	No boulders
6	200	198	199	199	11	119	Slight boulders
7	200	200	200	200	10	90	No boulders
8	200	197	199	199	10	89	Slight boulders
9	200	198	199	199	12	117	No boulders
10	200	198	199	199	12	110	No boulders
11	200	199	199	199	11	119	Slight boulders
12	200	200	200	200	10	90	No boulders
13	200	197	199	199	10	89	Slight boulders
14	200	198	199	199	12	117	No boulders
15	200	198	199	199	12	110	No boulders
16	200	198	199	199	11	119	Slight boulders
17	200	200	200	200	10	90	No boulders
18	200	197	199	199	10	89	Slight boulders
19	200	198	199	199	12	117	No boulders
20	200	198	199	199	12	110	No boulders

Table 5.11 Sishen mine Iron Ore mine results 2

Blast No:	Fragmentation				Vibration (mm/s)	Over-pressure (dB)	Comment
	P50 target (mm)	P50 prediction BlastLogic Kuz-Ram (mm)	P50 prediction BlastLogic Swebrec (mm)	P50 Split desktop (mm)			
1	200	198	199	199	11	133	No boulders
2	200	198	199	199	10	144	No boulders
3	200	198	199	199	11	124	No boulders
4	200	202	199	199	12	145	No boulders
5	200	198	199	199	12	131	No boulders
6	200	198	199	199	11	119	Slight boulders
7	200	198	199	199	10	90	No boulders
8	200	197	199	199	10	89	Slight boulders
9	200	198	199	199	12	117	No boulders
10	200	198	199	199	12	110	No boulders
11	200	198	199	199	11	119	Slight boulders
12	200	198	199	199	10	90	No boulders
13	200	197	199	199	10	89	Slight boulders
14	200	198	199	199	12	117	No boulders
15	200	198	199	199	12	110	No boulders
16	200	198	199	199	11	119	Slight boulders
17	200	198	199	199	10	90	No boulders
18	200	197	199	199	10	89	Slight boulders
19	200	198	199	199	12	117	No boulders
20	200	198	199	199	12	110	No boulders

Tables 5.10 and 5.11 show the results of target fragmentation distribution, contrasting it with both the predictions generated by the BlastLogic software. Among the various models employed, the Swebrec model appears to align most closely with our target fragmentation size, indicating a promising level of accuracy in BlastLogic software's predictions. However, it's important to note that there have been instances of small boulders observed within the pit, which deviate from the anticipated fragmentation sizes. These deviations can be attributed to several contributing factors, including variations in explosive performance, potential non-compliance by the charging crew on site, and variations in drilling accuracy. These elements collectively underscore the complexity of achieving precise fragmentation outcomes in our operational context.

Cost Analysis for Sishen Mine

The cost-benefit analysis was critical in showing how the project added value to the surface mine. This was from a period when BlastLogic software was implemented and used on-site for drilling and blasting management processes. Figure 5.5 shows the cost analysis associated with the fragmentation size distribution.

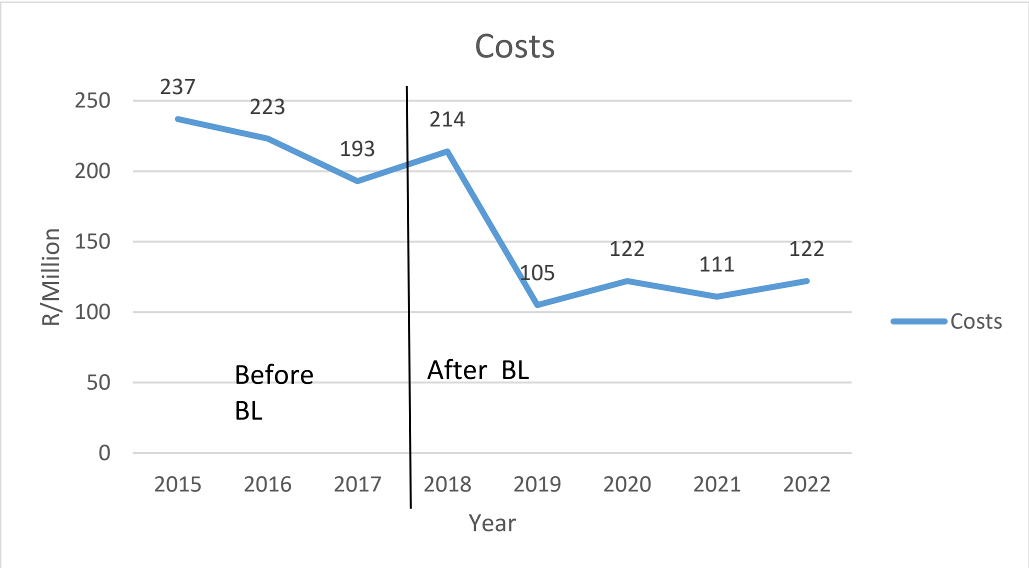

Figure 5.5 Cost analysis for Sishen Iron Ore mine

Figure 5.5 shows the cost analysis for the period of 5 years when BlastLogic software deployed on site. The graph shows a decreasing trend in the cost linked directly to the blasting size fragmentation after the implementation of the BlastLogic software.

5.3 Evaluation of BL Performance

Evaluating the performance of BlastLogic software at predicting fragmentation distribution is essential for ensuring the effectiveness of blasting operations in mining, construction, and quarrying industries. Accurate fragmentation prediction can lead to optimised blasting designs, improved ore recovery, and reduced downstream processing costs (Chiapetta and Postupack, 1995).

5.3.1 Evaluation of BL performance at Mogalakwena Platinum Mine

The Root Mean Square Error (RMSE) computations and prediction were done using BlastLogic software. The fragmentation measurements were provided by the image analysis. These provided valuable insights into the accuracy and reliability of the predictive model. Figures 5.6 and 5.7 show the correlation and regression analyses for fragmentation distribution size based on the Kuz-Ram and Swebrec models at Mogalakwena Mine respectively.

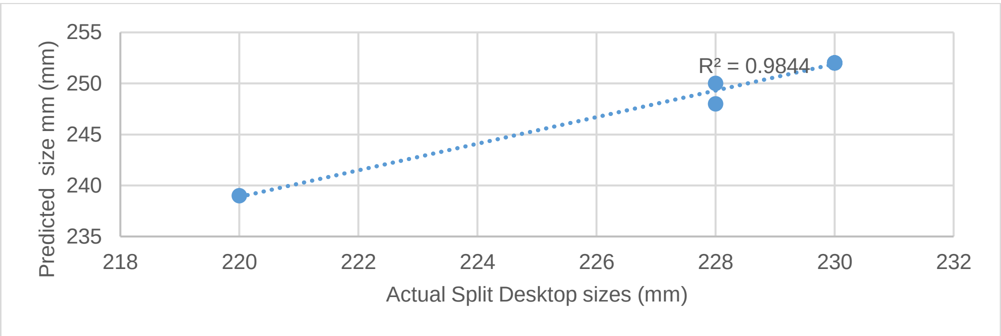

Figure 5.6 Correlation and regression for Mogalakwena mine for Kuz-ram model

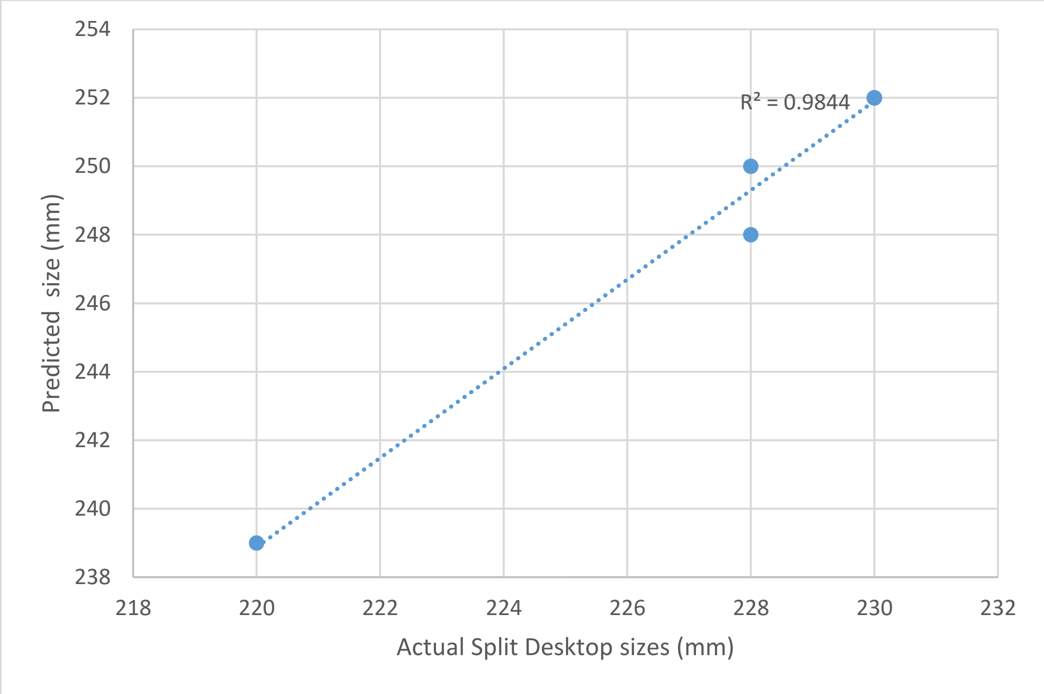

Figure 5.7 Correlation and regression for Mogalakwena mine for Swebrec model

In the Kuz- Ram model, R^2 is 0.9712 and Swebrec model R^2 is 0.9844. This indicates that there is a positive linear relationship between the two variables (actual fragmentation size and predicted sizes from BlastLogic software), and the regression model provides a reasonable fit to the data.

The standard deviation and skewness analysis results were also summarized in a Table format in Appendices. The details of the RMSE analyses, correlation and regression analyses are shown in Table 5.12. A summary of the results of the Root Mean Square Error (RMSE), variance, and standard deviation.

Table 5.12 Descriptive statistics for Mogalakwena Platinum results

Blast No:	Predicted size (mm)		Actual (mm)	Variance		Standard deviation		RMSE		Skewness	
	Kuz-Ram	Swebrec		Kuz-Ram	Swebrec	Kuz-Ram	Swebrec	Kuz-Ram	Swebrec	Kuz-Ram	Swebrec
1	250	253	252	4.33	1.52	2.08	1.23	8.91	8.93	0.50	-1.07
2	254	255	254	4.21	1.51	2.05	1.23	8.91	8.93	0.50	-1.16
3	253	254	254	4.30	1.54	2.07	1.24	8.91	8.93	0.54	-1.12
4	254	255	255	4.42	1.58	2.10	1.26	8.90	8.93	0.53	-1.13
5	253	255	199	4.51	1.61	2.12	1.27	8.90	8.93	0.57	-1.09
6	254	254	254	4.64	1.64	2.15	1.28	2.52	1.17	0.56	-1.05
7	250	251	252	4.75	1.69	2.18	1.30	2.52	1.17	0.61	-1.06
8	249	253	254	4.63	1.38	2.15	1.18	2.50	1.16	0.60	-0.99
9	253	255	255	4.24	1.35	2.06	1.16	2.37	1.15	0.77	-1.11
10	250	255	256	4.38	1.39	2.09	1.18	2.35	1.15	0.75	-1.07
11	253	255	255	4.19	1.43	2.05	1.20	2.15	1.14	0.80	-1.02
12	254	254	254	4.33	1.47	2.08	1.21	2.13	1.14	0.78	-0.97
13	240	254	255	4.47	1.52	2.11	1.23	2.13	1.14	0.81	-1.00
14	254	254	254	4.64	1.57	2.15	1.25	2.10	1.13	0.79	-1.03
15	253	255	255	4.80	1.62	2.19	1.27	2.10	1.13	0.82	-1.07
16	247	250	254	5.00	1.68	2.24	1.29	2.08	1.13	0.80	-1.02
17	253	255	255	3.48	0.84	1.86	0.92	1.76	0.94	2.73	1.86
18	261	258	257	3.62	0.87	1.90	0.93	1.73	0.94	2.66	1.89
19	253	255	255	0.98	0.36	0.99	0.60	1.61	0.92	-1.91	-0.74
20	254	254	254	1.03	0.36	1.01	0.60	1.58	0.92	-1.90	-0.66
21	253	254	255	1.04	0.37	1.02	0.61	1.58	0.92	-1.87	-0.78
22	254	255	253	1.10	0.37	1.05	0.61	1.55	0.91	-1.85	-0.92
23	250	253	254	1.11	0.38	1.06	0.62	1.54	0.85	-1.81	-0.84
24	251	255	255	0.57	0.26	0.75	0.51	1.41	0.84	-1.43	-0.39
25	254	255	252	0.25	0.26	0.50	0.51	1.25	0.84	0.57	-0.28
26	253	255	255	0.24	0.27	0.49	0.52	1.21	0.69	0.79	-0.15
27	253	254	254	0.25	0.27	0.50	0.52	1.17	0.69	0.67	0.00
28	254	255	255	0.26	0.27	0.51	0.52	1.16	0.69	0.54	-0.18
29	253	254	254	0.24	0.27	0.49	0.52	1.15	0.69	0.81	0.00
30	253	255	255	0.25	0.27	0.50	0.52	1.14	0.69	0.66	-0.21
31	254	254	254	0.27	0.28	0.52	0.53	1.10	0.69	0.48	0.00
32	253	255	255	0.25	0.28	0.50	0.53	1.10	0.69	0.86	-0.27
33	253	255	254	0.27	0.29	0.52	0.53	1.05	0.69	0.64	0.00
34	254	255	255	0.29	0.29	0.53	0.53	1.04	0.67	0.37	0.37
35	253	254	256	0.27	0.27	0.52	0.52	1.02	0.67	0.97	0.97
36	253	255	255	0.30	0.30	0.55	0.55	0.91	0.59	0.61	0.61
37	254	254	257	0.33	0.25	0.58	0.50	0.85	0.59	0.00	2.00
38	253	255	257	0.33	0.33	0.58	0.58	0.71	0.35	1.73	1.73
39	253	254	255	0.50	0.00	0.71	0.00	0.32	0.16	0.00	0.00
40	254	254	254	0.00	0.00	0.00	0.00	0.00	0.00	0.00	0.00

Table 5.12 shows the descriptive statistics for the Mogalakwena mine. A low standard deviation means that the data points are close to the mean value, indicating that the dataset has little variability or spread. In other words, the values are tightly grouped. A low RMSE means that the

predictions of the model are remarkably close to the actual values, indicating high accuracy. Low variance suggests that the data points are tightly clustered around the mean value, showing a small spread in the dataset.

5.3.2 Evaluation of BL performance at Isibonelo Colliery

The results of the Root Mean Square Error (RMSE) computations using the predictions from the BlastLogic software and fragmentation measurements from the image analysis. The correlation and regression graphs are from Isibonelo Colliery. Figures 5.8 and 5.9 show the correlation and regression analyses for Kuz-Ram and Swebrec models.

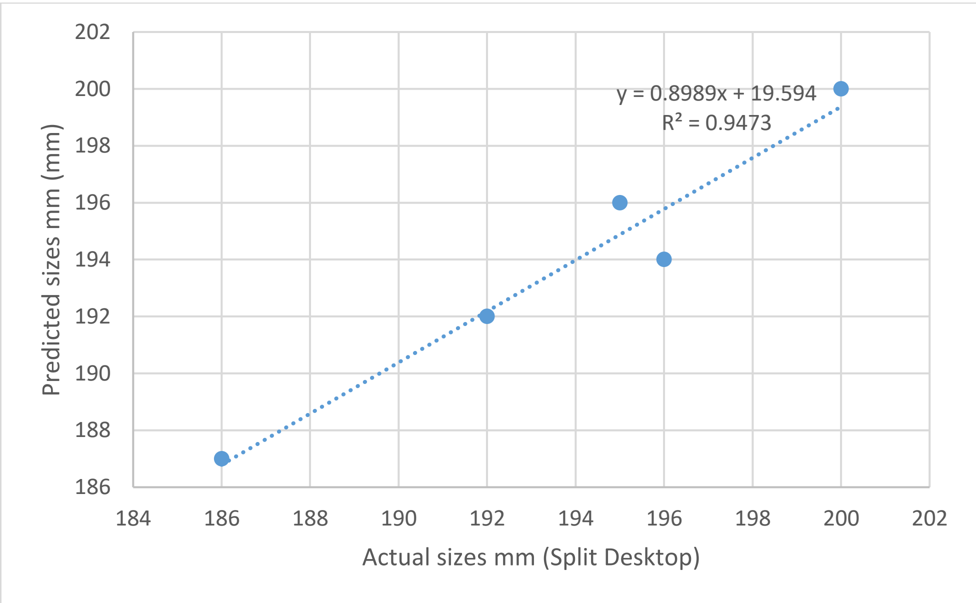

Figure 5.8 Correlation and regression for Isibonelo Colliery for Kuz-ram model

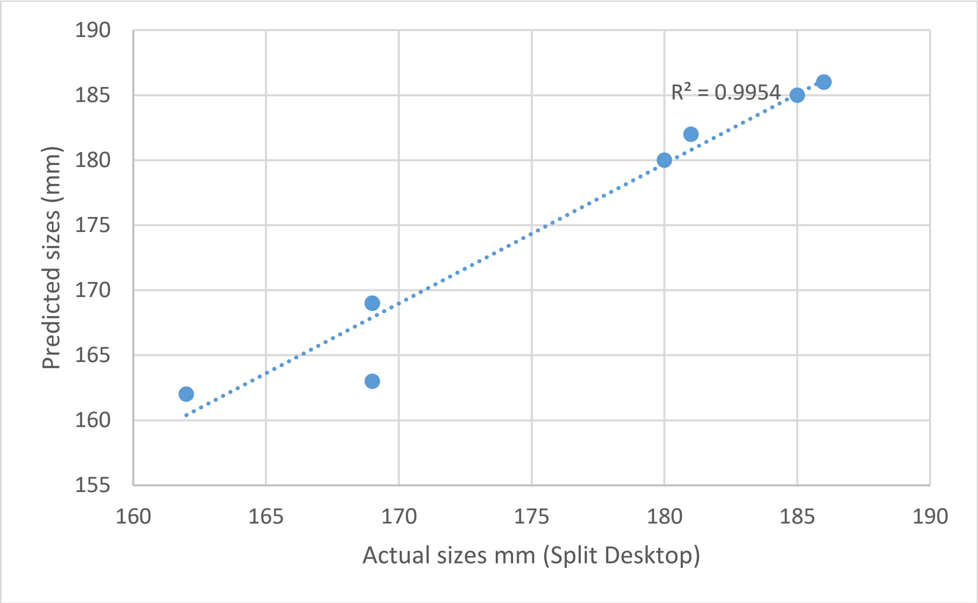

Figure 5.9 Correlation and regression for Isibonelo Colliery for Swebrec model

Figure 5.8 and 5.9 shows the correlation and regression analysis. In the Kuz- Ram model, R^2 is 0.9473 and Swebrec model R^2 is 0.9954. This indicates that there is a positive linear relationship between the two variables (actual fragmentation size and predicted sizes from BlastLogic software), and the regression model provides a reasonable fit to the data.

The details of the RMSE analyses, correlation and regression analyses are shown in Table 5.13. A summary of the results of the Root Mean Square Error (RMSE), variance, and standard deviation.

Table 5.13 The descriptive statistics for Isibonelo Colliery

Blast No:	Predicted size (mm)		Actual (mm)	Variance		Standard deviation		RMSE		Skewness	
	Kuz-Ram	Swebrec		Kuz-Ram	Swebrec	Kuz-Ram	Swebrec	Kuz-Ram	Swebrec	Kuz-Ram	Swebrec
1	206	199	199	5.31	2.61	2.30	1.62	2.70	2.04	1.60	-0.60
2	198	199	200	3.82	2.67	1.95	1.64	2.46	2.04	1.28	-0.58
3	195	199	199	3.92	2.74	1.98	1.66	2.44	2.03	1.26	-0.55
4	199	199	199	3.77	2.81	1.94	1.68	2.36	2.03	1.36	-0.52
5	198	199	200	3.85	2.88	1.96	1.70	2.36	2.03	1.39	-0.49
6	198	199	199	3.96	2.96	1.99	1.72	2.34	2.02	1.37	-0.47
7	198	199	199	4.08	3.05	2.02	1.75	2.33	2.02	1.35	-0.44
8	197	199	199	4.21	3.13	2.05	1.77	2.33	2.02	1.33	-0.41
9	198	199	199	4.31	3.22	2.08	1.80	2.31	2.02	1.28	-0.37
10	198	199	199	4.45	3.32	2.11	1.82	2.30	2.02	1.25	-0.34
11	198	199	200	4.60	3.43	2.15	1.85	2.30	2.02	1.23	-0.31
12	198	200	199	4.77	3.54	2.18	1.88	2.27	2.02	1.20	-0.27
13	197	199	199	4.94	3.57	2.22	1.89	2.27	2.01	1.18	-0.20
14	198	200	199	5.08	3.69	2.25	1.92	2.25	2.01	1.12	-0.16
15	198	199	196	5.28	3.72	2.30	1.93	2.24	2.01	1.09	-0.09
16	205	200	199	5.50	3.86	2.35	1.96	2.22	1.95	1.07	-0.04
17	198	199	201	3.64	3.88	1.91	1.97	2.01	1.94	0.42	0.04
18	197	200	199	3.81	4.03	1.95	2.01	1.95	1.92	0.41	0.10
19	198	199	199	3.95	4.05	1.99	2.01	1.92	1.91	0.35	0.20
20	198	199	199	4.15	4.20	2.04	2.05	1.92	1.91	0.35	0.27
21	203	203	199	4.37	4.37	2.09	2.09	1.91	1.91	0.34	0.34
22	198	198	199	3.12	3.12	1.77	1.77	1.80	1.80	-0.34	-0.34
23	198	198	199	3.29	3.29	1.81	1.81	1.80	1.80	-0.30	-0.30
24	202	202	199	3.49	3.49	1.87	1.87	1.79	1.79	-0.26	-0.26
25	198	198	200	2.38	2.38	1.54	1.54	1.72	1.72	-1.60	-1.60
26	197	197	199	2.52	2.52	1.59	1.59	1.70	1.70	-1.50	-1.50
27	200	200	200	2.71	2.71	1.65	1.65	1.67	1.67	-1.52	-1.52
28	197	197	199	2.31	2.31	1.52	1.52	1.67	1.67	-2.16	-2.16
29	195	195	199	2.52	2.52	1.59	1.59	1.64	1.64	-2.13	-2.13
30	198	198	199	2.25	2.25	1.50	1.50	1.51	1.51	-2.93	-2.93
31	198	198	200	2.46	2.46	1.57	1.57	1.50	1.50	-2.79	-2.79
32	198	198	199	2.69	2.69	1.64	1.64	1.47	1.47	-2.63	-2.63
33	197	197	199	2.98	2.98	1.73	1.73	1.46	1.46	-2.47	-2.47
34	198	198	199	3.48	3.48	1.86	1.86	1.42	1.42	-2.45	-2.45
35	198	198	199	4.00	4.00	2.00	2.00	1.41	1.41	-2.25	-2.25
36	198	198	200	4.70	4.70	2.17	2.17	1.41	1.41	-2.03	-2.03
37	198	198	199	5.67	5.67	2.38	2.38	1.37	1.37	-1.78	-1.78
38	197	197	200	7.00	7.00	2.65	2.65	1.36	1.36	-1.46	-1.46
39	198	198	199	12.50	12.50	3.54	3.54	1.27	1.27	1.20	1.37
40	193	193	201	0.00	1.22	0.00	0	1.26	1.26	1.22	1.10

Table 5.13 shows the descriptive statistics for Isibonelo Colliery. This shows the variance, standard deviation, RMSE and skewness of the results. The Swebrec model had the least RMSE compared to Kuz-Ram. Swebrec model prediction was close to the actual sizes from the Split Desktop. The results of the Root Mean Square Error (RMSE) computations using the predictions from the BlastLogic software and fragmentation measurements from the image analysis.

5.3.3 Evaluation of BL performance at Navigation Colliery

The results of the Root Mean Square Error (RMSE) computations using the predictions from the BlastLogic software and fragmentation measurements from the image analysis. The correlation and regression graphs are from Navigation Colliery. Figures 5.10 and 5.11 shows the correlation and regression analyses for Kuz-Ram and Swebrec models.

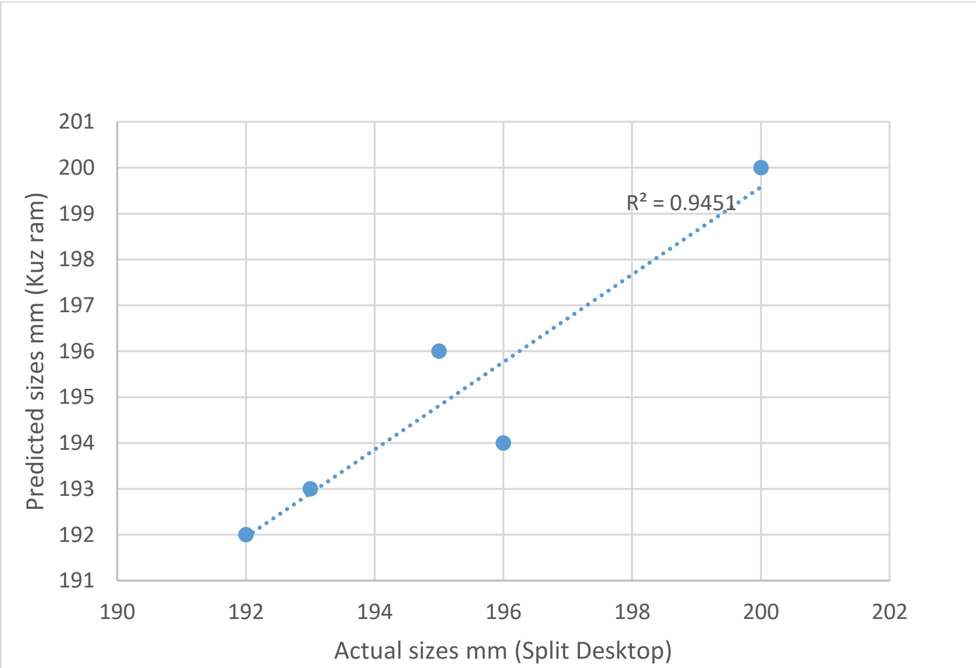

Figure 5.10 Correlation and regression for Navigation Colliery for Kuz-ram model

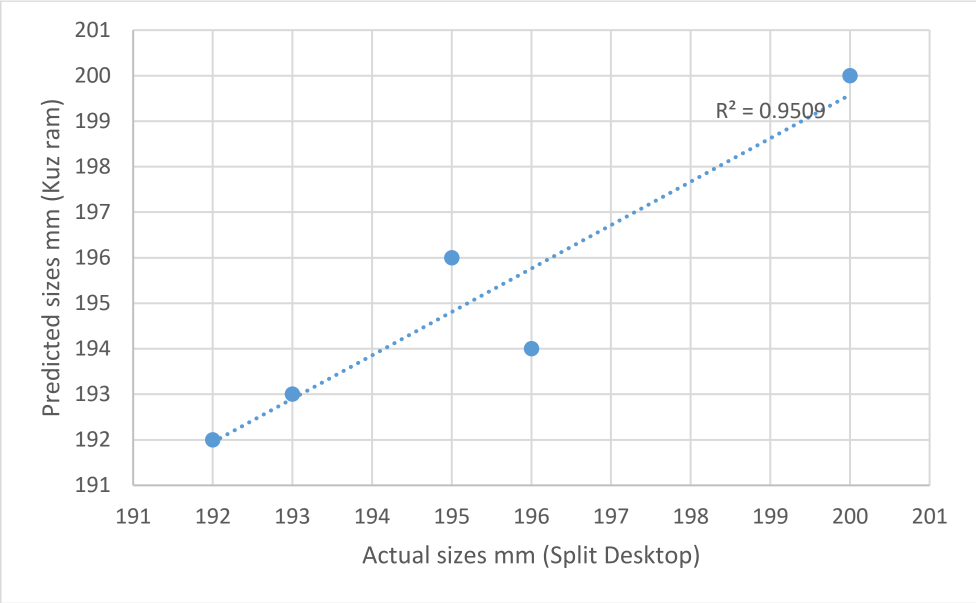

Figure 5.11 Correlation and regression for Navigation Colliery for Swebrec model

Figure 5.10 and 5.11 shows the correlation and regression analysis. In the Kuz- Ram model, R^2 is 0.9473 and Swebrec model R^2 is 0.9505. This indicates that there is a positive linear relationship between the two variables (actual fragmentation size and predicted sizes from BlastLogic software), and the regression model provides a reasonable fit to the data.

A summary of the results of the Root Mean Square Error (RMSE), variance, standard deviation and skewness for Navigation Colliery are presented in Table 5.14.

Table 5.14 The descriptive statistics for Navigation Colliery

Blast No:	Predicted size (mm)		Actual (mm)	Variance		Standard deviation		RMSE		Skewness	
	Kuz-Ram	Swebrec		Kuz-Ram	Swebrec	Kuz-Ram	Swebrec	Kuz-Ram	Swebrec	Kuz-Ram	Swebrec
1	206	199	199	5.31	2.61	2.30	1.62	2.70	2.04	1.60	-0.60
2	198	199	200	3.82	2.67	1.95	1.64	2.46	2.04	1.28	-0.58
3	195	199	199	3.92	2.74	1.98	1.66	2.44	2.03	1.26	-0.55
4	199	199	199	3.77	2.81	1.94	1.68	2.36	2.03	1.36	-0.52
5	198	199	200	3.85	2.88	1.96	1.70	2.36	2.03	1.39	-0.49
6	198	199	199	3.96	2.96	1.99	1.72	2.34	2.02	1.37	-0.47
7	198	199	199	4.08	3.05	2.02	1.75	2.33	2.02	1.35	-0.44
8	197	199	199	4.21	3.13	2.05	1.77	2.33	2.02	1.33	-0.41
9	198	199	199	4.31	3.22	2.08	1.80	2.31	2.02	1.28	-0.37
10	198	199	199	4.45	3.32	2.11	1.82	2.30	2.02	1.25	-0.34
11	198	199	200	4.60	3.43	2.15	1.85	2.30	2.02	1.23	-0.31
12	198	200	199	4.77	3.54	2.18	1.88	2.27	2.02	1.20	-0.27
13	197	199	199	4.94	3.57	2.22	1.89	2.27	2.01	1.18	-0.20
14	198	200	199	5.08	3.69	2.25	1.92	2.25	2.01	1.12	-0.16
15	198	199	196	5.28	3.72	2.30	1.93	2.24	2.01	1.09	-0.09
16	205	200	199	5.50	3.86	2.35	1.96	2.22	1.95	1.07	-0.04
17	198	199	201	3.64	3.88	1.91	1.97	2.01	1.94	0.42	0.04
18	197	200	199	3.81	4.03	1.95	2.01	1.95	1.92	0.41	0.10
19	198	199	199	3.95	4.05	1.99	2.01	1.92	1.91	0.35	0.20
20	198	199	199	4.15	4.20	2.04	2.05	1.92	1.91	0.35	0.27
21	203	203	199	4.37	4.37	2.09	2.09	1.91	1.91	0.34	0.34
22	198	198	199	3.12	3.12	1.77	1.77	1.80	1.80	-0.34	-0.34
23	198	198	199	3.29	3.29	1.81	1.81	1.80	1.80	-0.30	-0.30
24	202	202	199	3.49	3.49	1.87	1.87	1.79	1.79	-0.26	-0.26
25	198	198	200	2.38	2.38	1.54	1.54	1.72	1.72	-1.60	-1.60
26	197	197	199	2.52	2.52	1.59	1.59	1.70	1.70	-1.50	-1.50
27	200	200	200	2.71	2.71	1.65	1.65	1.67	1.67	-1.52	-1.52
28	197	197	199	2.31	2.31	1.52	1.52	1.67	1.67	-2.16	-2.16
29	195	195	199	2.52	2.52	1.59	1.59	1.64	1.64	-2.13	-2.13
30	198	198	199	2.25	2.25	1.50	1.50	1.51	1.51	-2.93	-2.93
31	198	198	200	2.46	2.46	1.57	1.57	1.50	1.50	-2.79	-2.79
32	198	198	199	2.69	2.69	1.64	1.64	1.47	1.47	-2.63	-2.63
33	197	197	199	2.98	2.98	1.73	1.73	1.46	1.46	-2.47	-2.47
34	198	198	199	3.48	3.48	1.86	1.86	1.42	1.42	-2.45	-2.45
35	198	198	199	4.00	4.00	2.00	2.00	1.41	1.41	-2.25	-2.25
36	198	198	200	4.70	4.70	2.17	2.17	1.41	1.41	-2.03	-2.03
37	198	198	199	5.67	5.67	2.38	2.38	1.37	1.37	-1.78	-1.78
38	197	197	200	7.00	7.00	2.65	2.65	1.36	1.36	-1.46	-1.46
39	198	198	199	12.50	12.50	3.54	3.54	1.27	1.27	0.00	0.00
40	193	193	201	0.00		0.00	0.00	1.26	1.26	0.00	0.00

Table 5.14 shows the descriptive statistics for Navigation Colliery. A low standard deviation means that the data points are close to the mean value, indicating that the dataset has little variability or spread. The values are tightly grouped. A low RMSE means that the predictions of the model are close to the actual values, indicating high accuracy. Low variance suggests that the data points are tightly clustered around the mean value, indicating a small spread in the dataset.

5.3.4 Evaluation of BL performance at Kolomela Iron Ore Mine

The results of the Root Mean Square Error (RMSE) computations using the predictions from the BlastLogic software and fragmentation measurements from the image analysis. The correlation and regression graphs are from the Kolomela Iron Ore mine. Figures 5.12 and 5.13 show the correlation and regression analyses for Kuz-Ram and Swebrec models.

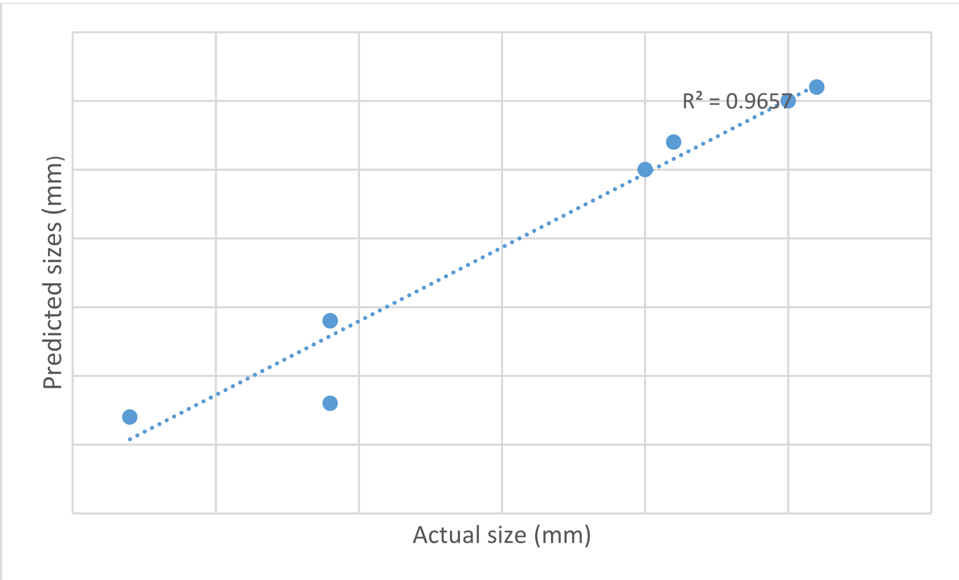

Figure 5.12 Correlation and regression for Kolomela Iron ore mine for Kuz-Ram model

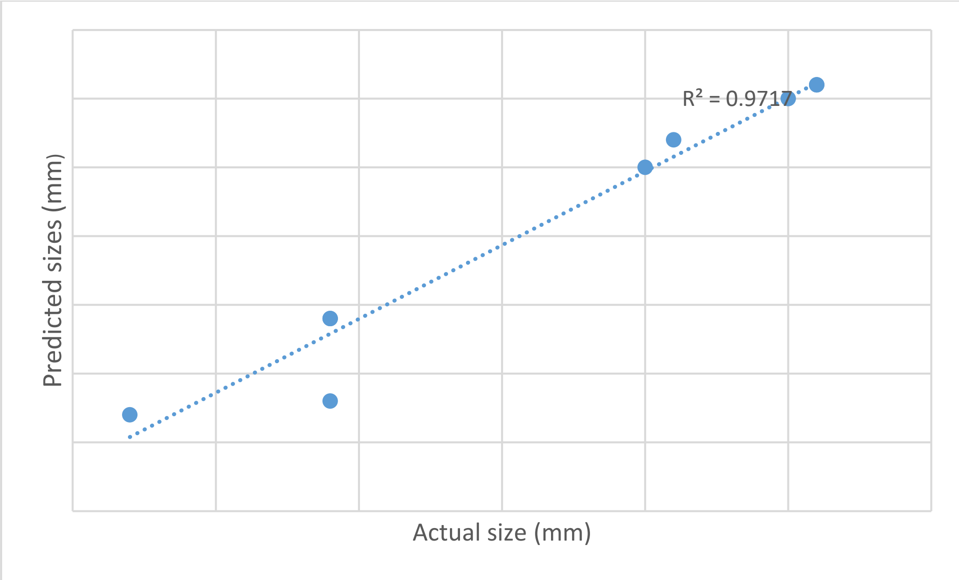

Figure 5.13 Correlation and regression for Kolomela Iron ore mine for Swebrec model

Figure 5.12 and 5.13 shows the correlation and regression analysis. In the Kuz- Ram model, R^2 is 0.9657 and Swebrec model R^2 is 0.9717. This indicates that there is a positive linear relationship between the two variables (actual fragmentation size and predicted sizes from BlastLogic software), and the regression model provides a reasonable fit to the data. Table 5.15 shows the descriptive statistics of the Kolomela mine.

Table 5.15 Table 5.15 Results of the descriptive statistics for Kolomela Iron Ore mine

Blast No:	Predicted size (mm)		Actual (mm)	Variance		Standard deviation		RMSE		Skewness	
	Kuz-Ram	Swebrec		Kuz-Ram	Swebrec	Kuz-Ram	Swebrec	Kuz-Ram	Swebrec	Kuz-Ram	Swebrec
1	204	200	199	14.32	26.89	3.78	5.19	4.36	4.17	c	1.05
2	208	211	210	14.50	27.50	3.81	5.24	4.28	4.16	1.78	1.02
3	200	200	200	13.62	25.98	3.69	5.10	4.27	4.16	1.99	1.13
4	200	199	199	13.97	26.62	3.74	5.16	4.27	4.16	1.94	1.09
5	198	200	199	14.33	27.15	3.79	5.21	4.27	4.16	1.90	1.05
6	200	200	201	14.46	27.85	3.80	5.28	4.27	4.16	1.88	1.01
7	211	202	203	14.85	28.57	3.85	5.35	4.26	4.15	1.83	0.97
8	211	203	199	12.25	29.47	3.50	5.43	4.07	4.15	2.08	0.96
9	198	195	199	9.27	30.38	3.05	5.51	3.60	4.10	2.36	0.97
10	198	200	200	9.35	29.74	3.06	5.45	3.60	4.05	2.34	0.98
11	211	199	199	9.41	30.60	3.07	5.53	3.58	4.05	2.34	0.93
12	207	201	199	5.90	31.31	2.43	5.60	3.04	4.05	2.52	0.88
13	200	201	200	4.47	32.40	2.11	5.69	2.77	4.04	3.14	0.84
14	198	198	199	4.64	33.56	2.15	5.79	2.77	4.04	3.08	0.80
15	198	203	200	4.62	34.09	2.15	5.84	2.76	4.03	3.15	0.74
16	198	197	199	4.58	35.50	2.14	5.96	2.74	4.01	3.25	0.74
17	198	199	199	4.52	35.62	2.13	5.97	2.74	3.99	3.39	0.68
18	205	201	200	4.43	36.55	2.10	6.05	2.73	3.99	3.58	0.61
19	209	199	198	3.68	38.09	1.92	6.17	2.62	3.99	4.69	0.55
20	200	197	199	16.58	39.11	2.43	6.25	1.96	3.99	0.34	0.47
21	200	198	200	17.15	38.99	2.11	6.24	1.95	3.97	-0.34	0.40
22	200	200	200	17.76	39.32	2.15	6.27	1.95	3.96	-0.30	0.30
23	200	211	202	16.23	40.69	2.15	6.38	1.95	3.96	-0.26	0.21
24	200	211	203	12.18	40.10	2.14	6.33	1.92	3.70	-1.60	0.35
25	200	198	195	10.15	39.00	2.13	6.24	1.86	3.47	-1.50	0.52
26	200	198	200	10.58	39.69	2.43	6.30	1.69	3.44	-1.52	0.41
27	200	200	200	11.04	40.15	2.11	6.34	1.69	3.43	-2.16	0.28
28	200	211	202	9.16	42.06	2.15	6.49	1.69	3.43	-2.13	0.14
29	200	211	203	9.50	41.48	2.15	6.44	1.66	3.12	-2.93	0.35
30	200	198	195	4.15	39.89	2.14	6.32	1.59	2.85	-2.79	0.61
31	200	198	200	4.37	41.16	2.13	6.42	1.38	2.81	-2.63	0.43
32	200	200	200	3.12	41.94	2.43	6.48	1.38	2.79	-2.47	0.22
33	200	211	202	3.29	45.07	2.11	6.71	1.38	2.79	-2.45	-0.03
34	200	211	203	3.49	45.14	2.15	6.72	1.34	2.40	0.34	0.33
35	200	198	195	2.38	42.27	2.15	6.50	1.25	2.04	-0.34	0.91
36	200	198	200	2.52	46.30	2.14	6.80	0.97	1.99	-0.30	0.55
37	200	200	200	16.58	48.67	2.13	6.98	0.97	1.96	-0.26	-0.07
38	200	211	202	17.15	56.33	2.43	7.51	0.97	1.96	-1.60	-1.73
39	200	211	203	17.76	84.50	2.11	9.19	0.92	1.35	-1.50	-2.03
40	200	198	195	16.23	6.80	2.15	6.80	0.79	0.47	-1.52	-1.78

Table 5.15 shows the descriptive statistics for the Kolomela Iron Ore mine. A low standard deviation means that the data points are close to the mean value, indicating that the dataset has little variability or spread. The values are tightly grouped. A low RMSE means that the predictions of the model are close to the actual values, indicating high accuracy. Low variance suggests that the data points are tightly clustered around the mean value, indicating a small spread in the dataset.

5.3.5 Evaluation of BL performance at Sishen Iron Ore Mine

The results of the Root Mean Square Error (RMSE) computations using the predictions from the BlastLogic software and fragmentation measurements from the image analysis. The correlation and regression graphs are from the Sishen Iron Ore mine. Figures 5.14 and 5.15 show the correlation and regression analyses for the Kuz-Ram and Swebrec models.

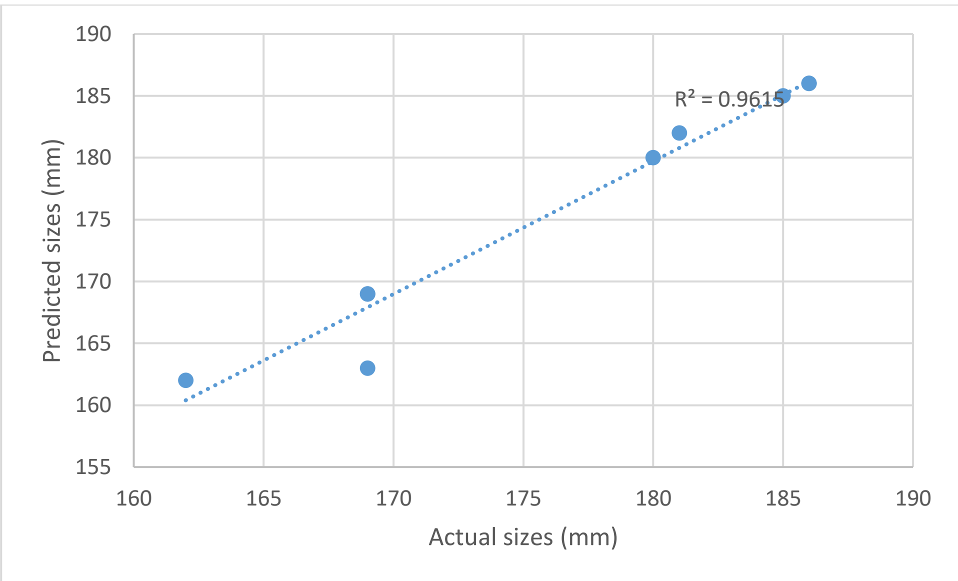

Figure 5.14 Correlation and regression for Sishen Iron Ore mine for Kuz-ram model

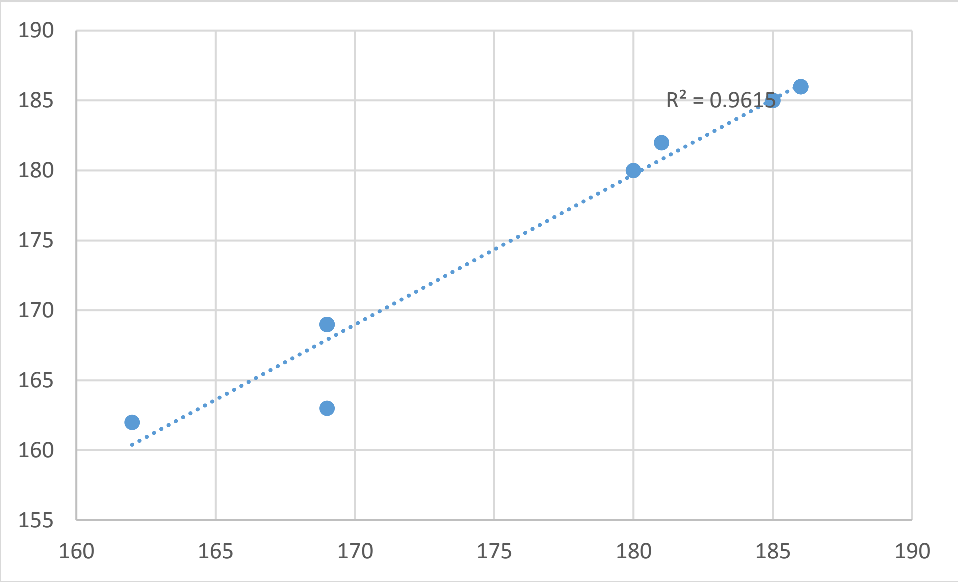

Figure 5.15 Correlation and regression for Sishen Iron Ore mine for Swebrec model

Figure 5.12 and 5.13 shows the correlation and regression analysis. The Kuz- Ram model, R^2 is 0.9613 and Swebrec model R^2 is 0.9613. This indicates that there is a positive linear relationship between the two variables (actual fragmentation size and predicted sizes from BlastLogic software), and the regression model provides a reasonable fit to the data.

A summary of the results of the Root Mean Square Error (RMSE), variance, standard deviation, and skewness for Sishen Iron Ore mine are presented in Table 5.16.

Table 5.16 Results of the descriptive statistics for Sishen Iron Ore mine

Blast No:	Predicted size (mm)		Actual (mm)	Variance		Standard deviation		RMSE		Skewness	
	Kuz-Ram	Swebrec		Kuz-Ram	Swebrec	Kuz-Ram	Swebrec	Kuz-Ram	Swebrec	Kuz-Ram	Swebrec
1	206	199	199	5.31	2.61	2.30	1.62	2.70	2.04	1.60	-0.60
2	198	199	200	3.82	2.67	1.95	1.64	2.46	2.04	1.28	-0.58
3	198	200	199	14.33	27.15	3.79	5.21	4.27	4.16	1.90	1.05
4	200	200	201	14.46	27.85	3.80	5.28	4.27	4.16	1.88	1.01
5	211	202	203	14.85	28.57	3.85	5.35	4.26	4.15	1.83	0.97
6	211	203	199	12.25	29.47	3.50	5.43	4.07	4.15	2.08	0.96
7	198	195	199	9.27	30.38	3.05	5.51	3.60	4.10	2.36	0.97
8	198	200	199	14.33	27.15	3.79	5.21	4.27	4.16	1.90	1.05
9	200	200	201	14.46	27.85	3.80	5.28	4.27	4.16	1.88	1.01
10	211	202	203	14.85	28.57	3.85	5.35	4.26	4.15	1.83	0.97
11	211	203	199	12.25	29.47	3.50	5.43	4.07	4.15	2.08	0.96
12	198	195	199	9.27	30.38	3.05	5.51	3.60	4.10	2.36	0.97
13	198	200	199	14.33	27.15	3.79	5.21	4.27	4.16	1.90	1.05
14	200	200	201	14.46	27.85	3.80	5.28	4.27	4.16	1.88	1.01
15	198	199	196	5.28	3.72	2.30	1.93	2.24	2.01	1.09	-0.09
16	205	200	199	5.50	3.86	2.35	1.96	2.22	1.95	1.07	-0.04
17	198	199	201	3.64	3.88	1.91	1.97	2.01	1.94	0.42	0.04
18	197	200	199	3.81	4.03	1.95	2.01	1.95	1.92	0.41	0.10
19	198	199	199	3.95	4.05	1.99	2.01	1.92	1.91	0.35	0.20
20	198	199	199	4.15	4.20	2.04	2.05	1.92	1.91	0.35	0.27
21	203	203	199	4.37	4.37	2.09	2.09	1.91	1.91	0.34	0.34
22	198	198	199	3.12	3.12	1.77	1.77	1.80	1.80	-0.34	-0.34
23	198	198	199	3.29	3.29	1.81	1.81	1.80	1.80	-0.30	-0.30
24	202	202	199	3.49	3.49	1.87	1.87	1.79	1.79	-0.26	-0.26
25	200	200	200	17.76	39.32	0.00	6.27	1.95	3.96	-0.30	0.30
26	200	211	202	16.23	40.69	0.00	6.38	1.95	3.96	-0.26	0.21
27	200	211	203	12.18	40.10	0.00	6.33	1.92	3.70	-1.60	0.35
28	200	198	195	10.15	39.00	0.00	6.24	1.86	3.47	-1.50	0.52
29	200	198	200	10.58	39.69	0.00	6.30	1.69	3.44	-1.52	0.41
30	200	200	200	11.04	40.15	0.00	6.34	1.69	3.43	-2.16	0.28
31	200	200	200	17.76	39.32	0.00	6.27	1.95	3.96	-0.30	0.30
32	200	211	202	16.23	40.69	0.00	6.38	1.95	3.96	-0.26	0.21
33	200	211	203	12.18	40.10	0.00	6.33	1.92	3.70	-1.60	0.35
34	200	198	195	10.15	39.00	0.00	6.24	1.86	3.47	-1.50	0.52
35	202	203	14.85	28.57	3.85	5.35	4.26	4.15	1.83	0.97	0.21
36	203	199	12.25	29.47	3.50	5.43	4.07	4.15	2.08	0.96	0.35
37	195	199	9.27	30.38	3.05	5.51	3.60	4.10	2.36	0.97	0.52
38	200	200	9.35	29.74	3.06	5.45	3.60	4.05	2.34	0.98	0.41
39	199	199	9.41	30.60	3.07	5.53	3.58	4.05	2.34	0.93	0.21
40	202	203	14.85	28.57	3.85	5.35	4.26	4.15	1.83	0.97	0.35

Table 5.16 shows the descriptive statistics for Navigation Colliery. A low standard deviation means that the data points are close to the mean value, indicating that the dataset has little variability or spread. In other words, the values are tightly grouped. A low RMSE means that the predictions of the model are close to the actual values, indicating high accuracy. Low variance suggests that the data points are tightly clustered around the mean value, indicating a small spread in the dataset.

5.3.6 Summary evaluation of BlastLogic software model performance

The root mean square of all the models was evaluated. With the correlation and regression analysis, the highest correlation coefficient, R, and coefficient of determination, R^2 values were considered as the best for the parameters and patterns used. The R values also establish the strength of the relationship between the design parameters and the actual fragmentation size distribution. The higher the R-value, the better the relationship that exists between the design parameters and the actual fragmentation. The results were calculated using Microsoft Excel.

In summary, when these terms are described as "low," it implies that the data points or predicted values are closely packed together, reflecting high precision or accuracy in the measurements or predictions. It is generally desired to have low standard deviation, low RMSE, and low variance in many applications as it indicates a more reliable and consistent dataset or model performance. A symmetric distribution has zero skewness, as both sides are balanced around the mean. However, most of the real-world problem datasets can exhibit some degree of skewness, and understanding the skewness is essential in interpreting and analysing the data correctly.

5.4 Summary of Chapter 5

Chapter 5 provided a comprehensive understanding of the discussion and analysis of results. It additionally looked at the cost analysis associated with the deviation from the fragmentation size distribution. The chapter also further evaluates the BL performance. The next chapter discusses the conclusions and recommendations for future work.

6 CONCLUSIONS AND RECOMMENDATIONS

6.1 Overview

The study's findings are presented in Chapter 5 in connection to the study's goals and problem description. An overview of the findings regarding the study's goals is provided in Section 6.2. The recommendations and ideas offered in Sections 6.3 and 6.4, respectively, could be taken into consideration for future development.

6.2 Conclusions and Contribution to Knowledge

In conclusion, this study investigated the evaluation of the BlastLogic software in predicting the fragmentation distribution for surface mines. The investigation aimed to highlight the software's capabilities and its potential impact on enhancing performance in this critical aspect of blasting operations. Through a comprehensive examination of its functionalities, the study addressed the significance of utilising modern technological solutions, such as BlastLogic software, in evaluating fragmentation distribution analysis. The findings highlighted the importance of accurate prediction of fragmentation data in mining activities, highlighting how software tools like BlastLogic software can potentially revolutionise traditional practices and contribute to more efficient and controlled blasting outcomes. As the mining industry continues to evolve, integrating advanced software solutions like BlastLogic can play a pivotal role in achieving safer, more productive, and environmentally conscious operations (Gadikor, 2018).

The research evaluated the performance of BlastLogic software predicting fragmentation size with a combined input data of 200 blast observations for five surface mines under study. The number of site observations provided valuable insight into the relative performance of the BlastLogic software. The accuracy level of BlastLogic software was tested against the actual fragmentation results obtained from the pit to verify the accuracy.

From the study conducted, the following conclusions can be drawn:

- Kuz-Ram and Swebrec models accurately predicted the fragmentation size distribution.
- Two models from the BlastLogic software—Kuz-Ram and Swebrec modified Kuz-Ram—had correlation coefficient, R, and coefficient of determination R^2 , high values (over 90%). The RMSE was modest (usually under 15%) in calculations. This showed improved fragmentation and a stronger correlation with the selected blast design parameters.
- The prediction errors for the Swebrec model compared to Kuz-Ram was less than 15%, it performed better in the fine regions.
- The BlastLogic software models performed well with the given blast designs to achieve the best fragmentation, as there has been a significant cost reduction.

6.3 Recommendations

The BlastLogic software offered accurate predictions as shown from the results analysis. Therefore, it is recommended that it be applied to other case studies in surface mines. In addition, the application of BlastLogic software is still amenable to improvements and makes it more practical and acceptable in the mining industry. The author recommends that:

- Ways to reduce computational time and computer memory requirements be explored to make the BlastLogic software amenable to mine fragmentation modelling requirements in terms of efficiency.
- For the chosen blast design parameters, there should be a comprehensive understanding of the pit geology and characteristics before applying them.

- The surface mining industry should adopt the Modified Kuz-Ram model (Swebrec model) to predict fragmentation size distribution.
- With sufficient understanding of the rock qualities, the outputs of the projections from all the models could be used to build blasts for unexplored areas because there was a high link between them.
- The average amount of fines produced from the 200 blasts studied was less than 15%, with an insignificant amount of oversized material less than 5%.
-

6.4 Limitations and Recommendations Future Research Work

This research focused on Platinum, Collieries, and Iron Ore surface mines, as these are part of the surface mines with BlastLogic software in South Africa. Based on the findings of this research, a similar study can be conducted on other different commodities in surface mines. Additional studies on the evaluation of the performance of the BlastLogic software in predicting fragmentation distribution with other mineral commodities would improve the available knowledge. The number of blasts was restricted to 50 blasts per mine observation for the study. Future work could consider more blasts beyond the regulated time. An additional limitation is that only historical data was used. For better fragmentation prediction, it would also be beneficial to compare different blast designs for the same rock type at the same mine. The aim of understanding the impact of BlastLogic software performance in predicting fragmentation distribution while using the new mining technologies.

7 REFERENCES

Abdallah, M. and Haidar, F. (2019). Modelling of dynamic fracture mechanism in rock masses due to wave propagation. *International Journal of Engineering and Technology*, Vol. 4, No. 4, pp. 4683-4690.

Adebola, J.M., Ajayi, O. D. and Peter, E. O. (2016). Rock fragmentation prediction using Kuz-Ram model. *Journal of Environment and Earth Science*, Vol. 6, No. 5, pp 111-113.

Alchin, D. and Botha, W. (2006). The structural/ stratigraphic development of the Sishen South (Welgevonden) iron ore deposit, South Africa, as deduced from ground gravity data modelling. *Applied Earth Science*, Vol. 115, No. 4, pp 174-186.

Altindag, R. (2012). Correlation between P-wave velocity and some mechanical properties for sedimentary rocks. *Journal of the Southern African Institute of Mining and Metallurgy*, Vol. 111, No.1, pp 36-45.

Armitage, P., McDonald, I., Edwards, S. and Manby, G. (2002). PGE Mineralisation in the Platreef and Calc-Silicate Footwall at Sandsloot, Potgiersrus District. *Applied Earth Science, Vol.* 111, No. 1, pp. 36-45.

Babaeian, M., Ataei, M., Sereshki, F., Sotoudeh, F., and Mohammadi, S. (2019). A new framework for evaluation of rock fragmentation in open pit mines. *Journal of Rock Mechanics and Geotechnical Engineering,* Vol. 11, No.2, pp 325-336.

Bahrami, A., Monjezi, M., Goshtasbi, K., and Ghazvinian, A. (2010). Prediction of rock fragmentation due to blasting using artificial neural network. *Engineering with Computers,* Vol. 27, No.2, pp 177-181.

Barakat, R. (1976). Sums of independent lognormally distributed random variables. *Journal of the Optical Society of America.* Vol. 66, No.3, pp 211-216.

Baumgardt, H.G., Schott, J.U., Sakamoto, Y., Schopper, E., Stöcker, H., Hofmann, J., Scheid, W., and Greiner, W. (1975). Shock waves and mach cones in fast nucleus-nucleus collisions. *Zeitschrift fur Physik A. Atoms and nuclei,* Vol. 273, No.4, pp 359-371.

Baxter, R. (2021). Facts and Figures 2021. Changing mines and lives, Pretoria*: Mineral Council of South Africa.* AVAILABLE AT. https://www.mineralscouncil.org.za/downloads/send/16-featured/1875-facts-and-figures-2021. [Accessed 12 December 2022].

Bekker, A., Slack, F., Planavsky, N., Krapez, B., Hofmann, A., Konhauser, O., and Rouxel, O.J. (2010). Iron formation: The sedimentary product of a complex interplay among mantle, tectonic, oceanic, and biospheric processes. *Economic Geology,* Vol. 105, No.3, pp 467-598.

Bennett, J. D. (1936). Broken Coal. *Journal of the Institute of Fuel,* Vol. 10, No.1, pp 22-39.

Bergmann, O., Riggle, J.W. and Wu, F. (1973). Model rock blasting effect of explosives properties and other variables on blasting results. *International Journal of Rock Mechanics and Mining Sciences & Geomechanics Abstracts,* Vol. 10, No.6, pp 585-612.

Bhandari, S. (1997). Operations, Engineering Rock Blasting. Netherlands, A. A Balkema: Rotterdam. Available at: https://miningandblasting.files.wordpress.com/2009/09/engineering-rock-blasting-operations_bhandari.pdf.

BME (2021). Bulk emulsions. Available at: https://bme.co.za/products/buk-emulsions. [Accessed 25 December 2022].

Bowa, V.M. (2015). Optimisation of blasting design parameters on open pit. A case study of Nchanga open pits. *International Journal of Scientific and Technology Research*, Vol. 4, No. 9, pp 45-51.

Borisson, G. (2003). Measurement of Size Distribution of Blasted Rock Using Digital Image Processing. *Fragblast*, Vol. 7, No. 3,pp 181-193.

Broadbent, S. R. and Callcott, G.T. (1956). A matrix analysis of process involving particle assemblies. *Philosophical Transactions of the Royal Society of London. Serw3sewies A, Mathematical and Physical Sciences*, Vol. 249, No. 960, pp 99-123.

Brunton, P. J., West, D. G. and McCormack, P. (2003). Fragmentation profile effects on excavator and loading unit efficiency. *International Journal of Mining Science and Technology*, Vol. 13, No. 2, pp 189-197.

Bye, A.R. (2005). Geotechnical, metallurgical, and blasting information for blast. Johannesburg Internal Anglo Platinum Report. PPL.

Chiapetta, R. and Postupack, C. (1995). An update on causes and recommendations for controlling coal damage when blasting overburden. *Brisbane, Explo*-95.

Chen, Y., Wang, X. and Li, H. (2018). Influence of rock strength and blast design parameters on rock fragmentation size distribution. Rock Mechanics and Rock Engineering, Vol. 51, No. 1, pp 165-177.

Chen, Y., and Zhang, J. (2021). Numerical modeling of rock fragmentation under blasting using the discrete element method. International Journal of Rock Mechanics and Mining Sciences, 143, 104752.

Chi, G., Fuerstenau, M., Bradt, R. and Ghosh, A. (1996). Improved communition efficiency through controlled blasting during mining. *International Journal of Mineral Processing,* Vol. 47, No. 1-2, pp 93-101.

Choudhary, B.S. (2013). Firing patterns and its effect on muckpile shape parameters and fragmentation in quarry blasts. *International Journal of Research in Engineering and Technology*, Vol. 2, No. 9, pp 32-45.

Choudhary, B.S. (2019). Effect of blast induced rock fragmentation and muckpile. Mining of Mineral Deposits, Vol.13, No. 3, pp 119-126.

Choudhary, B. S and Gupta, A. (2012). A comparative study on fragmentation measurement techniques. *Mining Engineers' Journal, Mining Engineers' Association of India*, Vol. 14, No. 3, pp. 16 – 24.

Chung, S. H. and Katsabanis, P. (2000). Fragmentation prediction using improved engineering formulae. *Fragblast: International Journal for Blasting and Fragmentation*, Vol.4, No. 3-4, pp 198-207.

Cundall, P. A., and Strack, O. D. L. (1979). A discrete numerical model for granular assemblies. Géotechnique, Vol. 29, No.1, pp 47-65.

Cunningham, C. (1983). The Kuz-Ram model for prediction of fragmentation from blasting. First International Symposium on Rock Fragmentation by Blasting, Vol.1, No. 1, pp 439-454.

Cunningham, C. (2005). The Kuz-Ram model 20 years on. Brighton conference proceedings, pp 201-210.

Dehran, S. (2018). Digital applications in metals and mining industry. *American Journal of Operations Management and Information Systems*, Vol. 3, No. 1, p 33.

Dimitraki, L., Christaras, B., Marinos, V., Vlahavas, L. and Arampelos, N. (2018). Predicting the average size of blasted rocks in aggregate quarries using artificial neural networks. *Bulleting of Engineering Geology and the Environment,* Vol. 78, No. 4, pp 2717-2729.

Drebenstedt, C and Singhal, R. (2013). *Mine Planning and Equipment Selection. Dresden,* Germany, Springs.

Dumakor-Dupey, N., Arya, S. and Jha, A (2021). Advances in blast-induced impact prediction. *A Review of Machine Learning Applications*, Vol. 31, No. 3, p 601.

Ediriweera, A. and Wiewiora, A. (2021). Barriers and enablers of technology adoption in the mining industry. *Resources Policy*, Vol.73, No. 10, pp 102-188.

Eloranta, J. (1995). Selection of powder factor in large diameter blastholes. *International Society of Explosives Engineers*, Vol. 6, No. 95, pp 25-34.

Entemann, C. (2000). A fuzzy logic with interval truth values. *International Journal of Fuzzy Sets and Systems*, Vol. 113, No. 2, pp 161-183.

Gadikor, J. (2018). Optimisation of drilling and blasting practices at a western US open pit copper mine. Nevada, University of Montana. Thesis, Nevada, University of Montana. Available at: https://digitalcommons.mtech.edu/grad_rsch/168. [Accessed 22 December 2022].

Garg, S., Brown, M. and Chen, X. (2021). Environmental impacts of poor fragmentation in surface mining: A case study. Environmental Science and Pollution Research, Vol.28, No. 9, pp 10629-10638.

Gates, A. (1915). Kick vs Rittinger an experimental investigation in rock crushing, performed at Purdue University. Transaction of the American Institute of Mining, Metallurgical, and Petroleum Engineers, pp 43-50.

Gaudin, T. and Meloy, T. (1962). Model and a comminution distribution equation for repeated fracture. *Transactions of the American Institute of Mining Metallurgical and Petroleum Engineers,* Vol.223, No. 47, pp. 43-50.

Gheibie, S., Aghababaela, H., Hoseinieb, H. and Pourrahmianc, Y. (2009). Modified Kuz-Ram fragmentation model and its use at the Sungun Copper Mine*. International Journal of Rock Mechanics and Mining Sciences*, Vol. 46, No. 6, pp 967-973.

Gloy, G. (2005). PPRust North Exploration Project: Mineralogical Investigation of Zwartfontein Boreholes. *Johannesburg, Ango Platinum*

Management Services, Anglo Platinum Research Centre- Mineralogical Research Department.

Gomes-Sebastiao, G. L and de Graaf, W. W (2017). An investigation into the fragmentation of blasted rock at Gomes Sand. Journal of the Southern African Institute of Mining and Metallurgy, Vol. 117, No. 4. Available at: http://dx.doi.org/10.17159/2411-9717/2017/n117n4a2, [Accessed 12 July 2022].

Grundstrom, C., Kanchobotla, S., Jankovic, A. and Thornton, D. (2011). Blast fragmentation for maximizing the SAG. Queensland, Proceedings of the Annual Conference on the Explosive and Blasting Technique.

Harris, C. (1968). The application of size distribution equation to multi-event communition processes. Transactions of the Metallurgical Society of the American Institute of Mining, Metallurgical and Petroleum Engineers, Vol. 241, No. 1, pp 343-358.

Heinz, W. (2009). Diamond Drilling Handbook. Fourth Edition. Johannesburg: Halfway House.

Higgins, M; Seppala, V; Kemeny, J; Bobo, T and Girdner, K. (1999). Integrated software tools and methodology for optimisation of blast fragmentation. Nashville, TN, Proceedings of the International Conference Society of Explosive Engineers Annual Conference. Available at: https://www.researchgate.net/publication/37618986_Improvements_in_Blast_Fragmentation_Models_Using_Digital_Image_Processing, [Accessed 17 October 2022].

Hjelmberg, H. (1983). Some ideas in how to improve calculations of the fragment size distribution in bench blasting using adaptive neuro-fuzzy inference system. *International Journal of Rock Mechanics and Mining Science and Geomechanics Abstracts,* Vol. 23, No. 6, pp 809-813.

Kassab, M.A. and Andreas, W. (2015) Study on P- wave and S-wave velocity in dry and wet sandstones of Tushka region, Egypt. AVAILABLE AT. https://www.sciencedirect.com/science/article/pii/S1110062115000003. [Accessed 10 November 2022].

Kemeny, J., Mofya, E., Kaunda, R. and Lever, P. (2002). Improvements in blast fragmentation models using digital image processing. *Fragblast*, Vol. 6, No. 3-4, pp 311-320. Available at: https://www.tandfonline.com/doi/abs/10.1076/frag.6.3.311.14051, [Accessed 11 March 2022].

Khomola, P. (2020). Monthly production meeting report, Postmasburg. Kumba Iron Ore, Kolomela.

Kinnaird, J., Hutchinson, D. and Nex, R.D (2005). Petrology and mineralisation of the southern platreef: northern limb of the bushveld complex. *Johannesburg, South Africa, Mineral Deposita*. Available at: *https://www.academia.edu/82494876/Petrology_and_mineralisation_of_the_southern_Platreef_northern_limb_of_the_Bushveld_Complex_South_Africa?f_ri=406,* [Accessed 11 November 2022].

Kopp, O.C. (2019). Bituminous Coal. Encyclopaedia Britannica. Available at: https://www.britannica.com/science/bituminous-coal. [Accessed 06 December 2021].

Kou, S. and Rustan, A. (1993). Computerised design and result prediction of bench blasting. Vienna, Austria, Fourth International Symposium on Rock fragmentation by Blasting. Available at: https://www.researchgate.net/publication/311099932_A_Distribution-Free_Description_of_Fragmentation_by_Blasting_Based_on_Dimensional_Analysis, [Accessed 12 October 2022].

Kulatilake, P., Hudaverdi, T. and Wu, Q. (2012). New prediction models for mean particle size in rock blast fragmentation. Geotechnical and Geological Engineering, Vol. 30, No. 3, pp 665-684.

Kuznetsov, V. (1973). The mean diameter of the fragments formed by blasting rock. *Soviet Mining Science*, Vol. 9, No. 2, pp 144-148.

Kuznetsov, Y., and Ramazanov, V. (1965). Fragmentation modeling in surface mining using the Kuz-Ram model. *International Journal of Mining Science and Technology*, Vol 28, No.3, pp 377-382.

Latham, J. P., and Ouchterlony, F. (2019). Advances in Modelling Rock Fragmentation and Fragmentation Energy Partitioning*. Geotechnical and Geological Engineeri*ng, Vol 37, No.1 , 411-433.

Leng, Z., Fan, Y., Gao, Q. and Hu, Y. (2020). Evaluation and optimisation of blasting approaches to reducing oversize boulder and toes in open pit. *International Journal of Mining Science and Technology*, Vol. 30, No. 3, pp 373-380.

Liu, Z., Xu, J., and Zhang, T. (2023). Numerical modeling of rock fragmentation under blasting using the finite difference method*. International Journal of Rock Mechanics and Mining Sciences*, Vol. 147, 105925.

Lu, H., and Wang, J. (2020). Advances in Numerical Simulation of Fragmentation and Damage Induced by Blasting. Advances in Civil Engineering, 2020, 8818629.

Malkowski, P., Ostrowski, L. and Brodny, J. (2018). Analysis of Young's modulus for carboniferous sedimentary rocks and its relationship with uniaxial compressive strength using different methods of modulus determination. *Journal of Sustainable Mining*, Vol. 17, No. 3, pp 145-15.

Maptek, (2021). Maptek blast design modelling and analysis to lower risk and increase productivity. AVAILABLE AT. https://maptek.com/products/blastlogic/index.html. [Accessed 13 April 2021].

McDonald, I., Holwell, D and Armitage, P.B. (2005). Stratigraphy and Platinum Group Element mineralization in the northern lobe of the Bushveld complex, South Africa, Cardiff University and University of Greenwich.

McMahon, G and Moreira, S. (2014). The Contribution of the Mining Sector to Socioeconomic and Human Development. Open knowledge repository. Available at: https://openknowledge.worldbank.org/handle/10986/18660. [Accessed 19 November 2022].

Milanović, S., Kričak, L., Negovanović, M and Marković, J. (2019). Application of softwares for drilling and blasting. *Podzemni radovi*, *Vol.* 34, No. 10, pp. 77-89.

Moghadam, M.J., Farsangi, M. and Mansouri, H. (2006) Muckpile fragmentation prediction using Artificial Neural Networks. *Journal of Mines, Metals and Fuels*, Vol. 54, No. 2, pp 421-423.

Monjezi, M., Amiri, h., Farrokhi, A. and Goshtasbi, K. (2010). Prediction of rock fragmentation due to blasting in Sarcheshmeh Copper Mine using artificia neural networks. *Geotechnical and Geological Engineering, Vol.* 28, No. 4, pp. 423-430.

Munjiza, A. (2004). The Combined Finite-Discrete Element Method. John Wiley & Sons.

Ndibalema, A. (2008). Capturing economic benefits from blasting. Southern African Institute of Mining and Metallurgy, pp 97-112. Available at: http://www.saimm.co.za/Conferences/SurfaceMining2008/097-112_Ndibalema.pdf, [accessed 02 January 2022].

Nembahe, R. and Ratshomo, K. (2016). *South African Coal Sector Report,* Pretoria: Energy Data Collection, Management and Analysis. Available at.

https://www.energy.gov.za/files/media/explained/2019-South-African-Energy-Sector-Report.pdf, [Accessed 12 October 2022].

Nex, P., Kinnaird, J., B, J. and Colloty, A. (2006) Platreef Rock Type Definitions and Descriptions*. Johannesburg, Anglo American Platinum.* Available at: https://www.researchgate.net/publication/262973972_A_geometallurgical_approach_at_Anglo_American_Platinum's_Mogalakwena_operation, [Accessed 11 July 2022].

Noy, M. (2013). Automated rock fragmentation measurements with close range digital photogrammetry. In Measurement and Analysis of Blast Fragmentation. Delhi, India, CRC Press/Balkema, pp 13-21.

Onederra, I., Thurley, M. J. and Catalan, A. (2014). Measuring blast fragmentation at Esperanza mine using high resolution 3D laser scanning. *Mining Technology*, Vol. 124, No. 1, pp 34-36.

Oraee, K. and Asi, B. (2006). Prediction of rock fragmentation in open pit mines using Neural Network Analysis. Torino, Italy, International Symposium on Mine Planning and Equipment Selection (MPES).

Orica, (2021). Optimising drill and blast operations with the next generation BlastIQ digital platform. Available at: https://www.orica.com/news--media/optimising-drill-and-blast-operations-with -the next generation-blastiq-digital-platform#Xt9VX0UzaUK. [Accessed 3 April 2021].

Otterness, R. E., Stagg, M. S., Rholl, S. and NS, S. (1991). Correlation of shot design parameters to fragmentation*. In Proceedings of the 7th annual symposium on explosives and blasting Technology.* Las Vegas, International Society of Explosives Engineers.

Ouchterlony, F. (2003). Influence of blasting on the size distribution and properties of muckpile fragments a state-of-the-art review*.* Luleå University of Technology, Sweden, MinFo Project P2000-10, Swebrec, Luleå University of Technology.

Ouchterlony, F. (2009). Fragmentation characterization; the Swebrec function and its use in blast *engineering.* London, UK, In: Fragblast 9, proceedings of the ninth international symposium on rock fragmentation by blasting. Taylor and Francis.

Ouchterlony, F., Johansson, D., and Håkansson, U. (2018). Modelling the influence of rock mass properties on fragmentation in bench blasting. International Journal of Rock Mechanics and Mining Sciences, Vol.107, pp 181-189.

Ouchterlony, F. and Sanchidrián, J. (2019). A review of development of better prediction equations for blast fragmentation. *Journal of Rock Mechanics and Geotechnical Engineering*, Vol.11, No. 5, pp.1094-1109.

Ozturk, C., Nasuf, E. and Kahraman, S. (2014). Estimation of rock strength from quantitative assessment of rock texture. *The Journal of the Southern African Institute of Mining and Metallurgy,* Vol. 116, No. 3, pp. 471-480.

Payne, B. (2019). Quarterly review production meeting. Mogalakwena Complex: Anglo American.

Potts, G. and Ouchterlony, F. (2006). The capacity of image analysis to measure fragmentation, an evaluation using Split Desktop®. Stockholm, Luleå University of Technology.

Petropoulus, N. (2015). Burden dynamics and fragmentation, thesis. Lulea University of Technology, Graphic Production.

Potyondy, D. O., and Cundall, P. A. (2004). A bonded-particle model for rock. International Journal of Rock Mechanics and Mining Sciences, 41(8), 1329-1364.

Randles, P. W., and Libersky, L. D. (1996). Smoothed Particle Hydrodynamics: Some Recent Improvements and Applications. *Computer Methods in Applied Mechanics and Engineering*, Vol. 139, No.1-4, pp 375-408.

Rosato, A., Strandburg, K. J., & Prinz, F. B. (1987). Why the Brazil nuts are on top: Size segregation of particulate matter by shaking. Physical Review Letters. Vol 58, No. 10, pp 1038-1040.

Roy, M., Ranjit Kumar, P. and Sarim, M. (2016) Rock Fragmentation by Blasting. *Journal of Mines, Metals and Fuels,* Vol. 64, No.9, pp. 424-431.

Schunnesson, H., Johansson, D., and Bergqvist, T. (2020). Using the Discrete Element Method to model fragmentation and damage in bench blasting. International Journal of Rock Mechanics and Mining Sciences, 135, 104403.

Service (1999). National Park Service Handbook for the Storage, Transportation, and Use of Explosives, *Washington, DC: U.S*. Department. of the Interior, National Park Service.

Sharma, P. D. (2011). *Expert opinion: mining consultant Partha Das Sharma Engineer Live.* Available at: https://www.engineerlive.com/content/expert-opinion-mining-consultant-parthadas-sharma. [Accessed 20 March 2022].

Sharma, A., Mishra A. K., B.S. Choudhary, and R Meena. (2019). Impact of Blast Design Parameters on Rock Fragmentation in Building Stone Quarries. Current Science, 116(2), pp 1861-1867.

Shi, P., Liu, S., and Zhu, H. (2017). A Numerical Model for Dynamic Damage and Fragmentation Analysis of Rock Blasting. Computers and Geotechnics, Vol. 90, pp 72-83.

Siddiqui, F., Shah, S. and Behan, M. (2009). Measurement of size distribution of blasted rock using digital image processing. *Journal of King Abdulaziz University: Engineering Sciences*, Vol. 20, No. 2.

Silva, J. D., Amaya, J. G. and Basso, F. (2017). Development of a predictive model of fragmentation using drilling and blasting data in open pit mining. *Journal of the Southern African Institute of Mining and Metallurgy,* Vol. 17, No. 11, pp. 1089-1094.

Singh, B. (2013). Firing patterns and their effect on muckpile shape parameters and fragmentation in quarry blasts. *International Journal of Research in Engineering and Technology, Vol.* 2, No 9, pp. 32-45.

Singh, S. (2007). New trends in drilling and blasting technology. *International Journal of Surface Mining, Reclamation and Environment, Vol* 14, No. 4, pp. 305-315.

Singh, T. and Sarkar, K. (2005). Geotechnical investigation of Amiyan landslide hazard zone in Himalayan region, Uttaranchal, India. Geotechnical Engineering, India: Word Scientific, pp 355-360.

Shi, X., Huang, D., Zhou, J. and Zhang, S. (2013). Combined ANN prediction model for rock fragmentation distribution due to blasting. *Journal of Information and Computational Science, Vol.* 10, No.11, pp. 3511-3518.

Spathis, A. (2006). Powder factors in asymmetric blast patterns: *Fragblast*, Vol. 10, No. (3-2), pp 97-109.

Spathis, A. (2013) A three parameter rock fragmentation distribution. Measurements, pp 73-86.

Spathis, S., Wesseloo, J., and Kizil, M. S. (2017). A review of the impact of blasting on the environment and geomechanics. *Mining Technology*, Vol. 126, No. 2, pp 70-78.

Souza, J.C., Silva, A.C. and Rocha, S.S. (2018). Analysis of blasting rocks prediction and rock fragmentation results using split-desktop software. *Tecnologia em Metalurgia Materiais e Mineração*, Vol 15, No 1, pp. 22–30.

Thornton, D. M., Kanchibotla, S. and Esterle, J. (2001). A fragmentation model to estimate ROM size distribution of soft rock types*.* The University of Queensland., In: Proceedings of the 27th annual conference on explosives and blasting Technology. International Society of Explosives Engineers.

Thread, S. (2019). What is Young's Modulus*.* Available at: *https://www.servicethread.com/blog /What is young Modulus.* [Accessed 21 November 2022].

Thurley, M. J.(2014). Automated, On-line, Calibration-Free, Particle Size. Measurement using*. Lulea, Sweden, Luleå University of Technology*.

Thurley, M. and Kim, C. (2005). Identifying, visualizing, and comparing regions in irregularly spaced 3D surface data. *Computer Vision and Image Understanding*, Vol. 98, No. 2, pp 239-270.

Wang, Z., Chen, X., and Zhang, Z. (2021). Artificial Neural Network modeling for rock fragmentation in surface blasting. International Journal of Mining Science and Technology, 31(5), pp 725-732.

Workman, L. (2001). The potential for unifying drilling, blasting and downstream operations by the application of technology*.* Cleveland, *International Society of Explosives Engineers*, pp. 83-97

Zhang, J. (2019). Rock strengths and rock failure criteria. Zhang, edition *Applied Petroleum Geomechanics.* Houston, Texas: Gulf Professional Publishing, pp. 85-131.

Zhang, Z.X. (2016). Basic Parameters of Rock Blasting. *Rock fracture and blasting theory and applications.* Amsterdam: Elsevier, Butterworth-Heinemann, an imprint of Elsevier, pp. 493-505.

Zhou, H., Cai, M., and Ma, G. (2023). Numerical modelling of rock fragmentation under blasting using the finite element method. *International Journal of Rock Mechanics and Mining Sciences*, Vol. 148, 105979.

8 APPENDICES

8.1 Fragmentation Challenges for Surface Mines

Mogalakwena Platinum Mine had challenges with boulders mostly of more 1 800mm in size after blasting. The target fragmentation size was 250mm. Figure 8.1 shows a fragmentation muckpile with different rock sizes loaded by the excavator.

Figure 8.1 Blasted muck pile boulders and destroyed high wall. Source: Payne (2019)

Figure 8.1 shows a blasted muckpile being loaded out by an excavator. There are different rock sizes within the muckpile and showing a large boulder of more than 1 800mm to the north-west of the figure. The large boulders could not be loaded onto trucks as they could not fit in the excavator bucket as indicated with the arrows. Additionally, Figure 8.1 shows a destroyed high wall comprised of loose hanging rocks, and this was a safety concern. The newly created high wall after the blast was not stable as it was collapsing during loading activity as shown with horizontal line. This posed a safety concern to the operator as the wall was collapsing and high wall instability. This reduced the productivity of the excavator.

Siddiqui *et al*. (2009) stated that most surface mines have fragmentation size distribution deviations from the design plan size distribution. This statement is true in respect of fragmentation deviations as observed at Mogalakwena mine. Table 8.1 shows the fragmentation deviations have been occurring over the recent years and documented on site.

Table 8.1 Target size and actual size. Source: Payne (2019)

Year	Target size (mm)	Average achieved size (mm)
2018	250	840
2019	250	640
2020	220	550
2021	220	490

At Mogalakwena mine, ten percent of the monthly blasting operations involve boulders that must be resized from over 1,800mm to less than 500mm before they can be loaded onto trucks. Boulder Secondary blasting was introduced as a strategy to mitigate the issue of oversized boulders. This approach involved the utilisation of additional explosives for secondary blasting, resulting in a heightened demand for explosive materials. Specifically, in the year 2019, Mogalakwena mine incurred an expense of R20 million on explosives, surpassing the budgeted amount by 30%, as reported by Payne (2019). Furthermore, across the coal surface mines included in the study, an extra R10 million was expended on additional explosives required to address the challenges posed by irregular fragmentation of boulders. This expenditure pattern underscores the consistency of the issue across the various mines, as identified during the annual review of explosive spending.

The Kolomela Iron Ore mine faced a series of challenges that severely affected its operations. These challenges included inconsistent fragmentation sizes, difficulties in excavator digging caused by poorly fragmented bench toes, and the scattering of fragments after blasting.

In particular, the desired fragmentation size was set at 200mm, but the actual results were often far from this target, ranging from fines as small as 55mm to imposing boulders of 1850mm. These deviations had a detrimental impact on the mine's overall efficiency, productivity, and safety.

Moreover, the issue extended to loading times, which were directly linked to the outcomes of the blasting. The loading cycles at Kolomela Iron Ore mine consistently exceeded the ideal duration, and this was primarily attributed to the problems with fragmentation (Khomola, 2020).

Kolomela Iron Ore mine faced challenges such as inconsistent fragmentation, difficult excavation conditions, and fragment dispersion post-blasting, which collectively undermined efficiency, productivity, and safety. The loading times at the mine were also adversely affected by these issues, highlighting the urgent need for resolution (Khomola, 2020). The muckpile shape and size were poor as it was not consistent. Boulders and fines in the blasted muckpile were prominent and it made it difficult for loading units to achieve the loading rates. Table 1.3 shows the average cycle time of loading and hauling at Kolomela mine.

Table 8.2 Load and haul cycle breakdown. Source: Khomola (2020)

Cycle activities	Actual site average (hh:mm:ss)	Mine ideal average (hh:mm:ss)	Deviations (hh:mm:ss)
Queuing	00:03:23	00:01:16	00:02:07
Spotting	00:00:55	00:00:20	00:00:30
Loading	00:03:45	00:02:24	00:01:21
Hauling	00:03:11	00:02:05	00:01:06
Tipping	00:00:45	00:00:40	00:00:05
Travelling empty	00:02:29	00:02:11	00:00:18
Total	00:14:28	00:09:04	00:05:27

Table 8.3 shows that the loading and hauling cycle time for the actual site average is more than the mine ideal cycle time. According to Khomola (2020), inconsistent fragmentation sizes solely resulted in a 36% increase in loading and hauling cycle time higher than the planned cycle time. The increased cycle time contributed to mine losing production time during loading and hauling (Khomola, 2020).

Isibonelo Colliery and Navigation Colliery struggled with significant fragmentation challenges that were having a profound impact on their operations. These issues encompassed coal pulverization, back-break, and inadequate high wall control, all of which were closely tied to the problem of fragmentation.

The intended coal fragmentation size for both sites, slated for feeding into the primary crusher, was set at 200mm. However, the mines were consistently achieving a much smaller fragment size of only 40mm and 65mm respectively. This finer coal size had adverse consequences on the mine's overall efficiency, productivity, and safety.

The process of coal pulverization during blasting was a primary culprit behind this predicament. It not only resulted in excessive fragmentation but also led to a decrease in the average size of the blasted coal. This, in turn, gave rise to several operational complications, including challenges in handling, transportation, and downstream processing. These complications, in addition to the heightened operational costs, also contributed to a reduction in the overall yield of the coal mining operations. Furthermore, the excessive pulverization had an adverse impact on the quality of the coal, potentially resulting in a substandard product that did not meet the expectations of customers (Kecojevic and Komljenovic 2006).

Isibonelo Colliery and Navigation Colliery were confronted with a series of fragmentation-related challenges, notably coal pulverization, which were causing a cascade of problems affecting efficiency, productivity, safety, operational costs, and ultimately, the quality of the coal product supplied to customers. Addressing these challenges was imperative for the mine's sustainable success.

Sishen Iron Ore mine had challenges in inconsistence fragmentation size, hard digging of excavators due to bench toe not fragmented and scattered muckpile after the blasting. The target fragmentation size was 200mm . The mine was achieving a fragment size of 870 mm. The achieved size was negatively impacting the overall efficiency, productivity, and safety of the coal mining operations. One of the issues was the loading times observed directly related to blasting results. The muckpile shape and size were far off from the intended fragmentation size. Additionally, addressing these challenges was imperative for mine’s operational efficiency.

In summary, the sites challenges and benefits, optimisation of the fragmentation size is achieved through optimisation of the drilling and blasting processes. When done properly, blasting can effectively decrease the particle size to the target sizes required by the mine, which lowers the costs of subsequent activities for mines.

8.2 Fragmentation Pictures for Surface Mines

In Figure 8.1 up to 8.22, we present the muckpile images extracted from several distinct surface mines. These images offer a striking visual representation of the variability in muckpile morphology and composition across different mining operations. These images show the fragmentation muckpiles.

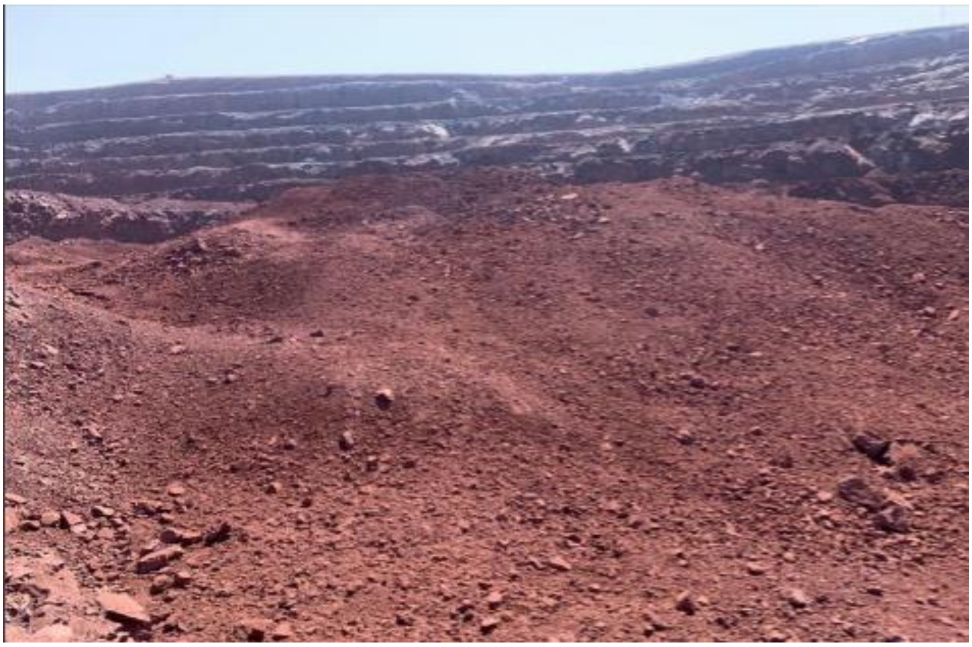

Figure 8.2 Muckpile picture for Kolomela Iron Ore mine

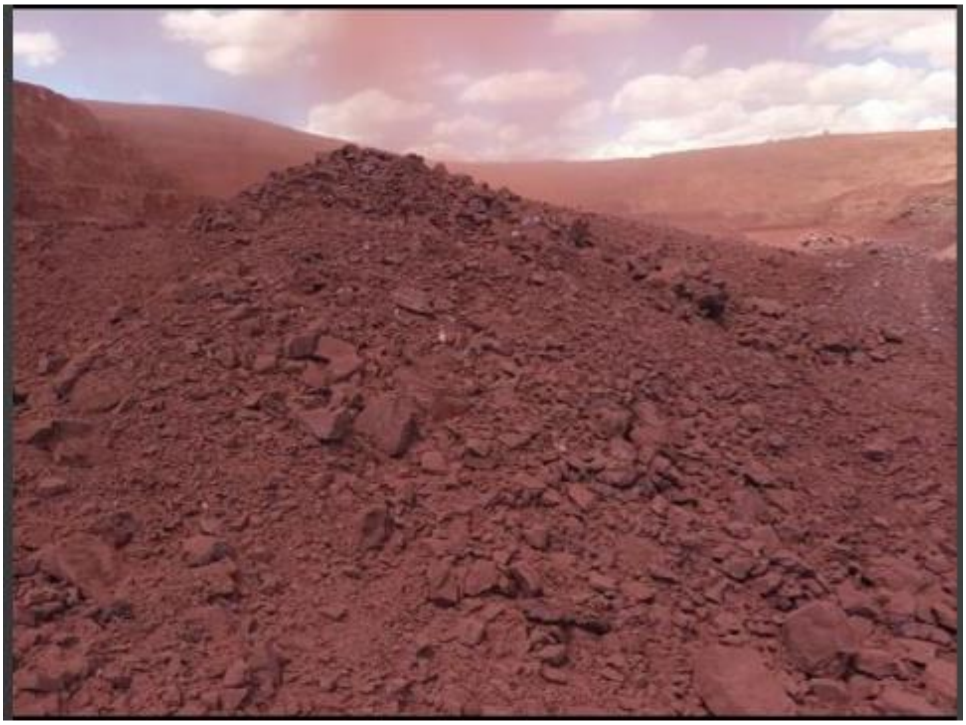

Figure 8.3 Muckpile picture for Kolomela Iron Ore mine

Figure 8.4 Muckpile picture for Kolomela Iron Ore mine

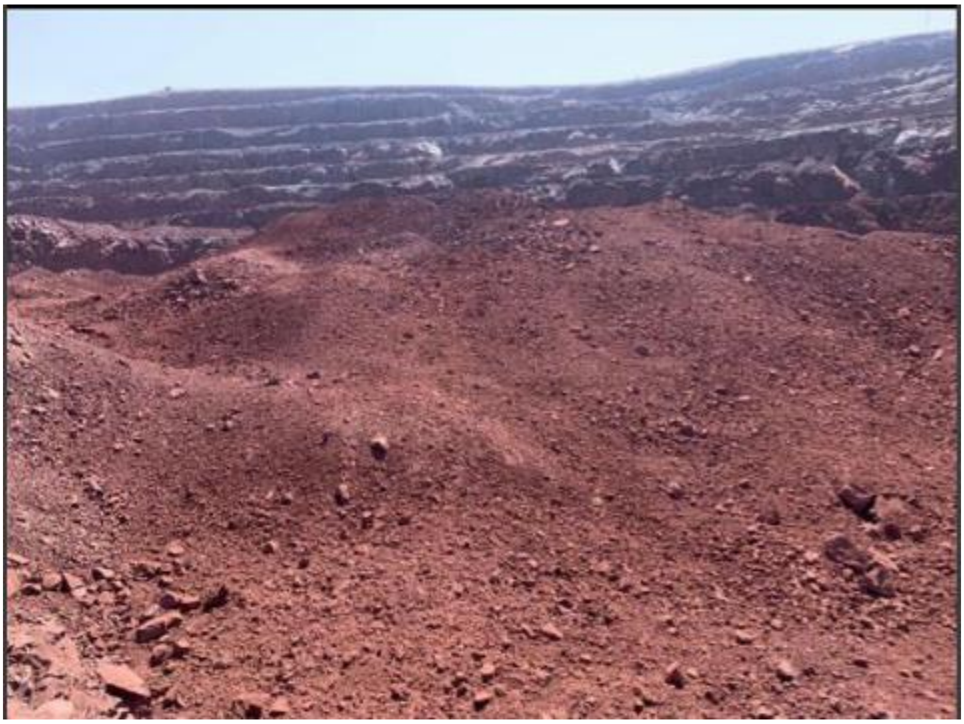

Figure 8.5 Muckpile picture for Kolomela Iron Ore mine

Figure 8.6 Muckpile picture for Kolomela Iron Ore mine

Figure 8.7 Muckpile picture for Kolomela Iron Ore mine

Figure 8.8 Muckpile picture for Sishen Iron Ore mine

Figure 8.9 Muckpile picture for Sishen Iron Ore mine

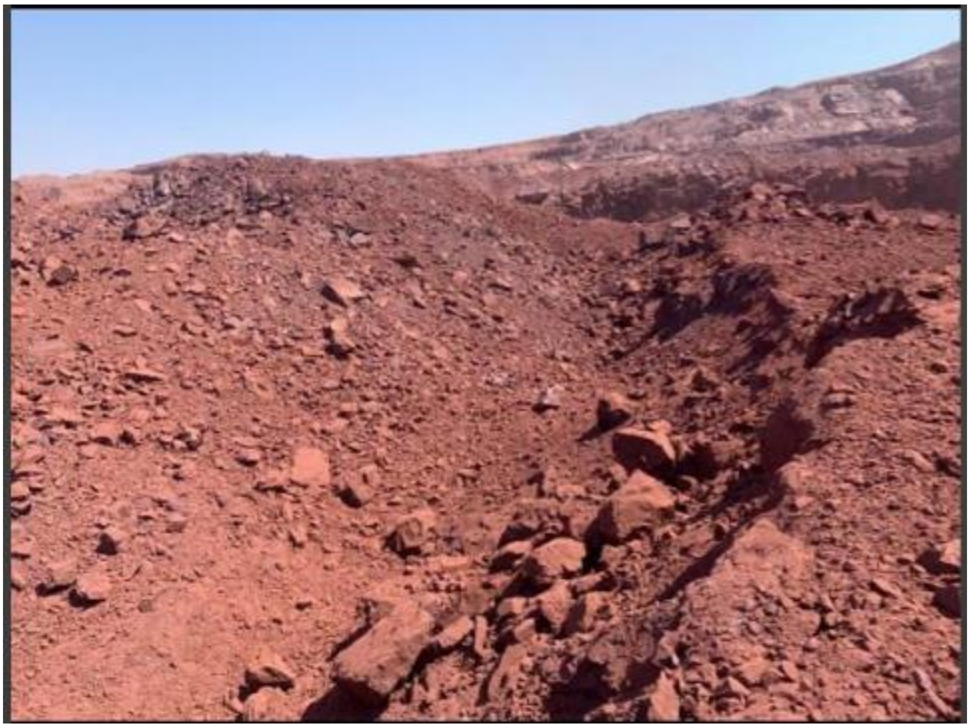

Figure 8.10 Muckpile picture for Sishen Iron Ore mine

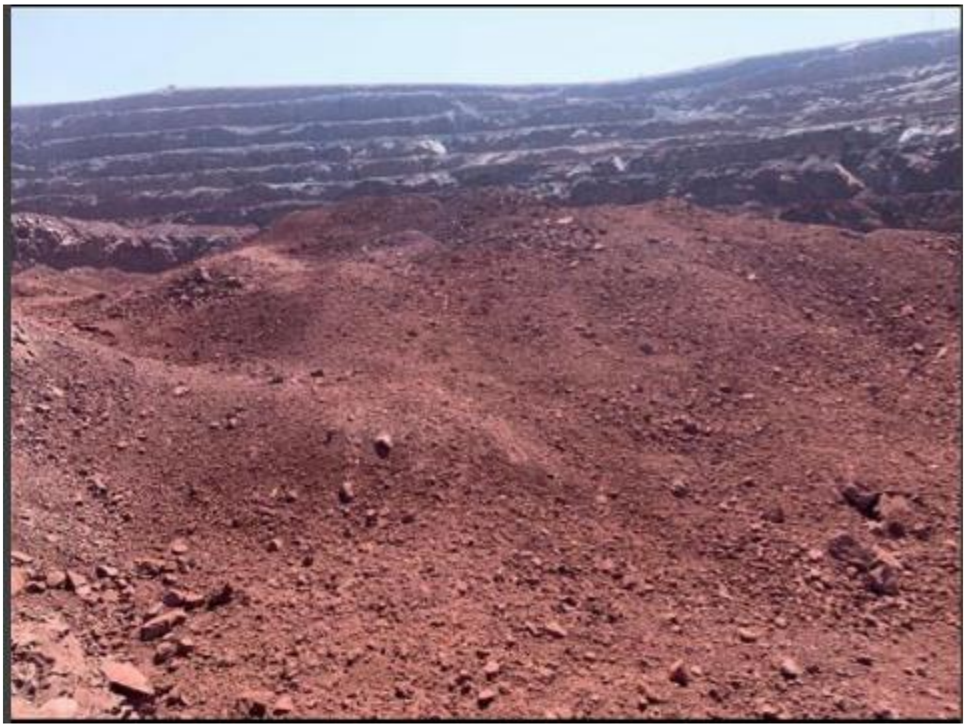

Figure 8.11 Muckpile picture for Sishen Iron Ore mine

Figure 8.12 Muckpile picture for Sishen Iron Ore mine

Figure 8.13 Muckpile picture for Sishen Iron Ore mine

Figure 8.14 Muckpile picture for Sishen Iron Ore mine

Figure 8.15 Muckpile picture for Sishen Iron Ore mine

Figure 8.16 Muckpile picture for Mogalakwena Platinum Mine

Figure 8.17 Muckpile picture for Mogalakwena Platinum Mine

Figure 8.18 Muckpile picture for Navigation Colliery

Figure 8.19 Muckpile picture for Navigation Colliery

Figure 8.20 Muckpile picture for Navigation Colliery

Figure 8.21 Muckpile picture for Navigation Colliery

Figure 8.22 Muckpile picture for Navigation Colliery

Table 8.3 to Table 8.7 shows some of the blasts results from split desktop results.

Table 8.3 Split Desktop results for Mogalakwena platinum mine

	MOG	IMG-20171128-WA0036	IMG-20171128-WA0037	IMG-20171128-WA0039	IMG-20171128-WA0038	IMG-20171128-WA0012	IMG-20171129-WA0010	IMG-20171129-WA0002	IMG-20171128-WA0041	IMG-20171128-WA0035
Size[mm]	% Passing	% Passing	% Passing	% Passing	% Passing	% Passing	% Passing	% Passing	% Passing	% Passing
2000	100	100	100	100	100	100	100	100	100	100
1000	99.47	100	100	100	100	100	96.23	100	100	100
750	97.88	100	100	100	100	100	84.81	100	100	100
500	93.74	100	100	99.37	100	100	60.19	96.99	100	100
300	78.77	93.65	92.76	83.22	84.04	92	34.39	78.45	78.75	96.19
250	68.9	83.83	83.76	73.76	70.72	81.62	28.33	66.73	65.4	89.45
125	29.97	33.84	41.34	31.73	27.25	38.63	15.25	21.76	26.84	44.19
100	22.19	24.92	30.72	23.46	20.68	29.04	12.31	14.8	20.68	31.46
75	15.03	16.48	21.06	15.82	13.97	19.99	9.35	8.91	14.42	20.64
53	9.39	9.96	13.35	9.84	8.7	12.74	6.7	4.83	9.33	12.31
38	6.01	6.14	8.62	6.24	5.53	8.27	4.87	2.69	6.15	7.51
27	3.81	3.74	5.51	3.91	3.47	5.31	3.51	1.47	4.01	4.52
19	2.4	2.25	3.47	2.42	2.15	3.37	2.51	0.79	2.58	2.68
13	1.46	1.3	2.11	1.44	1.29	2.06	1.74	0.41	1.61	1.53
10	1.04	0.89	1.5	1.01	0.9	1.47	1.35	0.26	1.16	1.04
7	0.66	0.53	0.94	0.62	0.56	0.93	0.96	0.14	0.74	0.61
5	0.43	0.33	0.61	0.39	0.35	0.6	0.7	0.08	0.49	0.37
2	0.14	0.09	0.19	0.11	0.1	0.19	0.29	0.02	0.16	0.1
1	0.06	0.03	0.08	0.05	0.04	0.08	0.15	0	0.07	0.04

Table 8.4 Split Desktop results for Isibonelo Colliery

	Isibonel0	IMG-20171128-WA0036	IMG-20171128-WA0037	IMG-20171128-WA0039	IMG-20171128-WA0038	IMG-20171128-WA0012	IMG-20171129-WA0010	IMG-20171129-WA0002	IMG-20171128-WA0041	IMG-20171128-WA0035
Size[mm]	% Passing	% Passing	% Passing	% Passing	% Passing	% Passing	% Passing	% Passing	% Passing	% Passing
2000	100	100	100	100	100	100	100	100	100	100
1000	99.47	100	100	100	100	100	96.23	100	100	100
750	97.88	100	100	100	100	100	84.81	100	100	100
500	93.74	100	100	99.37	100	100	60.19	96.99	100	100
300	78.77	93.65	92.76	83.22	84.04	92	34.39	78.45	78.75	96.19
250	68.9	83.83	83.76	73.76	70.72	81.62	28.33	66.73	65.4	89.45
125	29.97	33.84	41.34	31.73	27.25	38.63	15.25	21.76	26.84	44.19
100	22.19	24.92	30.72	23.46	20.68	29.04	12.31	14.8	20.68	31.46
75	15.03	16.48	21.06	15.82	13.97	19.99	9.35	8.91	14.42	20.64
53	9.39	9.96	13.35	9.84	8.7	12.74	6.7	4.83	9.33	12.31
38	6.01	6.14	8.62	6.24	5.53	8.27	4.87	2.69	6.15	7.51
27	3.81	3.74	5.51	3.91	3.47	5.31	3.51	1.47	4.01	4.52
19	2.4	2.25	3.47	2.42	2.15	3.37	2.51	0.79	2.58	2.68
13	1.46	1.3	2.11	1.44	1.29	2.06	1.74	0.41	1.61	1.53
10	1.04	0.89	1.5	1.01	0.9	1.47	1.35	0.26	1.16	1.04
7	0.66	0.53	0.94	0.62	0.56	0.93	0.96	0.14	0.74	0.61
5	0.43	0.33	0.61	0.39	0.35	0.6	0.7	0.08	0.49	0.37
2	0.14	0.09	0.19	0.11	0.1	0.19	0.29	0.02	0.16	0.1
1	0.06	0.03	0.08	0.05	0.04	0.08	0.15	0	0.07	0.04

Table 8.5 Split Desktop results for Navigation Colliery

	Navigation	IMG-20171128-WA0036	IMG-20171128-WA0037	IMG-20171128-WA0039	IMG-20171128-WA0038	IMG-20171128-WA0012	IMG-20171129-WA0010	IMG-20171129-WA0002	IMG-20171128-WA0041	IMG-20171128-WA0035
Size[mm]	% Passing	% Passing	% Passing	% Passing	% Passing	% Passing	% Passing	% Passing	% Passing	% Passing
2000	100	100	100	100	100	100	100	100	100	100
1000	99.47	100	100	100	100	100	96.23	100	100	100
750	97.88	100	100	100	100	100	84.81	100	100	100
500	93.74	100	100	99.37	100	100	60.19	96.99	100	100
300	78.77	93.65	92.76	83.22	84.04	92	34.39	78.45	78.75	96.19
250	68.9	83.83	83.76	73.76	70.72	81.62	28.33	66.73	65.4	89.45
125	29.97	33.84	41.34	31.73	27.25	38.63	15.25	21.76	26.84	44.19
100	22.19	24.92	30.72	23.46	20.68	29.04	12.31	14.8	20.68	31.46
75	15.03	16.48	21.06	15.82	13.97	19.99	9.35	8.91	14.42	20.64
53	9.39	9.96	13.35	9.84	8.7	12.74	6.7	4.83	9.33	12.31
38	6.01	6.14	8.62	6.24	5.53	8.27	4.87	2.69	6.15	7.51
27	3.81	3.74	5.51	3.91	3.47	5.31	3.51	1.47	4.01	4.52
19	2.4	2.25	3.47	2.42	2.15	3.37	2.51	0.79	2.58	2.68
13	1.46	1.3	2.11	1.44	1.29	2.06	1.74	0.41	1.61	1.53
10	1.04	0.89	1.5	1.01	0.9	1.47	1.35	0.26	1.16	1.04
7	0.66	0.53	0.94	0.62	0.56	0.93	0.96	0.14	0.74	0.61
5	0.43	0.33	0.61	0.39	0.35	0.6	0.7	0.08	0.49	0.37
2	0.14	0.09	0.19	0.11	0.1	0.19	0.29	0.02	0.16	0.1
1	0.06	0.03	0.08	0.05	0.04	0.08	0.15	0	0.07	0.04

Table 8.6 Split Desktop results for Kolomela Iron Ore mine

	Kolomela	IMG-20171128-WA0036	IMG-20171128-WA0037	IMG-20171128-WA0039	IMG-20171128-WA0038	IMG-20171128-WA0012	IMG-20171129-WA0010	IMG-20171129-WA0002	IMG-20171128-WA0041	IMG-20171128-WA0035
Size[mm]	% Passing	% Passing	% Passing	% Passing	% Passing	% Passing	% Passing	% Passing	% Passing	% Passing
2000	100	100	100	100	100	100	100	100	100	100
1000	99.47	100	100	100	100	100	96.23	100	100	100
750	97.88	100	100	100	100	100	84.81	100	100	100
500	93.74	100	100	99.37	100	100	60.19	96.99	100	100
300	78.77	93.65	92.76	83.22	84.04	92	34.39	78.45	78.75	96.19
250	68.9	83.83	83.76	73.76	70.72	81.62	28.33	66.73	65.4	89.45
125	29.97	33.84	41.34	31.73	27.25	38.63	15.25	21.76	26.84	44.19
100	22.19	24.92	30.72	23.46	20.68	29.04	12.31	14.8	20.68	31.46
75	15.03	16.48	21.06	15.82	13.97	19.99	9.35	8.91	14.42	20.64
53	9.39	9.96	13.35	9.84	8.7	12.74	6.7	4.83	9.33	12.31
38	6.01	6.14	8.62	6.24	5.53	8.27	4.87	2.69	6.15	7.51
27	3.81	3.74	5.51	3.91	3.47	5.31	3.51	1.47	4.01	4.52
19	2.4	2.25	3.47	2.42	2.15	3.37	2.51	0.79	2.58	2.68
13	1.46	1.3	2.11	1.44	1.29	2.06	1.74	0.41	1.61	1.53
10	1.04	0.89	1.5	1.01	0.9	1.47	1.35	0.26	1.16	1.04
7	0.66	0.53	0.94	0.62	0.56	0.93	0.96	0.14	0.74	0.61
5	0.43	0.33	0.61	0.39	0.35	0.6	0.7	0.08	0.49	0.37
2	0.14	0.09	0.19	0.11	0.1	0.19	0.29	0.02	0.16	0.1
1	0.06	0.03	0.08	0.05	0.04	0.08	0.15	0	0.07	0.04

Table 8.7 Split Desktop results for Sishen Iron Ore mine

	Sishen	IMG-20171128-WA0036	IMG-20171128-WA0037	IMG-20171128-WA0039	IMG-20171128-WA0038	IMG-20171128-WA0012	IMG-20171129-WA0010	IMG-20171129-WA0002	IMG-20171128-WA0041	IMG-20171128-WA0035
Size[mm]	% Passing	% Passing	% Passing	% Passing	% Passing	% Passing	% Passing	% Passing	% Passing	% Passing
2000	100	100	100	100	100	100	100	100	100	100
1000	99.47	100	100	100	100	100	96.23	100	100	100
750	97.88	100	100	100	100	100	84.81	100	100	100
500	93.74	100	100	99.37	100	100	60.19	96.99	100	100
300	78.77	93.65	92.76	83.22	84.04	92	34.39	78.45	78.75	96.19
250	68.9	83.83	83.76	73.76	70.72	81.62	28.33	66.73	65.4	89.45
125	29.97	33.84	41.34	31.73	27.25	38.63	15.25	21.76	26.84	44.19
100	22.19	24.92	30.72	23.46	20.68	29.04	12.31	14.8	20.68	31.46
75	15.03	16.48	21.06	15.82	13.97	19.99	9.35	8.91	14.42	20.64
53	9.39	9.96	13.35	9.84	8.7	12.74	6.7	4.83	9.33	12.31
38	6.01	6.14	8.62	6.24	5.53	8.27	4.87	2.69	6.15	7.51
27	3.81	3.74	5.51	3.91	3.47	5.31	3.51	1.47	4.01	4.52
19	2.4	2.25	3.47	2.42	2.15	3.37	2.51	0.79	2.58	2.68
13	1.46	1.3	2.11	1.44	1.29	2.06	1.74	0.41	1.61	1.53
10	1.04	0.89	1.5	1.01	0.9	1.47	1.35	0.26	1.16	1.04
7	0.66	0.53	0.94	0.62	0.56	0.93	0.96	0.14	0.74	0.61
5	0.43	0.33	0.61	0.39	0.35	0.6	0.7	0.08	0.49	0.37
2	0.14	0.09	0.19	0.11	0.1	0.19	0.29	0.02	0.16	0.1
1	0.06	0.03	0.08	0.05	0.04	0.08	0.15	0	0.07	0.04

Table 8.8 to Table 8.12 shows the remaining explosive parameters from the main results.

Table 8.8 Explosive parameters at Mogalakwena Platinum mine

Blast Number	Total Charge(kg)	Tons blasted (tons)	Powder Factor	Density (kg/m^3)
1	98 118	123 483	1.44	3 200
2	104 219	244 951	1.44	3 200
3	102 350	273 388	1.44	3 200
4	91 495	122 481	1.44	3 200
5	123 381	203 486	1.44	3 200
6	97 318	134 481	1.44	3 200
7	118 639	289 956	1.44	3 200
8	115 395	288 387	1.44	3 200
9	97 498	128 487	1.44	3 200
10	136 388	298 489	1.44	3 200

Table 8.9 Explosive parameters at Isibonelo Colliery

Blast Number	Total Charge(kg)	Tons blasted (tons)	Powder Factor	Density (kg/m^3)
1	17 640	25 200	0.70	1 200
2	13 770	24 097	0.68	1 200
3	12 960	22 680	0.65	1 200
4	16 200	28 350	0.60	1 200
5	17 460	30 555	0.70	1 200
6	18 360	32 130	0.68	1 200
7	10 260	17 955	0.65	1 200
8	9 360	16 380	0.60	1 200
9	18 000	31 500	0.70	1 200
10	16 290	28 507	0.68	1 200

Table 8.10 Explosive parameters at Navigation Colliery

Blast Number	Total Charge(kg)	Tons blasted (tons)	Powder Factor	Density (kg/m^3)
1	18 524	22 140	0.61	1 200
2	17 620	24 074	0.61	1 200
3	24 010	35 237	0.61	1 200
4	17 427	21 071	0.61	1 200
5	17 620	24 047	0.62	1 200
6	19 602	25 137	0.62	1 200
7	21 240	21 674	0.62	1 200
8	18 897	22 714	0.62	1 200
9	18 992	24 074	0.62	1 200
10	10 192	21 111	0.62	1 200

Table 8.11 Explosive parameters at Kolomela Iron Ore mine

Blast Number	Total Charge(kg)	Tons blasted (tons)	Powder Factor	Density (kg/m^3)
1	137 725	202 291	1.44	3 200
2	121 690	197 238	1.44	3 200
3	103 490	186 273	1.44	3 200
4	133 055	204 299	1.44	3 200
5	92 365	173 901	1.44	3 200
6	82 860	150 281	1.44	3 200
7	81 190	169 281	1.44	3 200
8	98 225	177 091	1.44	3 200
9	100 845	182 451	1.44	3 200
10	39 691	87 572	1.44	3 200

Table 8.12 Explosive parameters at Sishen Iron Ore mine

Blast Number	Total Charge(kg)	Tons blasted (tons)	Powder Factor	Density (kg/m^3)
1	139 725	171 282	1.45	3 200
2	173 282	282 182	1.50	3 200
3	182 582	282 928	1.50	3 200
4	171 928	292 914	1.50	3 200
5	62 915	179 928	1.50	3 200
6	89 978	141 290	1.50	3 200
7	111 290	191 372	1.50	3 200
8	94 382	199 031	1.50	3 200
9	110 231	93 318	1.50	3 200
10	93 319	131 482	1.50	3 200

8.3 Vibration and Overpressure Interface Layout

This section presents the guidelines to using vibration and overpressure models in BL. The models give the exclusions zones and the monitoring stations numbered. Figures 8.22 and 8.23 show the vibration models of the Kolomela and Mogalakwena surface mines.

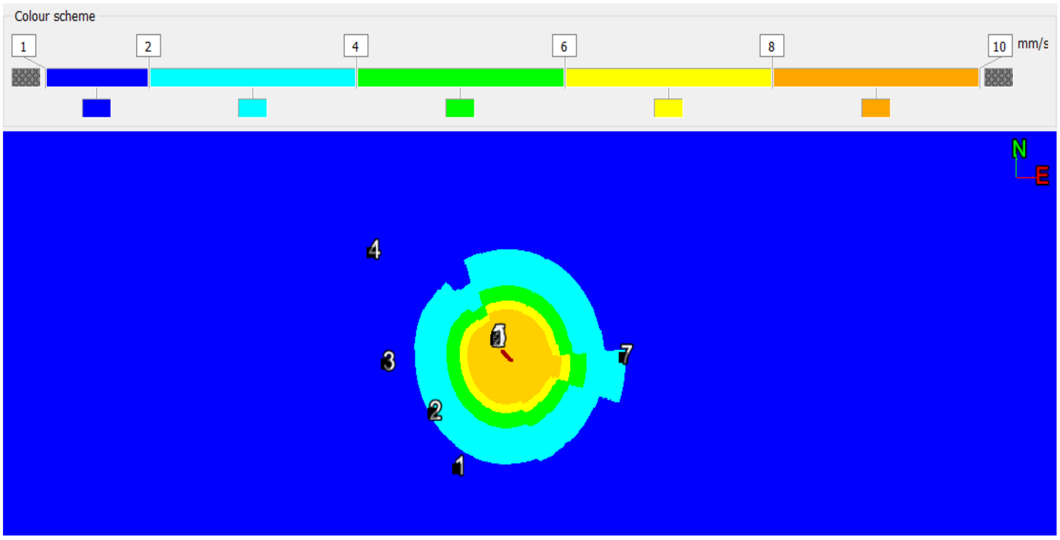

Figure 8.23 Vibration model Kolomela Iron Ore. *Source : Maptek (2021)*

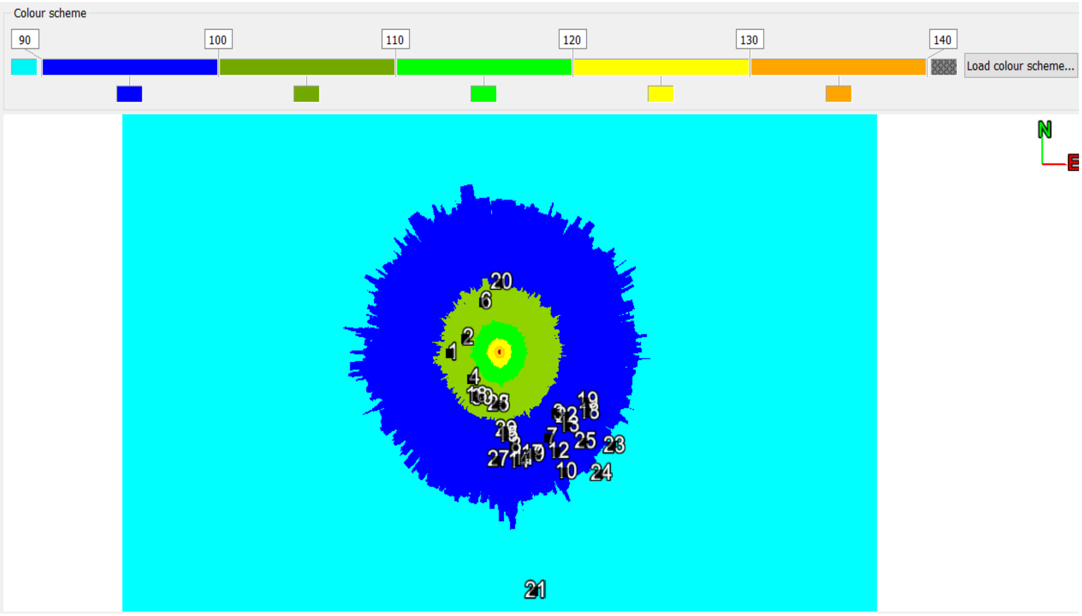

Figure 8.24 Vibration model Mogalakwena Platinum Ore

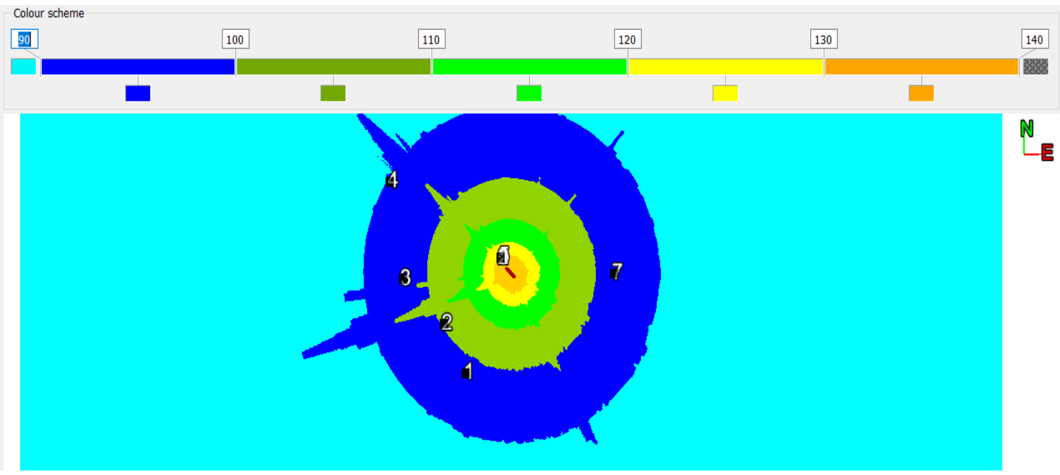

Figure 8.25 Vibration model. *Source : Maptek (2021)*

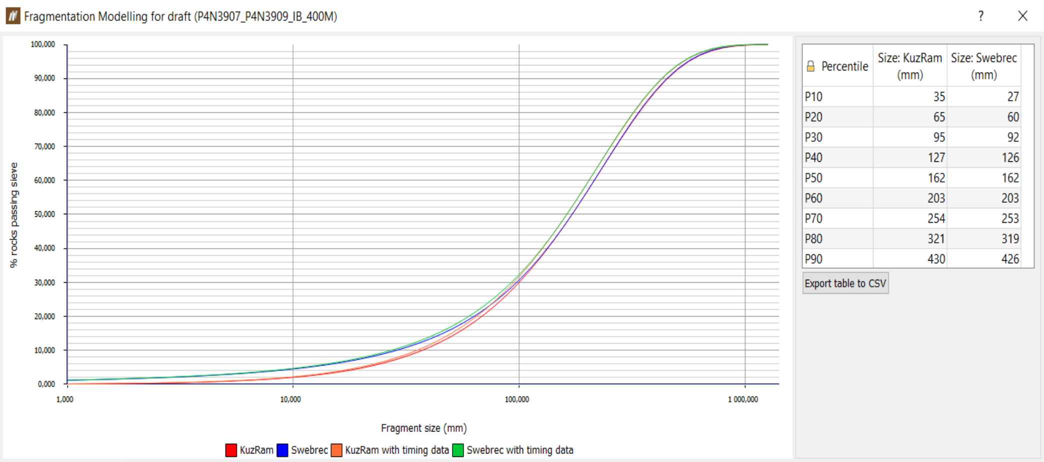

Percentile	Size: KuzRam (mm)	Size: Swebrec (mm)
P10	35	27
P20	65	60
P30	95	92
P40	127	126
P50	162	162
P60	203	203
P70	254	253
P80	321	319
P90	430	426

Figure 8.26 Fragmentation curves. **Source : Maptek (2021)**

8.4 Descriptive Statistics

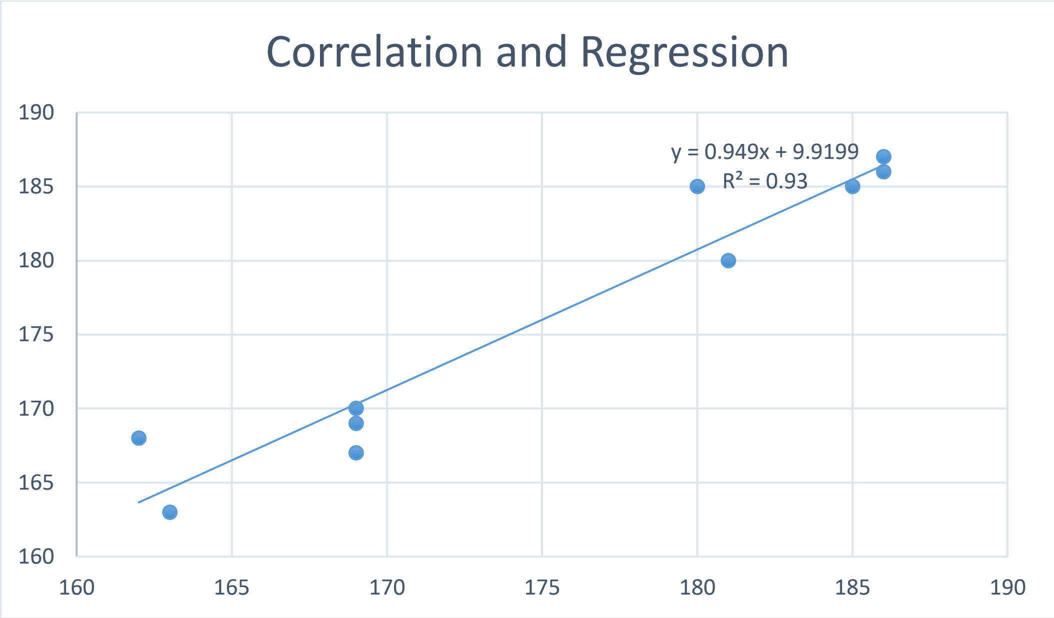

Figure 8.27 Correlation and regression for Mogalakwena Platinum mine

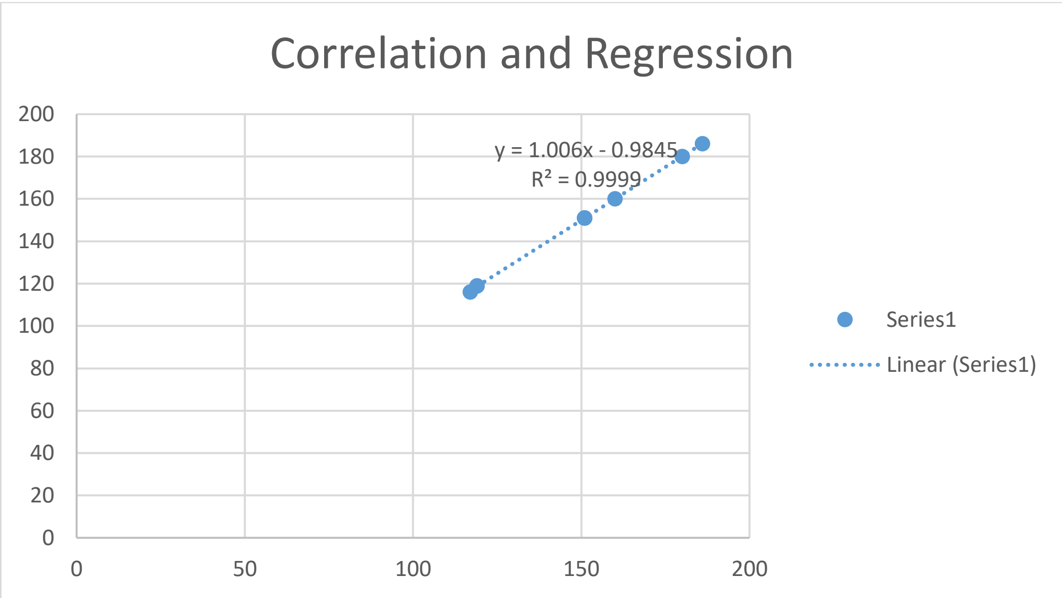

Figure 8.28 Correlation and regression for Isibonelo Colliery

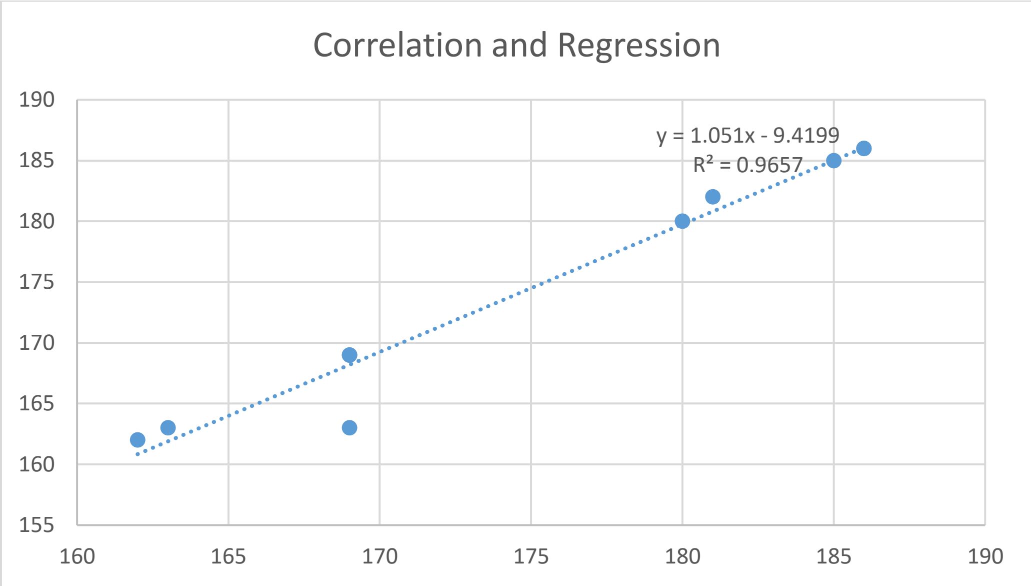

Figure 8.29 Correlation and regression for Navigation Colliery

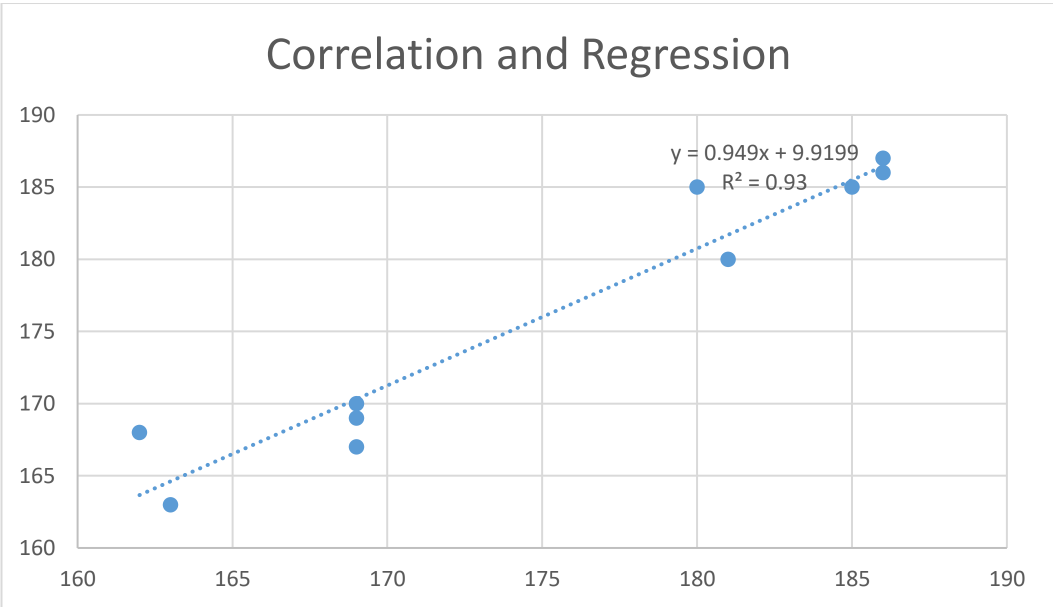

Figure 8.30 Correlation and regression for Kolomela mine

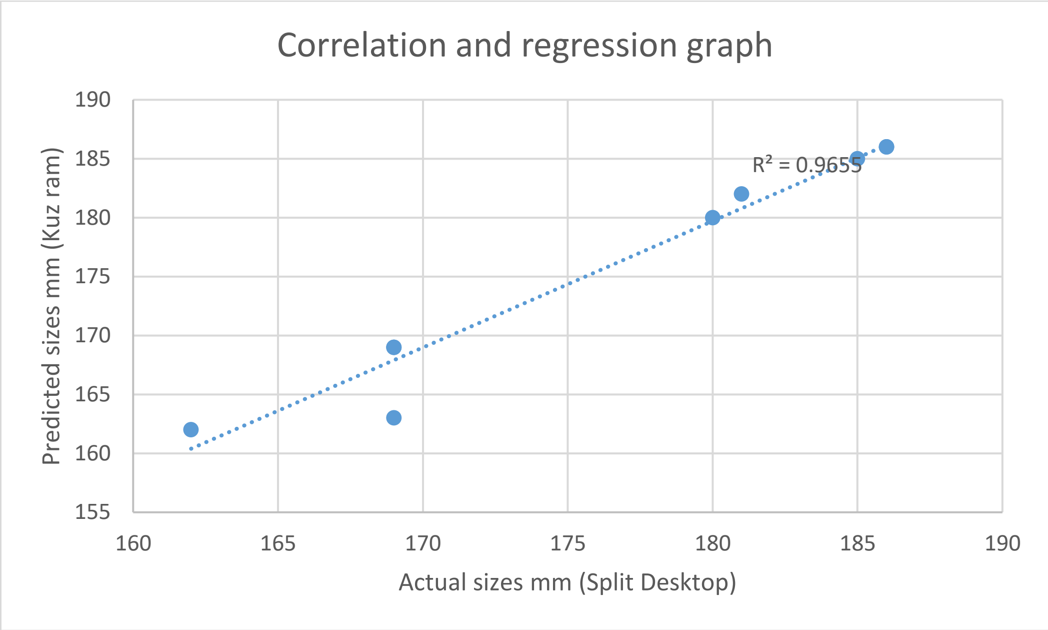

Figure 8.31. Correlation and regression for Sishen Iron Ore mine